Molecular bases of excitability and sexual dimorphism in the zebra finch song system

by

Samantha R. Friedrich

A DISSERTATION

Presented to the Department of Behavioral Neuroscience
and the Oregon Health & Science University
School of Medicine
in partial fulfillment of
the requirements for the degree of Doctor of Philosophy

October 14, 2021

CERTIFICATE OF APPROVAL

This is to certify that the PhD dissertation of

Samantha R. Friedrich

has been approved by

Claudio Mello, Ph.D., M.D. (Mentor)

Deb Finn, Ph.D. (Chair)

Lucia Carbone, Ph.D.

Stephen David, Ph.D.

Deena Walker, Ph.D.

This dissertation is dedicated to my gramma, Carolyn A. Friedrich, whose backyard bird game put Disney princesses to shame.

Abstract

Vocal learning is the ability to learn vocalizations through imitation, and is a rare trait shared by only a few lineages of mammals and three groups of birds. Songbirds more than any other animal model have been indispensable in elucidating the behavioral and neural mechanisms of vocal learning, and they share many key features with human speech circuitry and development. The most highly studied songbird species is the zebra finch (*Taeniopygia guttata*), whose song circuitry has been investigated through the many disciplines of genomics, neuroanatomy, neurophysiology, neuroendocinology, behavior, learning, and more. The brain circuitry that drives song learning and production, called the song system, is highly specialized functionally and molecularly, and strikingly sexually dimorphic. This dissertation aims to deepen our understanding of vocal learning and sexual differentiation in the brain through the detailed molecular lens of transcriptomics. In Chapter 2, I examine three major families of ion channel genes - sodium, calcium, and chloride channels. I use comparative genomic methods to rigorously confirm their orthology and improve gene models, and show how their expression in the song system is regulated to endow each song circuit element with unique excitability properties. In Chapter 3, I turn my focus toward the transcriptional dynamics that take place during the sexual differentiation of a key vocal motor nucleus in the song system. Comparisons of genome-wide expression across sex and age

reveal an abundance of sex-specific genes and functional networks that define distinct male and female developmental programs. Through these efforts, I demonstrate how heterogeneous gene expression across circuit elements, sexes, and developmental stages calibrates the neural substrate of a complex, sexually dimorphic behavior. More broadly, the work in this dissertation provides molecular resolution to both classic and emerging theories of how brain circuits are electrophysiologically tuned and sexually differentiated.

Acknowledgements

It really does take a village to raise a PhD student, and I am extremely fortunate to have been surrounded by so many wonderful friends and mentors throughout this undertaking. I would like to first thank my advisor, Dr. Claudio Mello, whose passion for birds is positively infectious and has deepened my appreciation of our flighted friends in ways I could not have imagined at the start of this journey. I find myself repeatedly in awe of your expansive knowledge and ability to relate seemingly disparate topics. I will never forget your ability to ask insightful questions at every seminar, no matter how distant the topic may be from our cozy corner of songbird neurobiology, nor the overflowing generosity and eagerness with which you share your scientific passion. I would like to thank the members of the Mello lab with whom I've had the pleasure of sharing a workspace and many grand experiences. Your friendliness and brilliance have made the Mello lab feel welcoming, warm, and something special. Peter Lovell, thank you for making the lab a communicative, social space, and teaching me everything I needed to know in lab to grow my own wings. Morgan Wirthlin, I met you years ago at a conference before I had even applied to grad school, and it was the highlight of that conference for me. Since that day I've modeled so much of how I conduct myself as a scientist after your shining example. Alex Nevue, you have a sharp

mind and you really are a natural in this field. I am so grateful to have you as a colleague and friend. Taylor Kaser and Allie Buckner, my songbird sweethearts, you brought brilliance and sunshine into the lab. It's not exactly easy to be a woman in science, but it was so much easier with you two around. I also want to acknowledge the help I received from Ben Zemel, Alex Wilmington, Chris Olson, and, through a serendipitous twist of fate that had nothing to do with birdsong, Devin Owen. I would like to thank the members of my Dissertation Advisory and Oral Exam Committees, Dr. Deb Finn, Dr. Lucia Carbone, Dr. Stephen David, and Dr. Deena Walker, for being generous with their time, as well as for their encouragement, curiosity, and insightful input. A heartfelt thank you to my many fairy godparents that made up the dream team of Behavioral Neuroscience (BEHN) administrators: Jeanne Sutter, Charlotte Wenger, Nicole Ernst, Amanda Asbrock, Josh Merrick, and Kris Thomason. And to all the BEHN program directors, Suzanne Mitchell, Garet Lahvis, Andrey Ryabinin, and Marina Guizzetti. Also to Jackie Wirz, shepherd to and advocate for all lost grad students during her time as Assistant Dean of Graduate Student Affairs. Extra-special thanks to Jeanne, Deb, Garet, Andrey, and Jackie for showing me support that went above and beyond program- or professional- related matters. You all deserve to be recognized and rewarded for the invaluable personal work that you do. A humongous thank you to all the students in the BEHN program I shared this experience with. Ya'll are both the reason I was excited to join the program in the first place, as well as what kept me from quitting altogether on numerous occasions. Warmest thanks to my brilliant classmates Elina Thomas and Nadir Balba; we survived grad school by celebrating every victory together, no matter how small. I do not know how to say a big enough thank you to Stark House and everyone in its magnetic orbit. Living with all you compassionate, hilarious, and loving

souls was truly a gift, and there is no other group I'd have rather been stuck with during the COVID pandemic. An infinite thank you to my parents, Melissa and Karl, for raising me to be an independent thinker and value education. Your love and support made it possible for me to blaze new trails and become a first generation PhD student. And to my brother Lukas, for being one of my biggest cheerleaders. And to my sister Carly, who is my other half; I am extremely grateful for the gift of getting to share a love of birds, and a personal closeness to them, with you. You are an amazing parrot-mom. And to my best friend, Victoria Nassif, who has been my soul mate and personal hero since we met in 9th grade. I have overflowing gratitude for my beloved partner and constant companion, Dr. Jon Savage, who provided me thoughtful and levelheaded advice as well as unconditional support through both my personal and professional pursuits the last 3+ years. You have been miracle grow to my healing and personal growth, and together, we have cultivated a companionship of incomparable ease and excitement. Thank you for bookending every day, even my worst ones, with laughter and many forms of cheese. And finally, I would like to thank Zip and Zephyr (AKA the "beep-beeps"), my adopted female zebra finches, whose bouncing, atmospheric chatters are now the sound of home, and whose flitting antics transformed a model organism into lively characters with individual charm.

Contents

List of Figures

List of Tables

List of Supplementary Figures

Chapter 1

Introduction

> What wild creature is more accessible to our eyes and ears, as close to us and everyone in the world, as universal as a bird?
>
> -David Attenbourough

Songbirds have long captured the curious minds of scientists and naturalists for their courtship displays of song and dance, drastic sex differences in plumage and behavior, and prolific speciation. While many different songbird species have been used in research, perhaps the most notorious and widely studied is the zebra finch (*Taeniopygia guttata*). Zebra finches are small, highly social songbirds of the family *Estrildidae* and valued by naturalists, researchers, and aviculturalists alike. Research using zebra finches has led to advances spanning a wide array of biomedical fields, and continues to expand since its humble beginnings in the 1950's [1]. Because zebra finches take so well to captivity, they allow for experimental ingenuity and controlled manipulation that are not feasible with wild avian models. Due to their imitative vocal abilities, zebra finches are an indispensable model for studying the speech and language deficits associated with several human conditions, including developmental verbal dyspraxia [2], fragile X syndrome [3], Huntington's disease [4],

and Parkinson's disease [5, 6]. Their unique reproductive behaviors and biology have shed light on mate choice [7], maternal effects [8], and sperm evolution [9]. Their bright red bills have prompted studies on the genetics and immune function of carotenoids [10, 11]. In addition to those mentioned above, there are numerous other research tracks that have benefited from zebra finches, but perhaps the most studied aspect of the zebra finch is their capacity for vocal learning [reviewed in 12, 13].

1.1 Zebra finches as models to study vocal learning

While it may seem counterintuitive to study a complex human trait using avian models, songbirds have illuminated the biological mechanisms of human speech more than any other animal model [14]. Vocal learning, or the ability to learn vocalizations through imitation, is a trait found in a select few animal groups including humans, dolphins, whales, possibly bats, elephants and pinnipeds, and three groups of birds – songbirds, parrots, and hummingbirds [15, 16]. The behavioral and neurobiological processes underlying avian vocal learning share remarkable similarity with human speech acquisition. Much like human infants learning to speak, young zebra finches produce unstructured vocalizations ("subsong") analogous to babbling, require a functioning auditory system and feedback to acquire and modify vocal sounds, learn optimally during critical periods of development, and exhibit considerable vocal variability from one individual to the next [reviewed in 17]. Despite major differences in gross brain organization between birds and mammals, the neural circuitry driving human speech and zebra finch song is wired with parallel blueprints, and homologous cortical and striatal vocal regions express similar groups of genes [18, 19].

For example, FOXP2 is a transcription factor gene directly linked to human speech that is expressed in striatal circuit elements of both human and songbird vocal learning pathways [20].

1.1.1 Singing is a complex, learned behavior

Zebra finch song is a learned vocalization used to attract mates, identify individual conspecifics, establish pair bonds, and maintain auditory contact [21]. Unlike many other songbirds, zebra finches do not use song for territorial defense. Singing is a sexually dimorphic behavior in zebra finches as only the males sing. Each male's song is made up of several complex syllables that occur in a faithfully repeated sequence called a motif, and multiple motifs sung in succession, and often preceded by a set of repeated introductory notes, constitute a song bout [22]. Juvenile zebra finches learn to sing through imitation, and generally copy the song of their father [reviewed in 12]. The song learning process takes place during a critical period spanning $\sim$20-90 days posthatch (DPH), beginning with a sensory phase in which juveniles listen to and acquire an auditory memory of the tutor's song, usually the father's song. Around 35 DPH, young males begin to produce highly variable and noisy syllables called subsong, which is considered analogous to the babbling phase in human speech development. This subsong progressively evolves into multiple distinct syllables sung in succession, forming recognizable song motifs that mark the plastic song phase beginning around 50 DPH. At this point, shared song elements between the tutor and juvenile also become recognizable. Juveniles continue to practice and polish their song and by 90 DPH, the song is "crystallized" into its final, stable form. Every male's song is unique but

similar to the tutor song, thus song serves as an acoustic signature of individual identity as well as signaling kinship [23].

Singing occurs in directed and undirected contexts. In both singing contexts, the acoustic nature of the song is largely preserved, with detectable but small changes in song tempo, variability across renditions, and number of introductory notes [24]. The associated behaviors and motivations are what mostly differentiate directed from undirected song. Directed song is that which is sung specifically to a mate as part of a courtship display. It is always accompanied by circumscribed posturing and movements, and its ultimate goal is to elicit copulation solicitation from a female. Undirected song is sung without the corresponding courtship dance, to no conspecific in particular, and in a wider array of contexts. Paired males sing undirected song just outside the nest to signal the female to stay put, and unpaired males sing undirected song to advertise their availability. Undirected singing in adults is also thought to reflect vocal practice [25]. Visually and acoustically isolated zebra finches will sing undirected song, and there is some evidence to suggest that singing is inherently rewarding [26].

1.1.2 The song system is a network of brain nuclei that coordinate song

The learning and production of song is orchestrated by a network of brain nuclei called the song system. The song system is anatomically discrete, and selectively active during listening to or producing song, implying this circuitry is highly specialized for song [27]. The song system is composed of the posterior direct motor pathway (DMP), necessary for song production [28, 29], and the anterior forebrain pathway (AFP) necessary for song learning

and adult song variability [14, 30–32]. Nucleus HVC (proper name) projects to both the DMP and AFP, and receives inputs from nucleus interfacialis of the nidopallium (NIf) [33] and thalamic nucleus uvaeformis (Uva) [34]. In the DMP, terminals from HVC synapse onto neurons of the robust nucleus of the arcopallium (RA), which are considered analogous to layer 5/6 motor neurons of mammalian laryngeal motor cortex [19]. RA then projects to the midbrain's dorsomedial (DM) nucleus of the intercollicular complex, to the tracheosyringeal subdivision of the XII cranial nerve nucleus (nXIIts), which innervates the syrinx (the avian vocal organ), and to medullary respiratory centers [35]. Lesioning RA or HVC fully disrupts song [28].

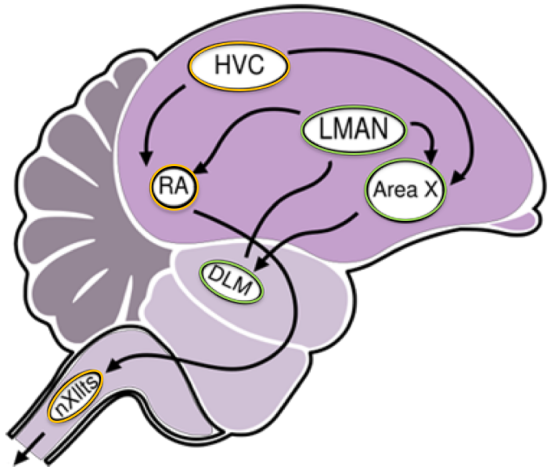

Figure 1.1: A simplified schematic of the song nuclei and their connections, shown from a parasagittal view. Yellow outlines indicate nuclei of the direct motor pathway (DMP) and green outlines indicate nuclei of the anterior forebrain pathway (AFP). Abbreviations: HVC: proper name; LMAN: lateral magnocellular nucleus of the anterior nidopallium; RA: robust nucleus of the arcopallium; X: Area X; DLM: dorsal lateral nucleus of the medial thalamus; DM: dorsomedial intercollicular nucleus; nXIIts: motonucleus of tracheosyringeal part of the XIIth cranial nerve.

In the AFP, striatal Area X receives projections from HVC and projects to the medial nucleus of dorsolateral thalamus (DLM), which projects to the lateral magnocellular nucleus of the anterior nidopallium (LMAN) [36]. LMAN projects to Area X [37] but also to RA,

converging with inputs from the DMP [38]. While lesioning LMAN in adults has no effect on song, lesioning LMAN in juveniles (<50 DPH) disrupts song development [30].

1.1.3 Song system gene expression is specialized and regulated by song

As the second avian species to have its entire genome sequenced [39], the zebra finch is well positioned to address questions surrounding genomic and transcriptomic influences on brain function. These endeavors encompass high-throughput studies using microarrays and RNA-seq, as well as more focused approaches using *in situ* hybridization and PCR. The activation of auditory and song system regions in response to song was revealed by immediate early gene expression, providing direct links between a specific behavior and concurrent gene regulation in the circuit elements driving that behavior [25, 40, 41]. This exploration of neurogenomic dynamics underlying a learned behavior was further expanded through the identification of additional genes and gene networks activated by singing and hearing song [42–45]. Furthermore, comparative transcriptomic analyses of song nuclei in birds and homologous speech processing regions in humans revealed shared molecular specializations, adding support to the theory that human and avian vocal learning systems are built on convergent neural mechanisms [19].

1.2 Songbirds as models to study neurobehavioral sex differences

In the last few decades, there has been an uptick in findings of sex differences in the brain that range in scale from molecular to brain network levels. Gauging the relative importance of these findings across varying levels of analysis has been a major source of controversy [46]. One major challenge studies face is relating molecular or structural findings to sex differences in specific behaviors, as it is not necessarily the case that all neural sex differences manifest in behavioral sex differences. This can be a challenge even for the rare instances of drastic sex differences in gross brain morphology; for example, the size of the mammalian sexually dimorphic nucleus of the preoptic area (SDN-POA) has been correlated with sexual preference, a trait that is expressed through many different sexual behaviors [47].

There are several considerable advantages of the songbird model that make the challenge of relating neural to behavioral sex differences far more tractable. For one, songbird sex differences in singing behavior are robust. In many songbird species including zebra finches, the sexually dimorphic nature of song is not just a matter of degree, but completely binary, in that only the males sing. Additionally, this behavior is driven by a discrete and sexually dimorphic network of brain nuclei. The song system is specifically activated by singing and hearing song, and does not appear to exhibit properties of a general purpose motor system [27]. Another advantage is that the window of song system development overlaps with song learning, allowing for manipulations of neural substrate to be evaluated by their effect on singing behavior and song learning. Finally, the abundance and diversity of songbird species provides a rich backdrop of natural variation in singing behavior. Comparative studies of

species that vary in the degree to which song is sexually dimorphic hold much promise in determining which neural sex differences drive behavioral sex differences.

Zebra finches are an excellent songbird model to study sex differences given their highly dimorphic singing behavior and brain circuitry. Males produce learned songs in addition to learned and unlearned calls, while females produce only unlearned calls [21]. This sex dimorphism in vocal behavior is reflected in the morphology of the underlying brain circuitry of the song system. When the gross anatomy of the mature song system was first characterized in the 1970's, the extreme sexual dimorphism was a main topic of interest, with some male song nuclei reaching five times greater volumes than their corresponding nuclei in females [48]. Also, the muscles of the vocal organ were found to be larger in males than females [49]. In zebra finches, the volumes of RA, HVC, and nXIIts are larger in adult males, and Area X is not cytoarchitecturally discernible in females [48–50](but see [51]). This prominent sex dimorphism in song nuclei volume led to the hypothesis that sex differences in the song system drive sex differences in singing behavior.

1.2.1 Sexual dimorphism emerges over song system development

The robust sexual dimorphism in song nuclei volume and cellular makeup develops during postnatal stages of brain development and overlaps with the critical period for song learning. In the first week or so after hatching, the song nuclei of male and female zebra finch nestlings are similar in size and morphology. Around 14-21 DPH, gross morphological sex differences begin to emerge and are elaborated over the course of sensorimotor learning [52, 53]. In general, song nuclei grow larger in males and regress in females.

Song nuclei vary in the particular timing and nature of sexually dimorphic metamorphoses. For example, both RA and HVC grow in males and shrink in females, however they differ in the timing of these changes, and in the cellular processes driving male growth. Around 10 DPH, well before zebra finches have left the nest, male and female HVC are equivalent in volume, but after this time point, they rapidly diverge in their growth trajectories. By $\sim$50 DPH, male HVC increases to more than double its 10 DPH volume, while female HVC shrinks to less than half its 10 DPH volume [53]. The growth of HVC in males is driven by an increase in the number of HVC neurons [54], specifically newborn RA-projecting neurons that migrate into HVC from the lateral ventrical dorsal to HVC [55–57]. The shrinkage of HVC in females is due to rapid cell loss beginning around 15 DPH, likely due to apoptotic mechanisms [56]. The development of sexual dimorphism in RA shows a similar but delayed trajectory relative to HVC. The volume of RA at 10 DPH is the same in males and females, and RA increases in volume and neuron number in both sexes until $\sim$20 DPH [50, 52, 53, 56, 58–60]. After 20 DPH, RA's trajectory diverges, growing rapidly in males and shrinking in females until 50 DPH, when RA volumes approximate those of adult birds. In contrast to HVC, the growth of male RA appears to be driven not by increases in cell number, but by increases in soma size and decreases in neuron density [54]. In females, RA shrinks, presumably through the same mechanisms proposed for female HVC, namely cell loss via programmed cell death pathways [56].

The molecular mechanisms driving sexual dimorphism in the song system are poorly understood. While sex differential cell survival seems to be a common theme in the development of multiple song nuclei, the different timings and types of changes associated with each nucleus' development strongly suggest that the underlying mechanisms are some-

what unique to each song nucleus. To gain insight into the molecular dynamics of sexual dimorphism, Chapter 3 investigates transcriptional regulation in RA during its divergent developmental trajectory.

1.2.2 The role of sex steroid hormones in song system development

There is a large and convoluted body of literature on the role of sex steroids in songbird brains, and despite many contradictions, it is undeniable that sex steroids affect song system development and sex differentiation [reviewed in 61]. As in mammals, hormones heavily influence the course of morphological and behavioral sex differentiation in birds. However, the influence of hormones on sexual differentiation is not as straightforward as gonadally secreted hormones acting on distal targets. In 1959, a landmark study by Phoenix et al. [62] introduced the idea that hormones exert long-lasting structural effects on the developing brain. This prompted a flood of investigations that eventually gave rise to a widely accepted model of sexual differentiation in which early gonadally-secreted hormones prompt the development of sexually differentiated tissue, and then gonadal hormones released in adulthood act within those differentiated neural substrates. While evidence from followup studies demanded some modifications to the theory, only in more recent decades has it been outright challenged by the discovery of sex differences that are not dictated by gonadal hormones [63]. From studies of zebra finches, the classic theory of sex differentiation has been challenged by contradictory evidence from hormone studies, as well as the discoveries of neurosteroidogenesis and brain cell-autonomous factors. To provide some background regarding the role of sex steroid action in the zebra finch song system, this section summarizes

brain expression patterns of sex steroid receptors and enzymes, evidence for neurosteroidogenesis, and some key hormone manipulation studies. The general consensus is that sex differences in song system and singing behavior are shaped in part through sex steroid signaling, but other factors are necessary.

The earliest detectable sexual dimorphism of the zebra finch song system is male-biased androgen receptor (AR) expression in HVC at 9 DPH [64]. ARs are expressed in virtually all song nuclei, showing greater expression in males within HVC, LMAN, and Area X, as well as in the syrinx [65, 66]. Compared to females, the proportion of androgen-concentrating cells is also much greater in adult male HVC and LMAN [65, 67, 68]. In contrast, expression of estrogen receptor (ER) and the estrogen-synthesis enzyme aromatase is notably lacking from song control regions [69], with the exception of very sparse ER expression in HVC [70]. No sex differences have been found in the expression levels of aromatase or estrogen receptors in the song system [71–73].

The origin of the hormones that act to masculinize the zebra finch song system is a matter of debate. In contrast to the classic mammalian paradigm, it does not seem to be the case that gonadal hormones are the master regulators of sexually dimorphic song system development. For one thing, circulating gonadal hormone levels do not show consistently significant sex differences in developing zebra finches [71, 74, 75]. Moreover, castrated males develop normal song [76, 77], and genetic females with induced testicular tissue show little to no masculinization of song circuitry [78, 79]. Gonadal hormones, however, do affect singing behavior. Compared to intact males, castrated male zebra finches sing less often and at a slower pace [76], and testosterone treatment prompts estrogen-masculinized females to start singing (see below).

In zebra finches, the critical source of sex steroid hormones that differentiate the song system may be the brain itself. Indirect evidence surfaced in the 1990's that zebra finches synthesize estrogen *de novo* within the brain [71, 80]. In support of *de novo* synthesis within the brain, estrogen levels from slice cultures of 25 DPH zebra finch telencephalon exceeded what could be derived from precursors provided in the medium [81]. This same study reported that estrogen levels were higher in male than female slice cultures, however this sex difference has not been observed *in vivo*.

One of the most intriguing outcomes of sex steroid manipulation in zebra finches is that early exposure to estradiol (E2) masculinizes female song system and behavior. E2-treated females develop robust song nuclei and sing multi-syllable songs that are comparable to males [82–88]. The earlier in development E2 is administered to females, the more complete the masculinization [85]. Early E2 treatment increases the volume of forebrain song nuclei in females as well as the size and number of neurons [82, 83, 89–91]. Additionally, E2 masculinizes the projection from HVC to RA *in vitro* [81]. While intriguing, it is important to note that the masculinizing effects of exogenous estrogen in females do not prove that estrogen is responsible for typical masculinization of the male song system.

Despite the widespread expression of androgen receptors in song system, androgens are far less effective at masculinizing females. Adult testosterone treatment does not induce song or masculinized song nuclei in female zebra finches [89, 92]. Treating young females with nonaromatizable androgens produces modest masculinizing effects on soma size and cell counts in some song nuclei, but these results are inconsistent across studies [80, 83, 89, 90, 93]. Some research suggests that androgens act in tandem with estrogens, wherein estrogens are necessary to prime song control areas to make them sensitive to androgen

action. In support of this paradigm, females masculinized with early E2 administration express androgen receptors at higher levels than control females in LMAN, HVC, and Area X [65, 94]. Additionally, treating young females with a combination of E2 and the androgen receptor blocker, flutamide, significantly dampens the masculinizing effects of E2 [95]. Collectively, the presence of androgen receptors [96], expression of a key androgen synthesis enzyme [97], and greater levels of cell proliferation [98] in the ventricular zone in males indirectly point to a possible role for androgens in sex-biased neurogenesis. Despite these findings, combined treatment with E2 and nonaromatizable androgen is no more masculinizing than E2 alone, nor does it lead to full masculinization of the female song system [91]. While not necessary to induce song, adult androgen treatment of early estrogen-treated females has been shown to increase song frequency [85, 99].

In contrast with the transformative power of E2 to masculinize females, attempts to shunt typical masculine development by blocking estrogen action through various methods have failed to demasculinize the song system or prevent singing [78, 100, 101]. Paradoxically, some manipulations using antiestrogens actually hypermasculinized the volume and cell size of song nuclei [102–104]. Modest demasculinization effects were observed in a few studies, however. When fadrozole, an aromatase inhibitor, was administered to young males over 10-30 DPH, the distribution of their mature (135 DPH) RA and HVC neuron sizes shifted toward smaller diameters [100]. Administration of fadrozole has also been shown to decrease the male-specific increase in brain-derived neurotrophic factor (BDNF) within HVC around 35 DPH [105]. *In vitro*, treating juvenile male slice cultures with fadrozole blocked the innervation of RA by HVC projections [81]. Although singing was unaffected by the aromatase inhibitor fadrozole, a different inhibitor called vorozole administered to

male hatchlings decreased the number of song bouts produced in adulthood [101]. Finally, a more recent study using the estrogen synthesis inhibitor exemestane showed that treated males sang simpler songs than untreated males, but reported little to no effects on the song system [106].

In summary, experiments using various hormone treatments and gonadectomies have produced singing female zebra finches with enlarged song nuclei and functional circuitry, but similar manipulations in males have had minimal effects on song nuclei or singing [reviewed in 61, 107]. To date, no hormone manipulation has completely masculinized the song system of a genetic female, nor demasculinized the song system of a genetic male, implying that other mechanisms must be invoked during development.

1.2.3 Genomic influences on sexual dimorphism

One of the most striking findings in support of genomic drivers of sexual differentiation is the case of the extraordinary zebra finch gynandromorph [108]. This bird, which arose spontaneously in a lab colony, acted like a male, producing a fully developed song and courting females. It presented male plumage on its right side, and female plumage on its left, divided neatly across the body's midline (Figure 1.2A). The gynandromorph's gonads followed the same laterality, with a testis on the right, and an ovary on the left. Consistent with the divided plumage and gonads, the brain was bisected into genetically male and female halves, confirmed by laterally confined expression patterns of sex-linked genes. Curiously, song nuclei on the right side of the brain were substantially larger than their corresponding nuclei on the left (Figure 1.2D). This finding was highly surprising con-

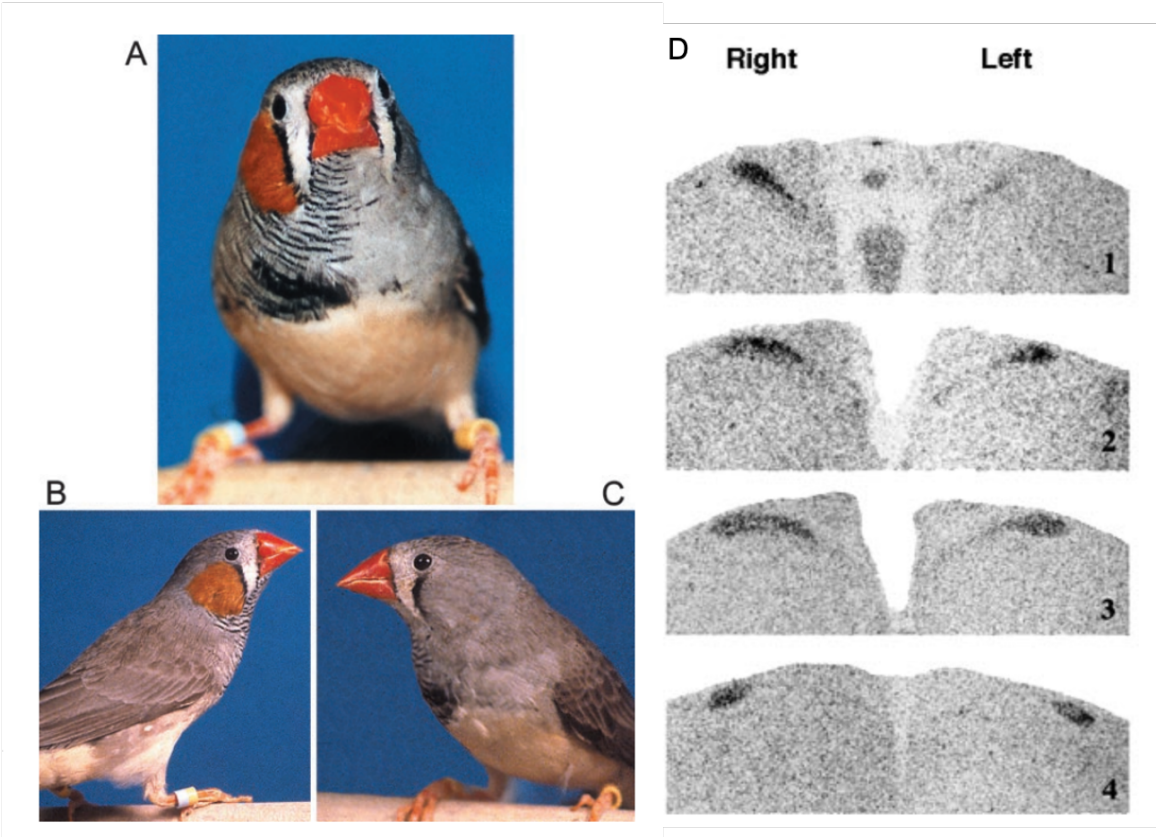

Figure 1.2: Zebra finch gynandromorph. (**A**) This bird showed a bilateral division of sex-specific plumage. Male plumage can be seen on its right side (**B**) and female plumage on its left side (**C**). (**D**) Inverted dark field autoradiograms of in situ hybridization showing the distribution of androgen receptor mRNA (dark areas) to mark HVC at various levels, revealing volume differences in HVC despite brain hemispheres being exposed to the same circulating hormone levels. Figure adapted from [108]

sidering that sex differentiation was thought to depend upon circulating hormones, to which both hemispheres were exposed. Instead, the song system showed sexual dimorphism between hemispheres, suggesting that cell-autonomous mechanisms contributed to processes of sexual differentiation in the zebra finch brain.

Reframing classic theories of sex differentiation

As one of the earliest sex differences to arise in a developing embryo, sex chromosome genes are poised to seed the signaling cascades that lead to multifaceted sexual differentia-

tion. Indeed, sex chromosome genes are fundamental to sex determination in many animal systems. In addition to sex determining genes, sex chromosomes contain many genes involved in sex-specific functions [109] and brain development [110]. For a long time, sex determination and sex differentiation were considered temporally and mechanistically discrete processes. Sex determination strictly concerned the fate of gonadal tissue, and sex differentiation referred to sex differences that arise in other tissues as a result of gonadal hormone secretions. Recent work in multiple species has blurred the line between the two, and they are now understood to be highly interdependent [111, 112].

In mammals, gonadal differentiation is under the control of the Y-linked gene *Sry* [113]. In males, *Sry* activates a cascade of pathways, including testosterone synthesis, that transforms undifferentiated gonad tissue into testis [114]. The classic theory of mammalian sex differentiation posited that sex chromosome genes trigger sex-specific gonadal development, and the gonads then secrete different levels of hormones into circulation, prompting the development of sex differences in various hormone-sensitive tissues throughout the body [115]. Framed this way, sex differentiation can be broken down into two subsequent mechanisms; a genetic, cell-autonomous mechanism driving gonadal differentiation, followed by a gonadal hormonal mechanism that acts in various target tissues. In line with the speculations put forth by Phoenix et al. [62], gonadal hormones were thought to act through two developmentally discrete mechanisms; the early "organizing" effects that direct the formation of permanent sex differences, and the transient "activating" effects of fluctuating hormone levels that act on mature, differentiated tissues in adults [116].

While tidy, this linear theory in which genetic sex determination sets the stage for hormone-mediated sexual differentiation is a gross oversimplification of the actual picture. Impor-

tantly, the classic theory fails to account for sex differences that arise prior to the differentiation of the gonads in both germline [117] and non-gonadal tissues [118–120]. A more cohesive and current theory places sex chromosome genes at the heart of sex-specific development, whereby sex chromosome genes initiate a myriad of downstream pathways that orchestrate sex differences, including but not limited to gonadal hormone secretions [111]. Much of our understanding of sex chromosome effects has resulted from research using the Four Core Genotypes (FCG) model, which is a mouse model developed to explore the effects of sex chromosomes independent of gonadal influence. In the FCG model, the SRY gene is optionally expressed as an autosomal transgene, allowing for comparisons between XX and XY mice that share the same gonad type [121]. Research using this FCG model revealed that sex chromosome complement affects a diversity of phenotypic endpoints, including the volumes of brain regions [122–124]. One unfortunate side effect of this model is that sex chromosome effects have been almost exclusively studied in mice, and thus also only in XY sex determination systems.

The avian ZW sex determination system

Nature has invented a wide and fascinating array of sex determination systems, of which the XY system is just one [125]. The ZW sex determination system underlies sex determination in birds, as well as some fish, reptiles, and insects. Parallel to the mammalian XY sex-determination system, genetic sex in birds depends on the combination of two asymmetric sex chromosomes. The ZW sex determination system can be thought of as the "mirror image" of the XY sex determination system; males are homogametic (ZZ), and females are heterogametic (ZW) (Figure 1.3). Analogous to the Y and X chromosomes, the W chro-

Figure 1.3: ZW sex chromosomes determine sex in zebra finches. Females (left) are heterozygous ZW, and males (right) are homozygous ZZ. Similar to the mammalian Y chromosome, the avian W chromosome is shorter and less gene-rich than the Z chromosome.

mosome is morphologically smaller and less gene-rich than the Z chromosome. While the evolution and genetic makeup of the Z chromosome has been studied in depth [126], far less is known about the avian W chromosome. Estimates suggest that avian W chromosomes contain around 30-50 genes, most of which have gametologous copies on the Z chromosome [127, 128]. Importantly, there are major differences in the gene composition of XY and ZW chromosome pairs. In fact, there are no shared genes between mammalian XY and avian ZW chromosomes; comparative analyses revealed that the avian Z chromosome contains many genes with orthologs on human chromosome 9, indicating that XY and ZW sex chromosomes evolved and diverged from different autosomes of the common ancestor to birds and mammals [128–131].

As with XY systems, male and female ZW genomes are not composed of the same gene set, nor the same gene dosage. Specifically, W chromosome genes are only present and expressed in female birds, and because males are homozygous (ZZ), their gene doseage of Z chromosome genes is double that of females. It is important to note, however, that

having two copies of the Z chromosome does not directly translate to double the levels of Z chromosome gene expression in males. This nonlinear relationship between gene doseage and gene expression is achieved through complex mechanisms of doseage compensation.

Doseage compensation is the process by which cells balance the expression of genes between sexes. In mammalian XX cells, doseage compensation is achieved through X-inactivation, the transcriptional silencing of one X chromosome of the pair [132]. This process is initiated by the expression of the XIST gene only in XX cells [133]. X-inactivation helps match the expression levels of X genes between XX and XY individuals, however some X genes escape inactivation, and thus show female-biased expression [134, 135]. Unlike mammals, there are no known mechanisms for global dosage compensation in birds [136–139]. Instead, avian genomes show incomplete dosage compensation, in which compensation level varies from gene to gene, with no obvious regional clustering along the Z chromosome [140]. In adult zebra finch brain, many Z genes are expressed at higher levels in males compared to females [39]. In another songbird, the blue tit (*Cyanistes caeruleus*), most male-biased genes expressed in brain were Z genes [141]. The mechanisms of this gene-by-gene dosage compensation are not yet fully understood, but there is some evidence that microRNAs are involved [142].

1.3 Introduction summary

To summarize, the zebra finch is the premier avian model to study vocal learning. Males produce complex, learned songs driven by a constellation of brain nuclei called the song system. This network of brain structures is functionally discrete and molecularly specialized,

and shows similarities in connectivity and gene expression to brain areas involved in human speech. Song is highly sexually dimorphic in zebra finches, as only the males sing. This sexual dimorphism in singing behavior is mirrored by sexual dimorphism in the underlying song system, circuit elements of which are several times larger in males. The processes that orchestrate the sexually dimorphic development of the song system take place during the critical window of song learning, and vary across song nuclei. The sexual differentiation of the zebra finch song system is influenced by sex steroid hormones, but deviates from the classic organizing theory in a few crucial ways. For one, sex steroids are not the only important factors, as all hormone manipulations have proven insufficient to completely block or reverse sex differentiation of the song system in males or females. Moreover, strong evidence of neurosteroidogenesis implies brain-derived steroids can act on brain development in a gonad-independent manner. In contrast to mammals, avian sex is determined by a ZW sex chromosome system that lacks global dosage compensation, resulting in sex-biased expression of many Z genes. Lastly, the classic sex differentiation model has been challenged by the discovery of cell-autonomous, genetic mechanisms, as illustrated by the size dimorphic song nuclei of a rare zebra finch gynandromorph.

Chapter 2

Exploring the molecular basis of excitability in a vocal learner

The contents of this chapter were originally published in:

S. R. Friedrich, P. V. Lovell, T. M. Kaser, and C. V. Mello, "Exploring the molecular basis of neuronal excitability in a vocal learner," BMC Genomics, vol. 20, no. 1, p. 629, Aug. 2019, doi: 10.1186/s12864-019-5871-2.

All supplementary tables and additional files can be found at `https://bmcgenomics.biomedcentral.com/articles/10.1186/s12864-019-5871-2`.

2.1 Background

Motor learning, the process by which motor skills are acquired and perfected through practice, requires fine-tuning of sensorimotor circuit elements to ultimately produce precise motor output. One remarkable example is vocal learning, a trait that allows individu-

als to learn their vocalizations through auditorily guided vocal practice. Vocal learning is demonstrated only by some mammals (humans, cetaceans, bats, and possibly pinnipeds and elephants), and three groups of birds (parrots, hummingbirds, and songbirds) [15]. Songbirds provide a particularly powerful model for studying the role of specific genes within vocal learning circuits. Decades of study in the zebra finch have revealed much about neuroanatomical substrates for vocal learning, including the connectivity and electrophysiological properties of a discrete set of vocal nuclei called the song system [12, 143]. Single-unit neural recordings and modeling have described the electrophysiological characteristics and underlying conductances of several song system neuron types [144–153]. Less established is how the regulated expression of genes - specifically ion channel genes - gives rise to the physiological and excitable properties of song system neurons.

The zebra finch song system is composed of the posterior direct motor pathway (DMP), necessary for song production [28, 29], and the anterior forebrain pathway (AFP) necessary for song learning and adult song variability [14, 30–32]. Nucleus HVC (proper name) projects to both the DMP and AFP (Figure 2.1), and receives inputs from nucleus interfacialis of the nidopallium (NIf) (cardinSensorimotorNucleusNIf2005) and thalamic nucleus uvaeformis (Uva) [34]. In the DMP, terminals from HVC synapse onto neurons of the robust nucleus of the arcopallium (RA), which are considered analogous to layer 5/6 motor neurons of mammalian laryngeal motor cortex [19]. RA then projects to the midbrain's dorsomedial (DM) nucleus of the intercollicular complex, to the tracheosyringeal subdivision of the XII cranial nerve nucleus (nXIIts), which innervates the syrinx (the avian vocal organ), and to medullary respiratory centers [35]. In the AFP, striatal Area X receives projections from HVC and projects to the medial nucleus of dorsolateral thalamus (DLM), which projects to

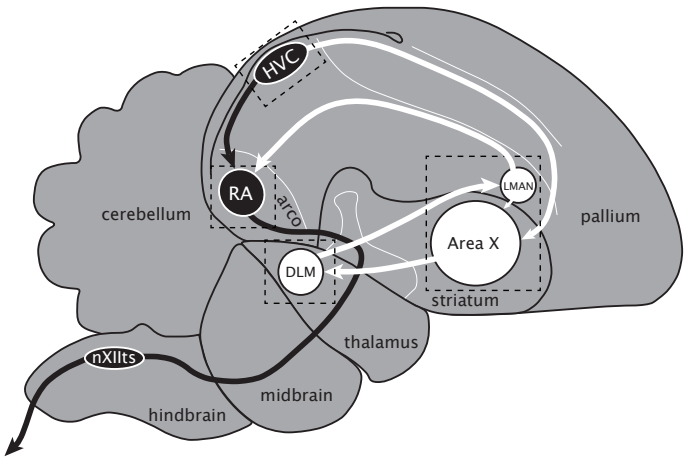

Figure 2.1: The zebra finch song system. Diagram of major brain areas collapsed across parasagittal planes to show the approximate locations and connections of the song control nuclei (not all connections are shown). The direct motor pathway (DMP; black arrows and nuclei) encompasses the projection from HVC to RA and from RA to vocal-motor nucleus nXIIts, the output of which controls the syrinx. The anterior forebrain pathway (AFP; white arrows and nuclei) encompasses the projection from HVC to Area X, from Area X to DLM, from DLM to LMAN, from LMAN back to Area X, and from LMAN to RA. Dotted boxes indicate approximate positions of the *in situ* hybridization photomicrographs presented in Figures 2.5 2.6, 2.7, 2.8, 2.9. See text for anatomical abbreviations.

the lateral magnocellular nucleus of the anterior nidopallium (LMAN) [36]. LMAN projects to Area X [37] but also to RA, converging with inputs from the DMP [38]. Detailed knowledge of this circuitry facilitates the identification of the molecular genetic determinants of its electrophysiological properties.

Given their direct effects on membrane potential, cell excitability, and neuronal firing, ion channels genes are among the most important determinants of neuronal function [154–156]. Their regulation and modulation is important in establishing electrophysiological properties of specific circuits, and may also contribute to nonsynaptic mechanisms of learning and memory [157–159]. As such, much can be learned about circuit function and excitability properties by identifying regional differences in ion channel gene expression. We previously examined the genomics and brain expression of potassium channel genes in ze-

bra finch [160] and uncovered evidence of differential expression for several key regulators of resting membrane and action potential repolarization. Here, we extend our analysis to sodium, calcium, and chloride channel families, all containing genes involved in determining neuronal excitability properties. Whereas sodium currents drive the rising phase of the action potential (AP) to ensure its initiation and propagation, calcium channels perform a wide array of functions such as regulating synaptic vesicle release, activating second messenger systems, and integrating signals over dendrites [155, 161, 162]. While less is known about chloride channels, some members of this family play a role in stabilizing resting membrane potential [163].

We identified 23 sodium, 38 calcium, and 33 chloride channel genes in the zebra finch genome - the majority with clear orthologs in mammals, indicating their broad conservation across vertebrates. We also established complements of ion channel genes that are differentially expressed within the major song system nuclei compared to the surround. These data represent the most comprehensive characterization of these ion channel gene families in a bird species to date. They also provide novel insights into how molecular specializations associated with neuronal excitability may have evolved to support a complex, learned vocal behavior.

2.2 Methods

2.2.1 Determining the full complement of sodium, calcium, and chloride channel genes in the zebra finch genome

We identified the sets of sodium, calcium, and chloride channel genes in zebra finch using a modified strategy of that previously used for potassium channels [160]. We first compiled the full set of human orthologs for these genes by navigating gene family hierarchies in HGCN (Ion channels > Ion channels by channel type > Sodium channels / Calcium channels / Chloride channels) and retrieving all gene names within all subfamilies for each of these three ion channel families [164]. Starting with human, arguably one of the most complete and best annotated genomes, allowed us to define a comprehensive set of genes to be examined. This effort identified a total of 108 ion channel genes, which included 23 sodium, 43 calcium, and 41 chloride channel and channel-related genes. This comprehensive set included genes encoding ion channels which have been linked to neuronal transmission, as well as the auxiliary subunits that modulate these channels. It also includes epithelial sodium channel (SCNN) genes, sperm-associated cation channel (CATSPER) genes, and volume-regulated anion channel subunits (LRRC8), even though these families have not been implicated in neuronal excitability and their expression in mammals is generally biased toward non-neuronal tissues [165–167]. We next searched for the orthologous genes in zebra finch using the following pipeline: (1) Obtain from NCBI (National Center for Biotechnology Information) the human records for the HGNC (HUGO Gene Nomenclature Committee) gene list; (2) Align the human models to the zebra finch genome to identify po-

tential orthologous loci; (3) Verify the synteny of the top-scoring alignment; 4) Demonstrate that the zebra finch gene aligns preferentially to the corresponding human locus; and (5) Demonstrate that secondary alignments represent other family members. These steps were also applied to identify chicken orthologs ("Chicken locus" column of Table S1, Additional file 1) in the galGal5 (GCA_000002315.3 (Warren, Hillier et al. 2017)) or updated galGal6 (GRCg6a; GCA_000002315.5) chicken genome. Each step is detailed next and summarized in Supplementary Figure S2.1. (1) We queried the NCBI Entrez Gene database with the names of the 108 genes in the starting HGNC gene list, to retrieve the corresponding human gene records. All 108 human genes were found in NCBI. (2) We retrieved the human RefSeq nucleotide sequences of the longest isoform for each annotated gene and used these as queries to search the zebra finch genome (taeGut1/WUGSC 3.2.4; GCA_000151805; Jul 2008) [39] using the UCSC Browser BLAT [168], noting all significant hits, defined as BLAT scores above 50 (top BLAT scores for human-to-taeGut1 alignments are reported in Table S1, Additional file 1). (3) We compared the synteny of the top scoring alignment in finch with that of the human query. We manually examined the immediately flanking genes on both sides of the alignment and query, if necessary expanding our analysis to genes farther up- or downstream. (4) The gene prediction (Ensembl release 95 [169]) at the top scoring finch locus was aligned back to human (using BLAT and/or BLAST) and the top-scoring alignment in human examined to confirm it was to the expected locus (same as initial query). For zebra finch gene models with multiple transcripts in Ensembl, we selected the longest variant. (5) All significant secondary alignments found in the finch genome were verified as done for the top hits (synteny comparison and back-alignment to human). This step served both to further confirm the orthology of the top hit and to identify possible novel paralogs or

paralogs missing from the human gene list (e.g. TPCN3) in the zebra finch genome. In the majority of cases, the top-scoring alignments in both finch and humans were reciprocally aligning models with conserved synteny across species, and all significant secondary alignments were to other genes of the same family, thus confirming orthology to human of the primary alignment in finch. These zebra finch Ensembl models that passed our synteny and alignment criteria are reported in Table 2.1 (n=61 genes, no symbols next to gene name and the "Zebra finch locus" column contains only Ensembl model(s)). We detected no cases of multiple top-scoring alignments with similar or different syntenies, thus we conclude that no novel paralogs and/or segmental duplications (e.g. of a cluster of syntenic genes) are present in the zebra finch genome for the gene families examined. In a few cases no Ensembl model was present but synteny of the top scoring finch locus was conserved with the human ortholog (n=2; chromosome location in taeGut1 is indicated in the "Zebra finch locus" column of Table 2.1). Lastly, secondary high scoring BLAT alignments to chrUn (chromosome Unknown) were not examined further, as those cases represent allelic variants in the zebra finch genome (as detailed in [39]). Several groups of genes required further verification efforts and/or variations of the main pipeline described above; these cases are discussed next and summarized in Supplementary Figure S2.1.

Case 1: Gene clusters. Some sodium channel (SCNxA) genes are arranged in clusters; in such cases, BLAT alignments tend to span multiple family members, or identify another family member in a given cluster. For these genes, we compared the syntenies within and around the clusters as a group across species, and closely examined the number, orientation and alignments of the individual genes in each cluster before deciding orthology. Both clusters in this family were found conserved between finch and humans (n=7 genes in 2

clusters: SCN5A, SCN10A, SCN11A, and SCN1A, SCN2A, SCN3A, SCN9A).

Case 2: Gene in taeGut1 but synteny diverges from human. Some genes met the reciprocal top-scoring alignment criteria but their synteny did not match that of human. To examine them further, we compared the synteny in zebra finch and human to that of orthologous loci in other birds, including Bengalese finch, medium ground finch, and tit (other passeriforms), falcon (outgroup to psitacopasseridae), chicken and/or quail (galliformes, basal neoaves), tinamou, ostrich, and emu (ratites, basal avian), lizard, alligator and turtle (non-avian sauropsids, outgroup to birds), Xenopus (amphibian, outgroup to amniotes), and platypus and opossum (basal mammals). We only used non-human orthologs that met two criteria: (1) conserved synteny and (2) aligned preferentially to the correct human locus. For 4 genes, this phylogenetic approach revealed an indirect relationship between the syntenies of the human query and the top scoring alignment in finch (indicated by a "$" in Table 2.1; details in "Synteny notes" column of Table S1, Additional file 1; examples in Figures 2.2 & 2.2). For another 2 genes (ASIC2 and CLIC2), human and zebra finch syntenies could not be fully linked through phylogenetic relationships, indicating weaker evidence of orthology (indicated by a "#" in Table 2.1).

Case 3: Gene detection in taeGut1 required non-human ortholog queries. In other cases, there were no significant alignments of the human query to taeGut1. For these genes, we pursued further searches in taeGut1 using as queries orthologs from the same list of other species discussed above in Case 2. For all 6 genes in this category, the top-scoring alignment identified a zebra finch Ensembl model that itself aligned to the correct locus in human, and whose synteny was conserved with human (indicated by a filled diamond in Table 2.1 and a chromosome location in the "Zebra finch locus" column). In the case of TPCN3, which

lacks a human model, we used orthologs from other species (chicken, dog) as queries to confirm the locus (initially identified from secondary alignments of human TPCN1 and 2) in taeGut1, and confirmed that synteny in zebra finch was conserved with those species.

Case 4: Synteny verification required examination of PacBio assembly. In yet other cases, a locus with an Ensembl model in taeGut1 was identified through alignments of human or other species' models and that Ensembl model aligned back to the correct locus in human but lacked syntenic context. This occurred when the top-scoring alignment in finch was located between gaps and/or on an unplaced scaffold or a chromosome "random" (e.g. chr13_random), or when the only significant alignment was to chrUn. For these genes, we next used the zebra finch Ensembl model to conduct searches of a newer zebra finch assembly (Tgut_diploid_1.0; GCA_002008985; [170]) built exclusively from PacBio reads (Pacific Biosciences). This PacBio assembly has higher contiguity, fewer gaps (individual scaffolds have no gaps), and often more genes and intergenic regions than the Sanger, 454, or Illumina assemblies. Since this PacBio assembly currently does not have gene predictions, the PacBio scaffolds found to contain the top scoring alignments were examined further by BLASTing against RefSeq databases [171]. Briefly, we BLAST searched the NCBI collections of avian and non-avian RefSeqs separately, using as query the identified PacBio scaffolds, broken down into 10-40 kb segments depending on gene size and gene density. The ion channel gene of interest was confirmed as present in zebra finch if the BLAST alignment output had high-scoring alignments of: a) the correct orthologs from multiple non-avian species at the same locus, and b) neighboring genes to that locus that confirmed a conserved synteny with human or other species as detailed in Case 2. All 8 genes in this category are indicated by the presence of both an Ensembl model and a PacBio location in

the "Zebra finch locus" column of Table 2.1). We note that in 2 of these 8 cases (ASIC3 and CATSPERE), the top scoring alignment back to human was not to the correct locus, but both Ensembl models are very partial relative to their full-length human ortholog. In such cases the query seems to be targeting a conserved region or motif rather than the entire gene, thus the reciprocal alignment is not an accurate criterion.

Case 5: Gene located only in PacBio. In several other cases, no locus could be found through alignments of human or other species' orthologs to taeGut1. For these genes, we searched the PacBio assembly with the human model and/or other species' orthologs and confirmed synteny using BLAST to explore the surrounding scaffold sequence (see example in Supplementary Figure S2.2), as described in Cases 3 and 4 above. As there are no models in the PacBio assembly, we did not perform alignments of the zebra finch locus to human. In all cases in this category, we found a correct ortholog (n=10; genes have a PacBio location instead of an Ensembl model in the "Zebra finch locus" column of Table 2.1). In 5 of these 10 cases (indicated by $\bigtriangledown$ in Tables 1 and S1), we found only short segments of the ion channel gene between its syntenic genes, indicating severe truncation. Because these PacBio scaffolds have no internal missing sequence due to gaps, such truncations point to likely examples of pseudogenization.

Case 6: Gene could not be found in either zebra finch assembly. When no significant hits could be recovered from alignments of orthologs in either taeGut1 or the zebra finch PacBio assembly, we followed a pipeline for candidate missing genes, specifically: (1) We BLAST searched the finch PacBio assembly using models of syntenic genes from comparative species as queries. When the syntenic genes were found on the same scaffold, we conducted additional BLAST searches of short segments (1-2 kb) of their intergenic region

at a time. We interpret cases in which syntenic genes were adjacent but no traces of the ion channel gene could be found intergenically as high likelihood cases of gene loss, noting again that finch PacBio scaffolds are gapless. (2) To better understand the origin of such losses, we systematically searched for the gene of interest and syntenic genes in all birds with an assembled genome deposited in NCBI, initially based on gene name searches in Entrez Gene. In cases where other avian species' scaffolds contained syntenic genes but lacked a model for the gene of interest, we conducted BLAST searches of the intergenic region as described in Case 4. In cases where we could not find evidence for the gene in any bird species, we applied the same general strategy above to search for the gene of interest and its syntenic context in representative outgroups (e.g. alligator, lizard), to trace the most likely pattern of gene loss in groups ancestral to birds (for example, see Figure 2.3). We note, however, that there are often gaps in the intergenic regions of these Illumina-based assemblies, which limits the certainty of conclusions regarding gene loss in species currently lacking a PacBio assembly. In all cases where the Ensembl model at the zebra finch locus was annotated, that annotation was correct. In cases where an Ensembl model was present but annotated as a "novel gene", we annotated it accordingly (n=34 models; indicated by a "$\wedge$" next to the Ensembl model in Table 2.1).

2.2.2 Assessing gene model completeness and expanding gene models with additional sequence

While inspecting taeGut1 loci to verify orthology, we found many Ensembl predictions that seemed very partial. As a first pass to estimate gene model quality and completeness,

we calculated a length ratio by dividing the length in bases of each zebra finch model by that of the orthologous human model (values in Table S1, Additional file 1; frequency histogram in Supplementary Figure S2.3A). As with the orthology analysis, we selected the longest transcript variant for zebra finch and human. If there were multiple non-overlapping zebra finch Ensembl models at a locus (i.e. split models), their lengths were summed. We also used an alignment-based method to evaluate the completeness of zebra finch models. Because chicken (galGal6) had a higher coverage (82x) and contig N50 (17,655,422) than taeGut1 (5.5x; 38,639) and thus had more reliable and complete gene predictions, we used chicken models from Ensembl (release 95). RYR1 was excluded from this analysis as it is >100 kb long, fragmented into at least 8 models across 8 different scaffolds that lack syntenic context in galGal5, and the only verified model in taeGut1 is highly partial and in a gappy region of chrUn. For all other genes with orthology-verified models in both zebra finch and chicken (n=79 genes, models in both "Zebra finch locus" and "Chicken locus" columns of Table S1, Additional file 1), we first obtained the transcript sequences of the orthologous chicken Ensembl models. As with zebra finch, we selected the longest transcript variant and concatenated split models. We then aligned the chicken and corresponding zebra finch models to taeGut1 using the UCSC Browser BLAT and exported the results as psl files. Using a custom Python (version 3.6.7) script (available at https://github.com/samifriedrich/seq-recovery), we compared the top-scoring alignments of chicken and zebra finch models for each locus to find blocks of aligned chicken model sequence that did not overlap with any blocks of aligned zebra finch model sequence. These blocks of aligned chicken sequence missing from the zebra finch Ensembl gene predictions highlight the incompleteness of the zebra finch models and define sequences that can be used to expand these incomplete models

(Supplementary Figure S2.4). We created a taeGut1 BED track that displays these additional sequence blocks in the UCSC genome browser (Additional file 6). For each gene in this analysis, we calculated the number of bases recovered, as well as a "percent of post-recovery length" (original model length / [original model length + number of bases recovered]; values in Table S1, Additional file 1; frequency histogram in Supplementary Figure S2.3B). Genes were considered problematic if the original Ensembl model length was less than 90% of the percent post-recovery length (indicated by a "*" in the "Zebra finch locus" column of Table 2.1, and values reported as % post-recovery length < 90% in Table S1, Additional file 1).

2.2.3 Animal subjects and brain tissue

Adult male zebra finches were obtained from a commercial supplier (Magnolia Bird Farm, Pasadena, CA) and acclimated in our animal facility in same-sex group cages for at least two weeks prior to the onset of experiments. The work described in this study was approved by the OHSU IACUC and is in accordance with NIH guidelines. To minimize the confound of song-induced gene expression, all birds were placed overnight in acoustic isolation chambers and monitored for singing for a period of 2 hours after lights-on. Verified non-singing birds were sacrificed by decapitation and brains were rapidly dissected, blocked in TissueTec OCT (Sakura Finetek USA, Inc.; Torrance, CA), then flash-frozen in a slurry of isopropanol and crushed dry ice. Frozen brains were sectioned in the sagittal plane on a Leica CM1850 cryostat at $10\,\mu\mathrm{m}$ and melted onto charged microscope slides (Colorfrost Plus; Thermo Fisher Scientific; Waltham, MA). Slides were stored at -80 °C until use.

2.2.4 cDNA clone selection and riboprobe synthesis

All probes were derived from clones selected from the ESTIMA zebra finch cDNA library (Replogle, Arnold et al. 2008). All genes present in taeGut1 were examined in the UCSC Genome Browser for the presence of ESTIMA clones. For genes found only in the PacBio assembly, we BLASTed each corresponding scaffold region against all NCBI zebra finch EST collections to evaluate potential evidence of expression and identify suitable cDNA clones (high alignment scores and alignments that mirrored the exon structure of aligned orthologs). Preference was given to clones representing the 3'UTR region, to minimize cross-alignment of conserved coding sequences with other gene family members. Candidate ESTs were aligned to the zebra finch genome using BLAT (UCSC Genome Browser) to confirm mapped unambiguous mapping to the target gene without significant hits to other loci. Clone IDs are provided for all genes for which an *in situ* was run ("EST evidence" column of Table S1, Additional file 1). We followed the protocol by Carleton et al. [172] to generate non-radioactive, digoxigenin (DIG)-labeled riboprobes. In brief, isolated plasmid DNA was restriction digested using BSSHII (New England Biolabs; Ipswich, MA), purified using Invitrogen's PureLink PCR kit (Invitrogen; Carlsbad, CA), and run on an agarose gel to verify digestion, DNA content, and correct template size. Antisense probes were synthesized by incubating template with T3 RNA polymerase (Promega; Madison, WI) and DIG labeling mix (Roche Applied Science) for 2 hours at 37 °C, purified using Sephadex G-50 columns and stored at -80 °C until use.

2.2.5 *In situ* hybridization and gene expression analysis

Non-radioactive *in situ* hybridizations to zebra finch sagittal brain sections were performed as in [172], using VectaMount Permanent Mounting solution for coverslipping. Expression for each gene was evaluated in sections from 2-3 different birds from a total of 10 birds. Brightfield microscopy was used to evaluate slides, and high-resolution images were acquired and uploaded to the Zebra Finch Brain Expression Atlas, ZEBrA . Genes that showed greater or lesser mRNA signal within a song nucleus relative to their surround were designated as higher or lower expression, respectively. Incubation with no probes or antisense riboprobes for genes of known expression pattern (e.g. GAD2) were routinely included in the hybridizations as negative and positive controls, respectively. The hybridization conditions used have been previously shown not to generate significant signal to various sense-strand riboprobes.

2.2.6 Microarray scoring

We also evaluated differential brain gene expression of ion channels based on data from four previous microarray experiments where the song nucleus of interest and a nearby region were microdissected using laser capture microscopy. The HVC dataset was generated using spotted glass ESTIMA:Song collection "20 k" cDNA microarrays as detailed in [173] and HVC was contrasted with the immediately ventral nidopallial shelf. Details on sample preparation, mRNA isolation, probe synthesis, and hybridization can be found in [174]. The RA, Area X, and nXIIts datasets were generated using Agilent microarrays spotted with oligonucleotides. RA and nXIIts samples were hybridized to the Duke University *Tae-*

niopygia guttata 45 K oligo array and Area X samples were hybridized to the 20 K Agilent-019785 Custom Zebra Finch Microarray. RA was contrasted to ventrolateral arcopallium, Area X was contrasted to ventral striato-pallidum, and nXIIts was contrasted with the supra-spinal medullary nucleus (SSP). Detailed methods of sample preparation, mRNA isolation, array hybridization, and first-pass analyses are available for RA [19], Area X [43], and nXI-Its [175]. To determine the expression of ion channel and related genes in the zebra finch song system, these microarray datasets were reanalyzed as detailed in [176, 177]. Briefly, this involved mapping the oligonucleotide sequences onto taeGut1, visualizing them as a BED track uploaded to the UCSC Genome Browser, manually annotating oligo and cDNA entries, and using *in situ* hybridization data from the ZEBrA database for establishing validated significance criteria of differential expression. Here we evaluated the differential microarray data for each ion channel gene present in taeGut1 by navigating to the locus to confirm oligo and cDNA annotation and verify the microarray data outcome for that gene as higher, lower, or non-differential expression in each song nucleus analyzed compared to its contrasting region. This effort led to annotation of previously unannotated oligos or correction of mis-annotated ones, contributing to the manual curation efforts outlined in [176, 177]. Differential expression tables constructed in Excel are presented in Figure 2.4. When the microarray outcome was in disagreement with the *in situ* hybridization data, the latter designation was used as the final outcome (indicated by "$" in Figure 2.4). Some of these discrepancies were likely due to the song nuclei and comparison regions being in the same sagittal plane for *in situ* hybridizations but not for microarrays (in the latter, RA was compared to ventrolateral arcopallium, and Area X was compared to ventromedial striato-pallidum). In some other cases, probes were not available for *in situ* hybridizations, so

expression data reflects microarray data only (indicated by asterisks in Figure 2.4).

2.3 Results

2.3.1 Determining the full complement of sodium, calcium, and chloride channel genes in the zebra finch genome

Genes that encode or modulate sodium, calcium, and chloride ion channels play important roles in determining the electrophysiological properties of brain circuits. In order to understand the potential contributions of these channels to functional circuits underlying vocal learning and production in songbirds, we started with a comprehensive analysis to define the full complement of these ion channel families in the zebra finch genome. Starting with a list of 108 ion channel genes previously identified in human plus one additional gene that lacks a human model (TPCN3), we used BLAT alignments and synteny analysis to identify orthologous loci in zebra finch and chicken. We identified 94 (23 sodium, 38 calcium, 33 chloride) of these genes in zebra finch (Table 2.1) and 98 in chicken (Table S1), the latter encompassing four genes (BEST2, BEST4, CLCA1, and CLCA2) not found in zebra finch (Tables 2.2 and S2). Of the identified zebra finch genes, 54 were predicted and correctly annotated by Ensembl (taeGut3.2.4 release 95), 27 genes comprising 34 models were annotated as “novel genes” in Ensembl (indicated by a "$\wedge$" in the “Zebra finch locus” column of Table 2.1), and 14 had no Ensembl predictions in taeGut1. Of these 14, four genes were found in taeGut1 through BLAT alignments of human or other species’ orthologs (indicated by a taeGut1 locus only in the “Zebra finch locus” column of

Table 2.1.) The remaining 10 genes were not in taeGut1, but were identified in the recently released zebra finch PacBio assembly (indicated by a PacBio locus only in the “Zebra finch locus” column of Table 2.1) through alignments of orthologous models. For five of these genes only very partial alignments were found, suggesting gene truncation (indicated by a "$\bigtriangledown$" in Table 2.1.) In most cases we established orthology by demonstrating reciprocal top-scoring alignments and similar syntenies in birds and humans. For 8 genes, we linked the zebra finch synteny with human through phylogenetic relationships (indicated by a “$” in Table 2.1), but for 2 genes we could not fully link the synteny in zebra finch with that of human (indicated by a “#” in Table 2.1, detail provided in “Synteny notes” column of Table S1, Additional file 1). For a total of 14 genes in this study, we used orthologs from other species to find the locus in zebra finch (indicated by a filled diamond in Table 2.1.) While no novel paralogs were found in zebra finch, we confirmed the presence of TPCN3 in birds and reptiles, a gene that is severely truncated in humans and chimp and completely missing from mouse and rat [178]. For 15 mammalian genes we did not find orthologs in zebra finch, but we established a possible origin of the loss by exploring outgroup species (Table 2.2; details in Table S2, Additional file 1). These genes are discussed further in the context of their respective subfamilies. We note these conclusions about gene losses are tentative given that many avian genomes are incomplete and phylogenetic representation of sequenced genomes is somewhat limited.

Sodium channel genes

Sodium voltage-gated channel alpha (α) subunits (SCNxA)

The subunits encoded by these genes form the pore of voltage-gated sodium channels [161], which play important roles in the initiation and rising phase of action potential (AP) generation, and are critical for AP propagation [155]. This family originated from a singular ancestral form that has undergone multiple duplications and diversified broadly [179, 180]. We found 9 of the 10 mammalian SCNxA genes in zebra finch and chicken. The missing gene was SNC7A, which arose in mammals and presumably functions not as a voltage-gated channel but rather as a sodium sensor [181].

Sodium voltage-gated channel beta (β) subunits (SCNxB)

Four genes encoding non-pore-forming, auxiliary β subunits have been described in mammals [182]. They are thought to modulate sodium currents by associating covalently (SCN1B and 3B) or non-covalently (SCN2B and 4B) with α subunits to form heteromeric complexes. We found all four β subunit genes in zebra finch and chicken, and note that in the latter, it was previously identified in a PacBio assembly [183]. SCN1B was missing from taeGut1 but limited evidence suggested its presence in songbirds [184]. We have now identified the complete gene and syntenic context in the PacBio assembly through ortholog alignments and verification of conserved synteny (Figure 2.2) and Supplementary Figure S2.2). The synteny of SCN1B throughout avian phylogeny was difficult to resolve as many avian models were either on short scaffolds with little syntenic context or on scaffolds with many gaps, but we identified a consistent group of syntenic genes across lineages.

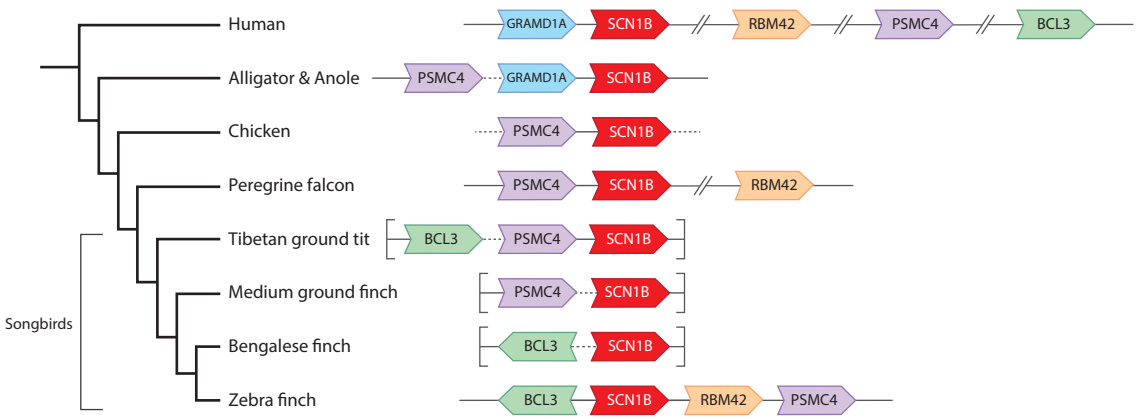

Figure 2.2: SCN1B is present in birds. SCN1B (red) is missing from taeGut1 but present in the zebra finch PacBio assembly. The different orientations (arrows point in 5' to 3' direction) and relative positions of BCL3, PSMC4, and RBM42 across birds suggest multiple rearrangement events in the avian phylogeny, even within different songbird lineages. GRAMD1A was not found in any avian species. Arrowheads indicate gene orientation; solid lines indicate gap-less intergenic regions; dotted lines indicate intergenic regions containing gaps; broken lines indicate interspersed genes not shown; brackets indicate the ends of scaffolds in the respective assemblies.

Acid-sensing ion channels (ASIC)

ASICs are proton-activated, nonselective cation channels that pass sodium, lithium, and potassium ions with the highest affinity for sodium [185]. All 5 mammalian ASIC genes were found in both zebra finch and chicken genomes.

Sodium leak channel (NALCN)

NALCN is a single gene that encodes a widely-expressed, nonselective, voltage-insensitive cation channel. This channel carries a persistent sodium leak current that sets excitability thresholds in virtually all neurons [186]. It is present in zebra finch and chicken genomes.

Epithelial sodium channels (SCNN)

Channel subunits in the SCNN family are encoded by four genes and drive active sodium reabsorption from extracellular fluid in epithelial tissues [187]. We found that all four genes are present in zebra finch and chicken genomes, confirming previous reports [188] and strengthening the evidence for orthology by confirming synteny.

Calcium channel genes

Calcium voltage-gated channel alpha (α)-1 subunits (CACNA1x)

Genes in this family encode the pore-forming $\alpha 1$ subunits that carry calcium across the plasma membrane [189]. In mammals, $\alpha 1$ subunits belong to three major subfamilies: Cav1 (L-type) channels (4 genes), Cav2 (P/Q-, N-, and R- type) channels (3 genes), and Cav3 (T-type) channels (3 genes). All genes were found in zebra finch and chicken, with CACNA1A and CACNA1F in the PacBio assembly.

HGNC Symbol	Alternate name	Full name	Zebra finch locus
A. Sodium channels			
α subunits			
SCN1A	Nav1.1	sodium voltage-gated channel alpha subunit 1	ENSTGUG00000007356^
SCN2A	Nav1.2	sodium voltage-gated channel alpha subunit 2	ENSTGUG00000007152^*
SCN3A	Nav1.3	sodium voltage-gated channel alpha subunit 3	ENSTGUG00000007034
SCN4A	Nav1.4	sodium voltage-gated channel alpha subunit 4	ENSTGUG00000003230
SCN5A	Nav1.5	sodium voltage-gated channel alpha subunit 5	ENSTGUG00000000531^
			ENSTGUG00000000533^
SCN8A	Nav1.6	sodium voltage-gated channel alpha subunit 8	ENSTGUG00000003307
SCN9A	Nav1.7	sodium voltage-gated channel alpha subunit 9	ENSTGUG00000007470^*
SCN10A	Nav1.8	sodium voltage-gated channel alpha subunit 10	ENSTGUG00000000476^*
SCN11A	Nav1.9	sodium voltage-gated channel alpha subunit 11	chr2:5686797–5,719,627
β subunits			
SCN1B[$]		sodium voltage-gated channel beta subunit 1	MUGN01000920.1818309–818,447
SCN2B		sodium voltage-gated channel beta subunit 2	ENSTGUG00000017358
			MUGN01000074.12766152–2,766,960
SCN3B		sodium voltage-gated channel beta subunit 3	ENSTGUG00000000607^
SCN4B		sodium voltage-gated channel beta subunit 4	ENSTGUG00000000230
			MUGN01000074.12777132–2,778,696
Acid-sensing			
ASIC1	ACCN2	acid sensing ion channel subunit 1	ENSTGUG00000003637
ASIC2[#]	ACCN1	acid sensing ion channel subunit 2	ENSTGUG00000003212^*
			ENSTGUG00000003215^*
ASIC3[◆]	ACCN3	acid sensing ion channel subunit 3	ENSTGUG00000016020^*
			MUGN01000217.1876923–883,599
ASIC4	ACCN4	acid sensing ion channel subunit 4	ENSTGUG00000006157*
ASIC5[◆]	ACCN5	acid sensing ion channel subunit 5	ENSTGUG00000005392
Leak channel			
NALCN		sodium leak channel, non selective	ENSTGUG00000010876
Epithelial			
SCNN1A[◆$]	SCNN1	sodium channel epithelial 1 alpha subunit	ENSTGUG00000013342*
SCNN1B		sodium channel epithelial 1 beta subunit	ENSTGUG00000005936
SCNN1D[◆]		sodium channel epithelial 1 delta subunit	ENSTGUG00000004091
SCNN1G		sodium channel epithelial 1 gamma subunit	chr14:8747853–8,755,433
B. Calcium channels			
L-type α subunits			
CACNA1S	Cav1.1	calcium voltage-gated channel subunit alpha1 S	ENSTGUG00000001142*
CACNA1C	Cav1.2	calcium voltage-gated channel subunit alpha1 C	ENSTGUG00000012529^
			ENSTGUG00000012538^
CACNA1D	Cav1.3	calcium voltage-gated channel subunit alpha1 D	ENSTGUG00000006839*
CACNA1F	Cav1.4	calcium voltage-gated channel subunit alpha1 F	MUGN01000244.140490–59,194
N/P/Q/R- type α subunits			
CACNA1A	Cav2.1	calcium voltage-gated channel subunit alpha1 A	MUGN01001147.1274884–306,034
CACNA1B	Cav2.2	calcium voltage-gated channel subunit alpha1 B	ENSTGUG00000002855*
CACNA1E	Cav2.3	calcium voltage-gated channel subunit alpha1 E	ENSTGUG00000017352
T-type α subunits			
CACNA1G	Cav3.1	calcium voltage-gated channel subunit alpha1 G	ENSTGUG00000009049*

Table 2.1: Ion channel genes in the zebra finch genome. Continues over next two pages. See symbol key under table.

HGNC Symbol	Alternate name	Full name	Zebra finch locus
CACNA1H	Cav3.2	calcium voltage-gated channel subunit alpha1 H	ENSTGUG00000006881*
CACNA1I	Cav3.3	calcium voltage-gated channel subunit alpha1 I	ENSTGUG00000010198*
α2/δ subunits			
CACNA2D1		calcium voltage-gated channel auxiliary subunit alpha2delta 1	ENSTGUG00000002536^*
			ENSTGUG00000002533^*
CACNA2D2		calcium voltage-gated channel auxiliary subunit alpha2delta 2	ENSTGUG00000004703^*
			ENSTGUG00000004711^*
			ENSTGUG00000004714^*
CACNA2D3		calcium voltage-gated channel auxiliary subunit alpha2delta 3	ENSTGUG00000006966^*
CACNA2D4		calcium voltage-gated channel auxiliary subunit alpha2delta 4	ENSTGUG00000012579^
β subunits			
CACNB1		calcium voltage-gated channel auxiliary subunit beta 1	MUGN01000261.12481145–2,492,038
CACNB2		calcium voltage-gated channel auxiliary subunit beta 2	ENSTGUG00000001247*
CACNB3		calcium voltage-gated channel auxiliary subunit beta 3	ENSTGUG00000015546
			MUGN01000394.1996686–999,415
CACNB4		calcium voltage-gated channel auxiliary subunit beta 4	ENSTGUG00000012082^*
γ subunits			
CACNG1		calcium voltage-gated channel auxiliary subunit gamma 1	ENSTGUG00000004397^
CACNG2	stargazer, stargazin	calcium voltage-gated channel auxiliary subunit gamma 2	ENSTGUG00000010725
CACNG3		calcium voltage-gated channel auxiliary subunit gamma 3	ENSTGUG00000006208*
CACNG4		calcium voltage-gated channel auxiliary subunit gamma 4	ENSTGUG00000004385*
CACNG5		calcium voltage-gated channel auxiliary subunit gamma 5	ENSTGUG00000004375*
CACNG7[§]		calcium voltage-gated channel auxiliary subunit gamma 7	MUGN01000421.1339861–356,707
CACNG8[§]		calcium voltage-gated channel auxiliary subunit gamma 8	MUGN01000421.1325281–333,090
Intracellular			
ITPR1	IP3R1	inositol 1,4,5-trisphosphate receptor type 1	ENSTGUG00000010241^
ITPR2	IP3R2	inositol 1,4,5-trisphosphate receptor type 2	ENSTGUG00000012196^
ITPR3	IP3R3	inositol 1,4,5-trisphosphate receptor type 3	ENSTGUG00000001798
RYR1		ryanodine receptor 1	ENSTGUG00000016333^
			MUGN01000615.12737–83,931
RYR2		ryanodine receptor 2	ENSTGUG00000010491
RYR3		ryanodine receptor 3	ENSTGUG00000011653^
TPCN1	TPC1	two pore segment channel 1	ENSTGUG00000009086
TPCN2[◆]	TPC2	two pore segment channel 2	ENSTGUG00000005328
TPCN3[◆✣]	TPC3	two pore segment channel 3	ENSTGUG00000007338^*
			ENSTGUG00000015038^*
Sperm associated			
CATSPERB[▽◆]	C14orf161	cation channel sperm associated auxiliary subunit beta	MUGN01001095.110976025–10,976,136
CATSPERD[▽◆§]	TMEM146	cation channel sperm associated auxiliary subunit delta	MUGN01000898.110200480–10,200,746
CATSPERE[▽◆]	C1orf101	catsper channel auxiliary subunit epsilon	ENSTGUG00000008288^*
			MUGN01000667.120007852–20,020,082
CATSPER3[▽◆]		cation channel sperm associated 3	chr13_random:2493868–2,500,983
			MUGN01000154.1512621–517,332

HGNC Symbol	Alternate name	Full name	Zebra finch locus
C. Chloride channels			
CLCNs			
CLCN1	CLC1	chloride voltage-gated channel 1	ENSTGUG00000013222*
CLCN2	CLC2	chloride voltage-gated channel 2	ENSTGUG00000010323*
CLCN3	CLC3	chloride voltage-gated channel 3	ENSTGUG00000006161
CLCN4	CLC4	chloride voltage-gated channel 4	ENSTGUG00000008365
CLCN5[$]	CLC5	chloride voltage-gated channel 5	ENSTGUG00000005324
CLCN6	CLC6	chloride voltage-gated channel 6	ENSTGUG00000002366*
CLCN7	CLC7	chloride voltage-gated channel 7	ENSTGUG00000004211*
CLCNK[†]	CLCK1	chloride voltage-gated channel K[†]	ENSTGUG00000002023^*
BSND	BART, DFNB73	barttin CLCNK type accessory beta subunit A	chr8:22970234:22970413
CLICs			
CLIC2[#]	CLIC2b	chloride intracellular channel 2	ENSTGUG00000004925
CLIC3[$]		chloride intracellular channel 3	ENSTGUG00000002341*
CLIC4	CLIC4L	chloride intracellular channel 4	ENSTGUG00000001132^*
CLIC5		chloride intracellular channel 5	ENSTGUG00000013246
CLIC6[◆]	CLIC1L	chloride intracellular channel 6	ENSTGUG00000004696
			MUGN01000638.1213150–238,240
CLCC1[◆]	MCLC	chloride channel CLIC like 1	ENSTGUG00000004508*
Calcium-activated			
ANO1	TMEM16A	anoctamin 1	ENSTGUG00000005385*
ANO2	TMEM16B	anoctamin 2	ENSTGUG00000011938
ANO3	TMEM16C	anoctamin 3	ENSTGUG00000004669
ANO4	TMEM16D	anoctamin 4	ENSTGUG00000009008
ANO5	TMEM16E	anoctamin 5	ENSTGUG00000004532*
ANO6	TMEM16F	anoctamin 6	ENSTGUG00000006024*
ANO7[▽]	TMEM16G	anoctamin 8	MUGN01000068.1571318–573,272
ANO8	TMEM16H	anoctamin 8	ENSTGUG00000015909^*
ANO9	TMEM16J	anoctamin 9	ENSTGUG00000006753
ANO10	TMEM16K	anoctamin 10	ENSTGUG00000003830
BEST1[◆]	VMD2	bestrophin 1	ENSTGUG00000005934^*
BEST3	VMD2L3	bestrophin 3	ENSTGUG00000006968^
Volume regulated			
LRRC8A	LRRC8	leucine rich repeat containing 8 VRAC subunit A	ENSTGUG00000004233
LRRC8B		leucine rich repeat containing 8 VRAC subunit B	ENSTGUG00000006230*
LRRC8C		leucine rich repeat containing 8 VRAC subunit C	ENSTGUG00000006226
LRRC8D	LRRC5	leucine rich repeat containing 8 VRAC subunit D	ENSTGUG00000006223
Other			
CFTR		cystic fibrosis transmembrane conductance regulator	ENSTGUG00000004828
CLNS1A[◆]		chloride nucleotide-sensitive channel 1A	ENSTGUG00000013030^

[▽] Highly partial or truncated
[†] Suggested name (not clear whether this locus is orthologous to mammalian CLCNKA or CLCNKB)
[$] Synteny traced through phylogenetic relationships
[#] Synteny could not be linked through phylogenetic relationship
[◆] Non-human ortholog used to find locus
[✣] No human ortholog
* Less than 90% of post-recovery length
^ Annotated as a "novel gene" in Ensembl

HGNC Symbol	Alternate names	Full name
Missing in finches		
BEST2	VMD2L1	bestrophin 2
Missing in Passeriformes		
CATSPER2	SPGF7, CATSPER	cation channel sperm associated 2
BEST4	VMD2L2	bestrophin 4
CLCA1	CaCC1	chloride channel accessory 1
CLCA2	CaCC3	chloride channel accessory 2
CLCA4	CaCC2	chloride channel accessory 4
Missing in Neognathae		
CATSPERG	C19orf15	cation channel sperm associated auxiliary subunit G
CATSPER1		cation channel sperm associated 1
CATSPER4		cation channel sperm associated 4
CLIC1	CL1C1	chloride intracellular channel 1
Missing in all birds		
CACNG6		calcium voltage-gated channel auxiliary subunit gamma 6
LRRC8E		leucine rich repeat containing 8 VRAC subunit E
Unique to mammals		
SCN7A	Nav2.1, Nav2.2, SCN6A	sodium channel, voltage-gated, type VII alpha subunit
CATSPERZ	TEX40, C11orf20	catsper channel auxiliary subunit zeta
CLCNKA or CLCNKB	CLCK1, ClC-K1; CLCKB, ClC-K2	chloride voltage-gated channel K A or B

Table 2.2: Ion channel genes missing from the zebra finch genome

Calcium voltage-gated channel alpha-2-delta (α2/δ) subunits (CACNA2Dx)

Calcium channels are modified by non-conducting subunits, including α2 and δ. α2/δ genes are unique in that each gene codes for both the α2 and δ subunits: α2 is an extracellular glycoprotein that forms a disulfide linkage to the δ subunit, and the δ subunit keeps the complex tethered to the plasma membrane [190]. All four human α2/δ genes were found in zebra finch and chicken.

Calcium voltage-gated channel auxiliary beta (β) subunits (CACNBx)

These modulatory subunits are entirely intracellular and attached to the calcium channel complex through binding sites on the α1 subunit [191]. All four human genes were found in zebra finch and chicken. CACNB1 in zebra finch was found only in the PacBio assembly.

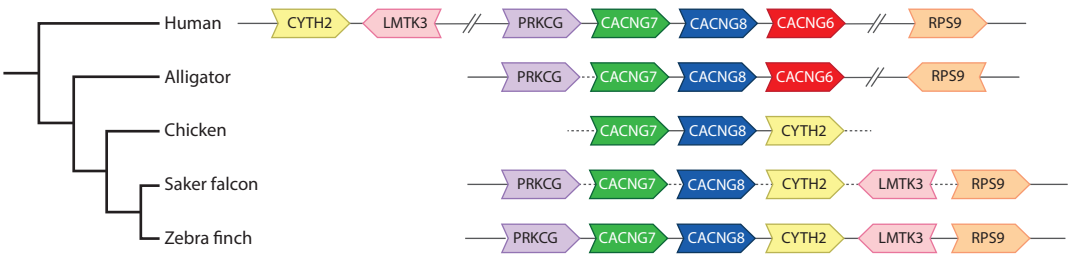

Figure 2.3: CACNG6 is missing from birds. While CACNG7 and CACNG8 are present, the syntenic paralog CACNG6 cannot be found in birds. The different orientations (arrows point in 5' to 3' direction) and relative positions of CYTH2, LMTK3, and RPS9 across phylogeny suggests multiple rearrangement events in this genomic region, possibly in an avian ancestor. Arrowheads indicate gene orientation; solid lines indicate gap-less intergenic regions; dotted lines indicate intergenic regions containing gaps; broken lines indicate interspersed genes not shown.

Calcium channel auxiliary gamma (γ) subunits (CACNGx)

Gamma subunits are glycoproteins with four transmembrane domains that associate with calcium channel complexes in the membrane [192]. Of the eight human genes, three (CACNG6, CACNG7, and CACNG8) occur in a syntenic block within a region of human Chr19 that is largely missing in birds, possibly due to chromosomal rearrangements in ancestral archosaurs and/or dinosaurs [184]. Subsequent assessments have identified CACNG7 and CACNG8 but not CACNG6 in the galGal5 chicken assembly [183]. Here we have confirmed with high confidence that CACNG6 is missing in zebra finch and other avian lineages based on BLAST searches and synteny verification of bird genomes including chicken and zebra finch PacBio assemblies (Figure2.3), suggesting an ancestral avian loss. We also found evidence that CACNG7 is present and likely complete in zebra finch, while CACNG8 is present but appears truncated in both zebra finch and chicken.

Sperm associated cation channels (CATPSER)

This family encodes four α subunits (CATSPER1-4) and five auxiliary subunits (CATSPER B, D, E, G, & Z) essential to sperm activation and motility [193, 194]. In zebra finch, we found fragments of CATSPER3, B, D, and E, but no trace of CATSPER1, 2, 4, G and Z. Chicken shares the same pattern, but retains fragments of CATSPER2. Because CATSPER1, -4, and -G are present in ratites, their absence in zebra finch and chicken appears to reflect loss in Neognaths. Our conclusions are partially consistent with previous reports [183, 195, 196], but due to the higher quality PacBio scaffolds and examination of additional birds, we provide stronger evidence with regards to truncation and phylogenetic patterns of gene loss. We note that the chicken gene annotated as CATSPER2 in NCBI (Gene ID: 395985) is misannotated – the correct annotation is CACNA1S.

Other calcium channel genes (ITPR, RYR, TPCN)

Other calcium channels may impact neuronal function by regulating internal calcium stores, including inositol 1,4,5-trisphosphate receptors (ITPR), ryanodine receptors (RYR), and two-pore channels (TPCN) [178, 197, 198]. Each family has 3 genes, all of which were identified in zebra finch and chicken. TPCN3 appears to have been lost in rodents and truncated in primates, including humans [178]. Interestingly, the truncated gene appears to have been duplicated in human, as can be seen in the UCSC Browser (GRCh38/hg38 chr2:109947776-109974086 and chr2:110397405-110423734).

Chloride channel genes

Voltage-dependent chloride channels (CLCN)

This family is composed of channels that open and conduct chloride ions in response to changes in membrane potential [163]. Mammals have 10 CLCN genes, of which 9 were identified in zebra finch and chicken. Two adjacent human genes - CLCNKA and CLCNKB - have high sequence identity and appear to be the result of a duplication specific to mammals. Both chicken and finch have a single gene at this locus that mirrors the ancestral condition. Because of their high similarity, sequence alignments could not resolve which human paralog is the ancestral form present in birds or reptiles. As the nomenclature in ancestral species is inconsistent, we suggest the name "CLCNK" for the single gene found at this locus in birds and reptiles.

Chloride intracellular channels (CLIC)

These channels are integrated into the membranes of organelles and participate in processes like membrane trafficking and cytoskeleton dynamics [199]. They can also exist in a soluble state in the cytoplasm, the function of which is poorly understood. Of the 7 functional genes in mammals, we found all but CLIC1 in chicken and zebra finch. We could not conclusively establish a CLIC1 loss because the syntenic genes are at the ends of different scaffolds in both zebra finch and chicken PacBio assemblies. It thus remains possible that CLIC1 is not in these assemblies due to incompleteness of the scaffolds. Consistent with this possibility, CLIC1 and syntenic genes are present in alligator and in kiwi (a ratite). Alternatively, the gene was lost in neognaths, as kiwi is currently the only bird with a detectable

CLIC1.

Calcium-activated chloride channels (ANO, BEST)

Some anoctamin (ANO1 & ANO2) and bestrohpin (BEST2) genes encode channels that conduct chloride currents in response to surges in intracellular calcium, but the function of most other family members remains speculative [200, 201]. Mammals have 10 ANO genes, of which we found 9 in chicken and zebra finch, and 4 BEST genes, of which we found 4 in chicken and 2 in zebra finch. ANO7 lacks models in zebra finch and chicken, but traces were detected by aligning orthologs to the zebra finch and chicken PacBio assemblies. The synteny in these and other birds (kiwi, goose, golden eagle, and rifleman) is conserved with mammals and alligators. Given that only a few 3' exons from orthologous models of this gene aligned to the chicken and zebra finch PacBio assemblies, combined with the lack of EST-based expression evidence, we conclude that ANO7 has likely become a pseudogene in some avian lineages, including oscines and galliformes. BEST4 is present and complete in galliforms (chicken) and psittaciformes (budgie), but appears pseudogenized in passerines, as only short segments of the 5' and 3' UTR regions were detected in zebra finch (PacBio), Bengalese finch, great tit, and starling. While BEST2 seems complete in chicken and songbirds like Tibetan tit and starling, we did not detect it at the corresponding locus in the zebra finch PacBio assembly. The upstream genes are in zebra finch similarly as in other birds, reptiles, and mammals, while the genes downstream of this locus reflect a synteny shared by Tibetan tit and starling that is presumably unique to songbirds. Because there are no BEST2 models and syntenic genes are isolated on short scaffolds in Bengalese and medium ground finch, we cannot distinguish between a loss in the finch lineage and a zebra finch-

specific loss. Similar to CACNG6/7/8, BEST2 is located in a region of human chromosome 19 associated with extensive rearrangements and gene losses in birds [184].

Chloride channel accessory subunits (CLCA)

Mammals have several non-pore-forming accessory subunits with a broad functional repertoire that includes modulating chloride channels, cell adhesion, and tumor suppression [202]. In humans, three functional CLCAs are in a syntenic cluster (CLCA1, CLCA2, and CLCA4) along with a pseudogene (CLCA3P). We found at least one CLCA gene with conserved synteny in psittaciformes (budgie), accipitriformes (eagles), and more basal birds (chicken, guinea fowl, and tinamou). In zebra finch and other passerines (e.g. golden-collared manakin), the immediately syntenic genes were adjacent to one another, with no trace of CLCA and no gaps in the intergenic region. From this, we conclude that CLCA genes were likely lost in Passeriformes.

Volume-regulated chloride channels (LRRC8)

LRRC8 channels are activated by cell swelling and may influence extracellular signaling by transporting neurotransmitters [203, 204]. Mammals have five LRRC8 subunits, and all but one (LRRC8E) were found in zebra finch and chicken. This gene appears to have been lost in birds [205].

Other chloride channel genes

Cystic fibrosis transmembrane conductance regulator (CFTR) is a chloride channel gated by ATP [206]. Chloride nucleotide-sensitive channel 1A (CLNS1A) is expressed at rela-

tively high levels in human [165] and mouse [166] brain tissue, and strongly implicated in cell volume regulation [207]. Both genes are present in zebra finch and chicken.

2.3.2 Evaluating zebra finch gene models

While examining zebra finch gene orthology, we noticed that many human models were noticeably longer than the corresponding zebra finch Ensembl models, suggesting that the latter may be incomplete predictions. To record this difference, we calculated a ratio (Table S1, Additional files 1 and 3A) of zebra finch to human transcript model length, and found that 28 of the 80 existing zebra finch Ensembl models were less than 90% of the human length, and 19 were less than 75%, even after summing the lengths of partial models, when present. To further evaluate model completeness, we compared the alignments of orthologous chicken and zebra finch Ensembl models at each gene locus in taeGut1 (n=79 genes with an Ensembl model in both species). Because Ensembl chicken models are from a higher quality genome and are generally more complete than zebra finch models, this method revealed sequence blocks where the chicken model aligned but that are not present in the zebra finch Ensembl models (example in Supplementary Figure S2.4). We recovered these additional sequences for 66 of the 79 genes analyzed (Table S1, "Additional bases recovered" > 0), and created a taeGut1 BED track for their visualization in the UCSC Browser (Additional file 6). We also calculated a percent of post-recovery length (Table S1, Additional file 1; Supplementary Figure S2.3B) and found 36 genes for which the original model length was less than 90% of the post-recovery length (indicated by a "*" in the "Zebra finch locus" column of Table 2.1), and 16 that were less than 75%. This effort demonstrates that

many zebra finch Ensembl models are incomplete, but additional genomic sequence related to those genes exists and should be taken into account in future studies.

2.3.3 Differential expression of sodium, calcium, and chloride channel genes in the song system

To assess the expression of ion channel genes in the song system of adult male zebra finches, we analyzed previously generated microarray data and conducted *in situ* hybridizations on brain sections containing the 4 major telencephalic song nuclei (HVC, RA, LMAN, and Area X), and a brainstem motor nucleus, nXIIts. Because our focus was on vocal control circuitry, not all brain areas of relevance for vocal learning (such as auditory forebrain) were assessed. This analysis encompassed 55 ion channel genes (14 sodium, 25 calcium, 16 chloride) that were part of the microarrays and/or for which cDNA clones were available in zebra finch. Summaries of the data are presented in Figure 2.4, and robust examples of differential *in situ* patterns are presented in Figures 2.5- 2.7 and Supplementary Figure S2.5. For a few genes, *in situ* hybridizations also revealed differential expression in DLM and Uva. For all genes analyzed, the terms higher, lower and non-differential below refer to expression compared to the respective surrounds (nidopallium for HVC, LMAN and NIf, arcopallium for RA, striatum for Area X, dorsal thamalus for DLM and Uva, rostral medulla for nXIIts).

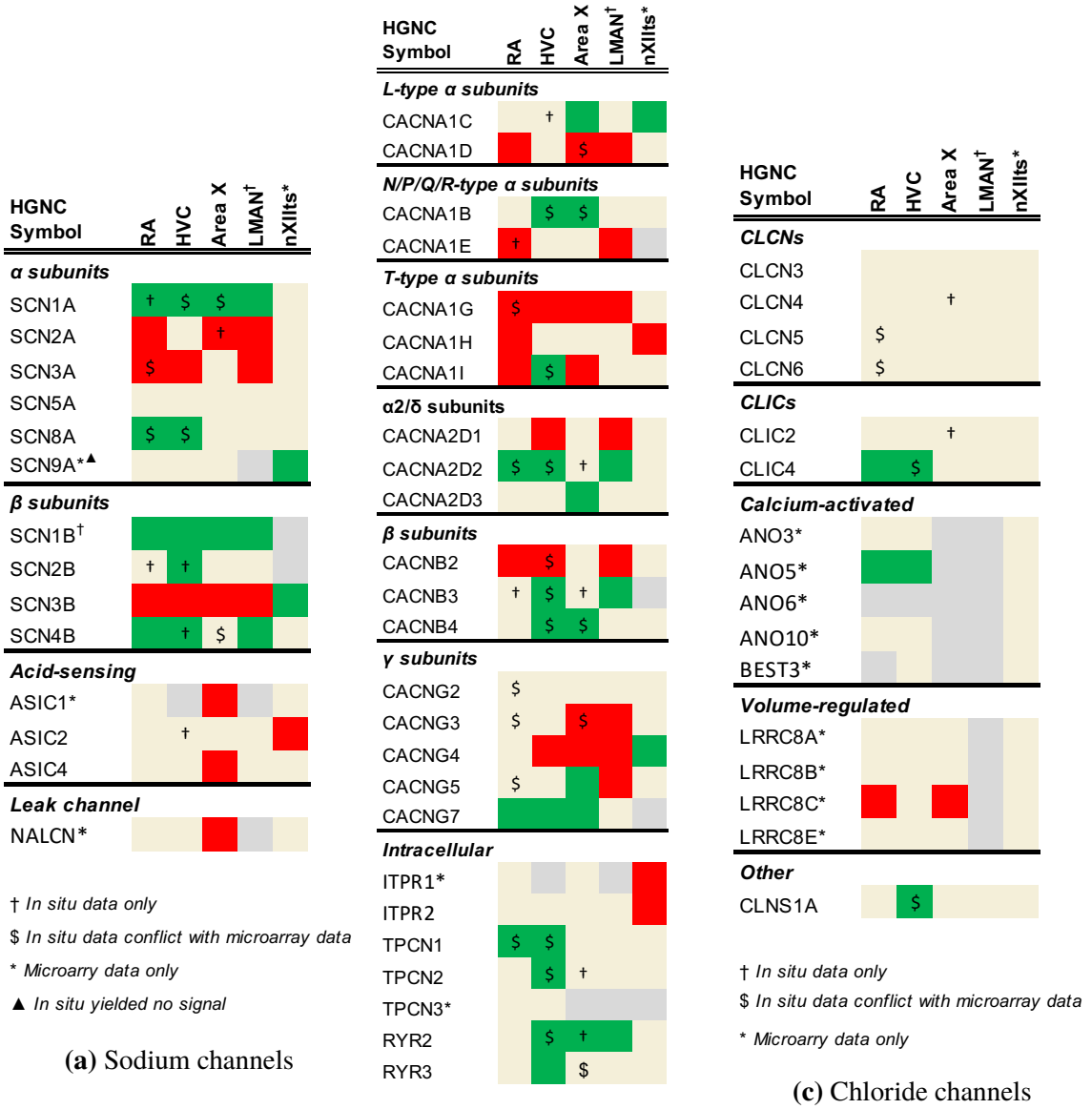

(a) Sodium channels

(b) Calcium channel

(c) Chloride channels

Figure 2.4: Regulation of (**a**) sodium, (**b**) calcium, and (**c**) chloride channel genes in adult male song nuclei. Color shading indicates a gene that is higher (green), lower (red), or non-differential (shaded tan) in each song nucleus examined compared to the surrounding areas. Genes not assessed in a given nucleus are in grey. Gene expression was assessed by microarray and/or *in situ* hybridization

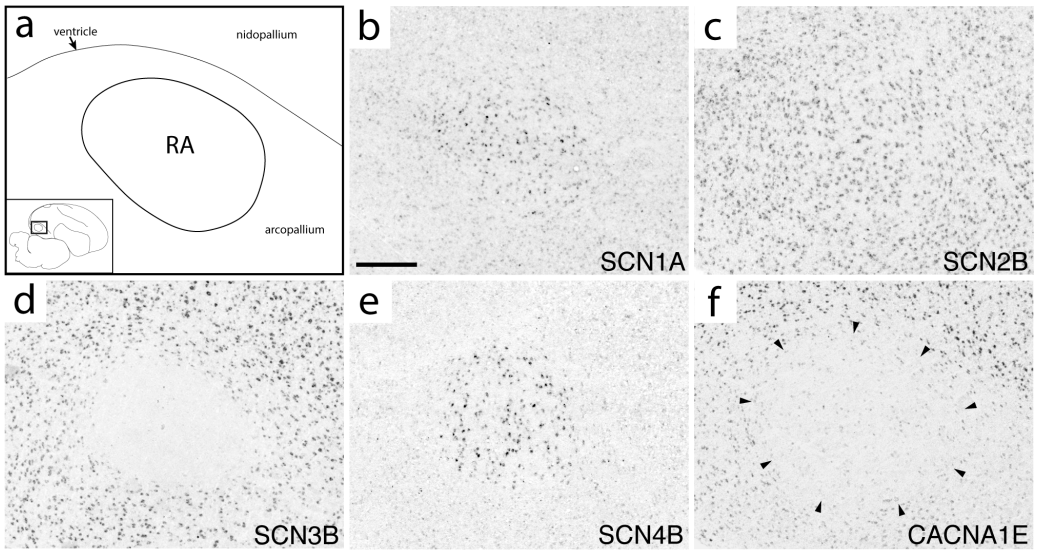

Figure 2.5: Expression of select ion channel genes in RA. (**a**) Camera lucida drawing depicting RA and surrounding arcopallium & nidopallium in the parasagittal plane (approximate location is indicated in inset; the dorsal arcopallial lamina is depicted by thin line.) (**b-f**) Representative *in situ* hybridization photomicrographs of select ion channel genes that show differential (**b, d-f**) and non-differential (**c**) expression in RA compared to the surrounding arcopallium. Gene abbreviations are given in Table 2.1. Scale bar: $500\,\mu\mathrm{m}$.

Sodium channels

The four alpha subunits with the highest brain expression in mammals (SCN1A/2A/3A/8A) showed varied patterns within the song system (Figure 2.4a). SCN1A was higher in RA (Figure 2.5b), HVC (Figure 2.6b), LMAN (Figure 2.7j), Area X, and DLM (Figure 2.8b). SCN2A was lower in RA (Supplementary Figure S2.5), Area X, LMAN, and DLM (Figure 2.8c), but non-differential in HVC (Figure 2.6c). SCN3A was lower in RA (Figure 2.5d), HVC (Supplementary Figure S2.5), and LMAN. SCN8A was higher in RA (Supplementary Figure S2.5) and HVC (Supplementary Figure S2.5). In contrast, SCN5A was non-differential in all nuclei, and SCN9A was non-differential except in nXIIts where it was higher and the only alpha subunit to show differential expression in this nucleus.

SCN1B showed higher expression in all telencephalic nuclei, including NIf, as well as

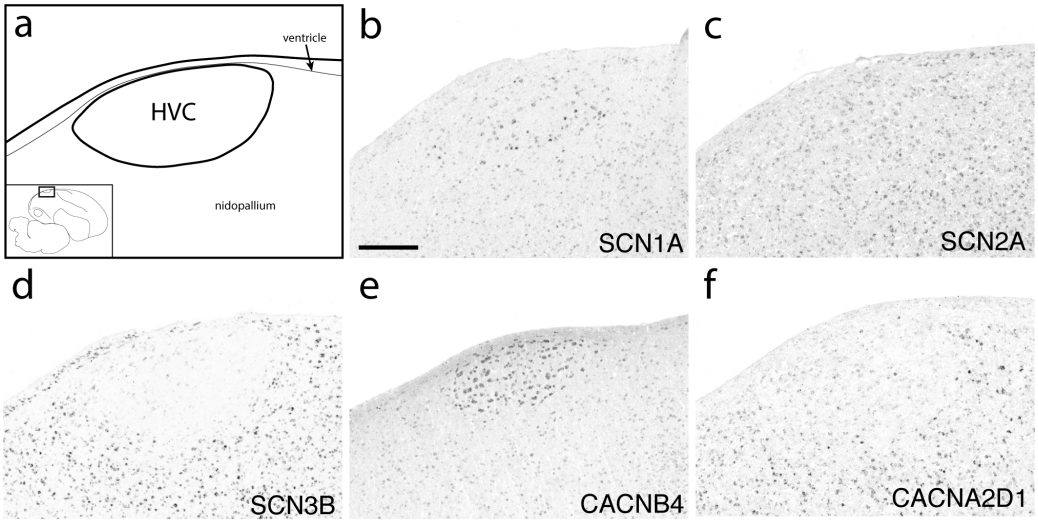

Figure 2.6: Expression of select ion channel genes in HVC. (**a**) Camera lucida drawing depicting HVC and surrounding nidopallium in the parasagittal plane (approximate location is indicated in inset.) (**b-f**) Representative *in situ* hybridization photomicrographs of select ion channel genes that show differential (**b, d-f**) and non-differential (**c**) expression in HVC compared to the adjacent nidopallium. Gene abbreviations are given in Table 2.1. Scale bar: $500\,\mu\mathrm{m}$.

in DLM (Figure 2.9). In contrast, SCN2B was non-differential across song nuclei (e.g. RA in Figure 2.5c) except for higher expression in HVC (Figure 2.6c). SCN3B was an exquisite negative marker of all telencephalic song nuclei (Figures 2.5d, 2.6d, 2.7b, and 2.8c), but higher in nXIIts. Interestingly, SCN3B was highly expressed in a sparse cell population in Area X (Supplementary Figure S2.5). SCN4B was higher in RA (Figure 2.5e), HVC, and LMAN (Figure 2.7k). Area X showed lower expression of ASIC1 and ASIC4, and ASIC2 was lower in nXIIts. NALCN, the only sodium channel that is a leak channel, showed lower expression in Area X.

Calcium channels

Among Cav1s, CACNA1C was higher in Area X and nXIIts, while CACNA1D was lower in RA, Area X, and LMAN. Among Cav2s, CACNA1E was lower in RA (Figure 2.5f)

and LMAN, while CACNA1B was higher in HVC and Area X (Figure 2.7c) where it was particularly strong in a sparse population of Area X cells (Supplementary Figure S2.5). Differential expression of Cav3's was biased toward lower expression, except for higher expression of CACNA1I (Cav3.3) in HVC (Supplementary Figure S2.5), the only calcium channel α subunit to exhibit opposing expression in two different song nuclei. All three Cav3 channels were lower in RA, the only nucleus to show differential expression in the same direction of every gene within a channel subfamily.

CACNA2D1 and CACNA2D2 were complementary in their differential expression; CACNA2D1 was lower in HVC (Figure 2.6f) and LMAN, and CACNA2D2 higher in HVC and LMAN (Figure 2.7d). In Area X, CACNA2D2 was non-differential but strongly expressed in a sparse cell population, with a similar pattern throughout the striatum (Figure 2.7d). CACNA2D2 was also higher in RA, and CACNA2D3 higher only in Area X. The only calcium channel β subunit to show lower expression was CACNB2, which was turned down in RA, HVC (Supplementary Figure S2.5), and LMAN (Figure 2.7l), but higher in DLM (Supplementary Figure S2.5). CACNB2 was also generally lower throughout much of the anterior striatum, but a sparse cell population showed enhanced expression (Supplementary Figure S2.5). CACNB3 was higher in HVC and LMAN and CACNB4 higher in HVC (Figure 2.6e) and Area X (Figure 2.7e).

Differential expression of γ subunits in the song system was predominantly in the AFP. CACNG5 was lower in LMAN (Figure 2.7g) and higher in Area X, and CACNG3 was lower in Area X and LMAN. CACNG5 also showed enhanced expression in a sparse cell population of Area X (Supplementary Figure S2.5), and in Uva (Figure 2.8d). CACNG4 was lower in HVC, LMAN and Area X (Figure 2.7f), but higher in nXIIts. All γ subunit

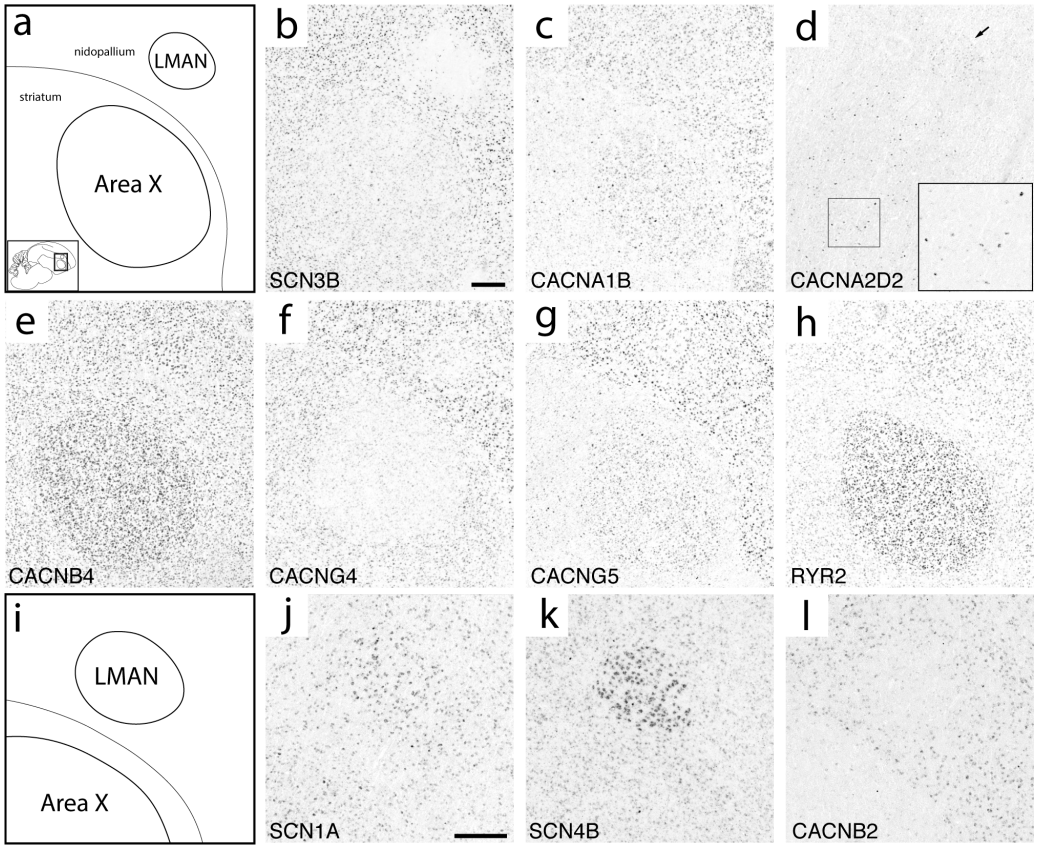

Figure 2.7: Expression of select ion channel genes in LMAN and Area X. (**a**) Camera lucida drawing depicting anterior portions of the nidopallium and medial striatum including song nuclei LMAN and Area X in the parasagittal plane (approximate location is indicated in inset; the pallial-subpallial lamina is depicted by thin line). (**b-h**) Representative *in situ* hybridization photomicrographs of select ion channel genes that show differential expression in Area X (all panels except d) and LMAN (**b, d, f-h**) compared to adjacent regions. Arrow in (**d**) indicates LMAN and inset shows enhanced labeling in a population of sparse cells from the indicated region of Area X. (**i**) Camera lucida drawing depicting LMAN and dorsal Area X at same level as in (**a**). (**j-l**) Representative *in situ* hybridization photomicrographs of select ion channel genes that show differential regulation in LMAN compared to the adjacent nidopallium. Note the sparse, darkly stained cells in Area X in panel (**j**). Gene abbreviations are given in Table 2.1. Scale bars for each panel series are $500\,\mu\mathrm{m}$.

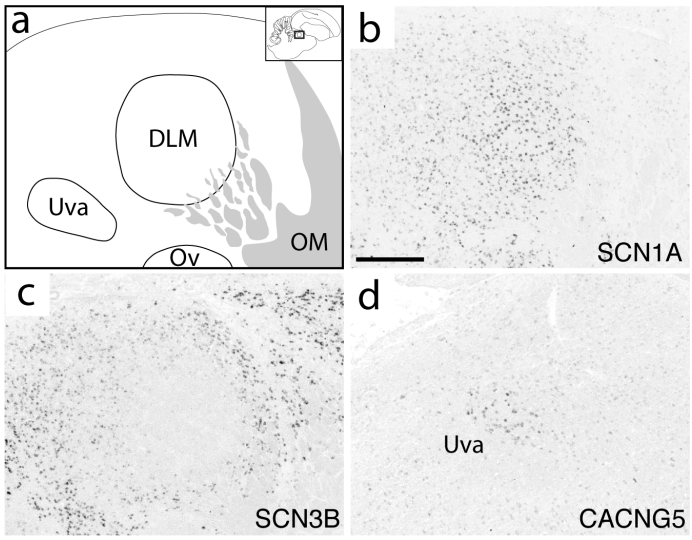

Figure 2.8: Expression of select ion channel genes in DLM and Uva. (**a**) Camera lucida drawing depicting DLM, Uva, and surrounding thalamic areas in the sagittal plane (approximate location is indicated in inset.) (**b-d**) Representative *in situ* hybridization photomicrographs of select ion channel genes that show differential regulation in DLM (**b, c**) or Uva (**d**). Gene abbreviations are given in Table 2.1. Scale bar: $500\,\mu\mathrm{m}$.

genes examined were non-differential in RA (e.g. Supplementary Figure S2.5), except for CACNG7, which was higher in RA as well as in HVC and Area X. Differential expression for TPCN and RYR genes was always higher, including RYR2 in HVC (Supplementary Figure S2.5), Area X and LMAN (Figure 2.7h), and RYR3, TPCN -1 and -2 in HVC. Only nXIIts showed differential expression of ITPRs, which were lower.

Chloride channels

The majority of identified chloride channels lacked zebra finch ESTs. Among assessed genes, most were non-differential, except for three genes with higher expression - ANO5, CLIC4, and CLNS1A - which were all higher in HVC, with ANO5 and CLIC4 also higher in RA, and one gene with lower expression, LRRC8, in RA and Area X. Thus, differential expression of chloride channel genes was biased toward nuclei of the DMP and higher

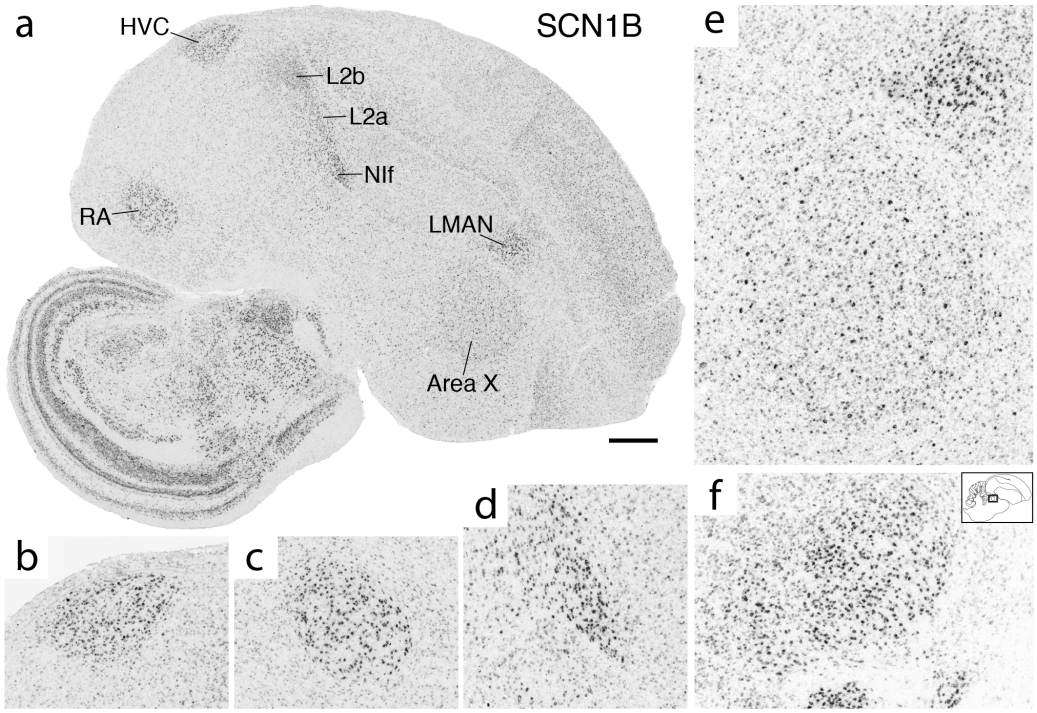

Figure 2.9: SCN1B is strongly upregulated in multiple song system nuclei. (**a**) *In situ* hybridization photomicrograph of a whole parasagittal section. Individual song nuclei in (**a**) are shown in detail in (**b**) HVC, (**c**) RA, (**d**) NIf, and (**e**) Area X and LMAN. SCN1B is also noticeably upregulated in Field L2a and L2b as shown in (**a**). (**f**) SCN1B upregulation in DLM (approximate location shown in inset and comparable to Figure 2.8). Scale bar in (**a**): $1\,\mathrm{mm}$.

expression.

2.4 Discussion

In spite of the wealth of information on song system connectivity and neurophysiology, an understanding of the molecular basis for the intrinsic electrophysiological properties of its constituent neurons is lacking. Here we report on the genomics and song system expression of sodium, calcium, and chloride ion channel genes in the zebra finch, including pore-forming and modulatory subunits. This effort annotated 34 “novel gene” Ensembl models, detected additional sequences for several partial gene models in taeGut1, and established

what we believe is the full complement of these gene families in zebra finch and chicken, with no novel paralogs detected. PacBio assemblies were particularly helpful to: (1) identify previously undetected genes; (2) confirm with high confidence gene truncation; (3) define orthology based on synteny; (4) suggest a likely phylogenetic path to previously reported avian gene losses or truncations [183, 184]. A large number of zebra finch gene models are partial relative to human and chicken models, but we detected additional sequences in taeGut1 that could expand those models. Incomplete gene predictions (indicated by "*" in Table 2.1) cast doubt on "off-the-shelf" dN/dS values from automated algorithms. Thus, conclusions regarding positive selection or rapid gene evolution in these families (e.g. [39, 208, 209]) should be treated as provisional until more complete gene models are available.

Each song nucleus examined differentially expresses a unique complement of ion channels, suggesting that diverse expression of these genes is fundamental to shaping excitability within the song system. With few exceptions, differential expression of individual genes was in the same direction across nuclei. Area X and HVC showed enhanced expression of more calcium channel genes than other song nuclei, suggesting a more prominent role of calcium currents in governing electrophysiological properties of the AFP. In contrast, chloride channel genes were mostly non-differential. Compared to other nuclei, nXIIts differentially expressed the fewest number of genes. We note that most genes that lacked brain expression evidence in zebra finch (e.g. SCN4A, CACNG1, and CLCN1) are primarily expressed in non-neural tissues (e.g. skeletal muscle) in other organisms [165, 167].

Some genes were strongly expressed in sparse cells and might contribute to defining the unique neuronal populations reported in Area X [149, 210, 211], HVC [145, 146], and RA [148]. We acknowledge, however, that several of these genes participate in processes other

than excitability (e.g. cell signaling and metabolism), and expression in specific cell types or non-neuronal cells (e.g. glia) was not assessed. Furthermore, protein-based assays and coexpression analysis are needed to determine the subcellular localization of the channels and their possible interactions. We did not evaluate splice variants, but note that in mammals, genes like T-type calcium channels give rise to variants with distinct gating properties and spatiotemporal regulation [212]. We also note that while differential expression provides clues as to regulatory mechanisms, non-differentially expressed ion channels may still contribute to excitability. Below we discuss the main implications of the brain expression findings with regards to gene families.

Sodium channels

Based on its known role in in mammals, the higher expression of SCN1A (Nav1.1) in all major song nuclei suggests an essential function of somatodendritic signal integration and action potential (AP) thresholding in the song system [213]. SCN1A also confers fast spiking in a diversity of GABAergic interneurons [214–216]. Because in most nuclei SCN1A was enhanced in small, sparse cells reminiscent of interneurons, the enhanced expression of SCN1A may contribute to the fast-spiking behavior of interneurons that has been described in multiple song nuclei [144, 145, 148, 149, 210]. In mammals, SCN8A (Nav1.6) facilitates AP initiation and propagation [213, 217–219]. Its higher expression in RA and HVC could thus reinforce rapid and reliable axonal propagation in the DMP. SCN3A (Nav1.3) brain expression is high early in mammalian development but is progressively replaced by SCN1A, SCN2A, and SCN8A [220–222]. In adult zebra finch, SCN3A is widely expressed through-

out the brain but lower in RA, HVC and LMAN - a species discrepancy that highlights the diversity in sodium channel expression across phylogenies. β subunits alter cell surface expression, gating properties, and voltage sensitivities of α subunits [182], and high levels of β subunits are likely necessary to shuttle and modulate a high volume of voltage-gated sodium channels. Thus, it is not surprising that some α and β subunits were highly expressed within the same song nuclei. In mammals, SCN1B increases the surface expression and current densities of α subunits [182, 223, 224]. It also supports resurgent sodium currents that enable high-frequency firing ([225], and reinforces AP initiation by targeting SCN8A to the axon initial segment [219]. Additionally, SCN1B can modulate voltage-gated potassium (Kv) family channels [226–228], several of which are higher in multiple song nuclei, including Kv1.1, Kv4.2, and Kv4.3 [160]. Collectively these features suggest that SCN1B may be an important regulator of neuronal excitability in song nuclei by supporting fast, reliable spiking. HVC was the only nucleus to show higher expression of both SCN1B and SCN2B, consistent with the higher expression of α subunits in HVC, and the observation that the sodium current-boosting effects of SCN2B require SCN1B coexpression [182, 223]. SCN4B induces resurgent sodium current, an important adaptation for neurons that exhibit high-frequency firing [218, 229–233]. Its high expression suggests that resurgent currents might support the high-frequency and bursty firing characteristic of neurons in RA [234, 235], HVC [236, 237], and LMAN [238]. SCN4B also supports persistent sodium currents [231], which might account for the non-inactivating sodium conductances of HVC neurons [150]. While the effects of SCN3B on excitability are inconsistent [239–244], its high brain expression in adult zebra finches contrasts with rodents, where expression is high during development and lower in adulthood [245]. Much like SCN3A, this stark divergence ex-

emplifies how gene expression patterns can differ in birds versus mammals. As for ASICs, little is known about the role of acid signaling in neurotransmission, although there is evidence of their role in dendritic spine remodeling [185]. Lastly, leak currents carried by NALCN play roles in rhythmic and spontaneous firing [186, 246], thus NALCN differential expression might contribute to the heterogeneity in spontaneous firing rates across Area X cell types [149].

Calcium channels

Calcium channels influence input processing in dendrites and signal transmission in synaptic terminals, which links them to plasticity mechanisms that serve learning and memory [189]. Voltage-gated calcium channels (Cav's) are vital to dendritic processing, burst firing, and neurotransmitter release. Among pore-forming alpha subunits, L-type (Cav1) channels conduct large, long-lasting currents in response to strong depolarization [247]. The higher expression of the L-type channel CACNA1C suggests that integration of synaptic input is important in Area X and nXIIts. CACNA1C can also associate with BK channel KCa1.1 (KCNMA1) to modulate repolarization and spiking frequency [248, 249]. While not differential, KCNMA1 is expressed in Area X [160] and may interact with CACNA1C to shape repolarization and repetitive firing. Compared to CACNA1C, CACNA1D activates at lower membrane potentials and is slower to inactivate [250]. Thus, its lower expression may refine the timing and restrict the duration of depolarization-induced calcium influx in song nuclei. T-type (Cav3) channels create low-threshold calcium potentials that are integral to driving rebound and burst firing in neurons [212, 247, 251]. The lower expression of

all T-type channels in RA is intriguing given that low expression of T-type channels is associated with single or tonic AP firing [212], yet RA neurons exhibit bursty, high-frequency firing [234, 235, 252]. This suggests that high-frequency firing in RA might instead be driven by voltage-gated sodium channel beta subunits (SCN1B, SCN4B) and/or potassium channel subunits like Kv3.1 [155, 253], which show high expression in RA [160], or by hyperpolarization-activated (HCN; Ih) channels as suggested by electrophysiology studies of HVC [150]. HVC was the only nucleus to highly express a T-type channel (CACNA1I / Cav3.3), providing a candidate for the low-threshold calcium conductances recorded in HVC's Area X-projecting neurons and interneurons [150, 254]. Relative to other T-type channels, CACNA1I channels are the most resistant to attenuation during high-frequency firing, exhibit current amplitude facilitation, and have more positive thresholds of activation and inactivation [212, 255, 256]. These properties might help to regulate excitability in HVC, which shows temporally-precise bursting during production of mature song [236]. CACNA1I is also an attractive candidate for development studies given that T-type calcium channels may underlie changes in intrinsic electrophysiological properties of HVC neurons during song learning [159]. CACNA1B, an N-type calcium channel, has a large single-channel conductance and is closely associated with the calcium-sensitive presynaptic vesicle release machinery [257–260]. The distinctive higher expression of CACNA1B in HVC and Area X suggests that these song nuclei are specialized for rapid and efficient neurotransmission. CACNA1E, an R-type calcium channel, functions in both dendritic calcium signaling and neurotransmitter release [162, 261]. In mammalian hippocampal neurons, these channels activate potassium channels within dendritic spines to limit depolarization in response to excitatory post-synaptic potentials [262, 263]. Additionally, CACNA1E-/- mice

are more resistant to seizure [264], possibly due to dampened excitability [265]. Depending on CACNA1E subcellular localization, lower expression in RA may translate to larger calcium transients in dendritic spines and/or reduce the potential for run-away excitability. The modulatory $\alpha 2\delta$ (CACNA2D) and β (CACNB) subunits increase calcium currents as well as vesicle release probability [189, 190, 266–268]. Their widespread high expression, particularly in the AFP, might thus relate to more efficient neurotransmission. The nearly identical expression patterns of $\alpha 2\delta$ and β in HVC and LMAN contrast with the divergent patterns of $\alpha 1$ subunits in these nuclei, suggesting that differences in calcium conductance might arise from unique combinations of $\alpha 1$ subunits rather than different auxiliary subunits. In turn, the higher expression of both modulatory $\alpha 2\delta$ subunits and pore-forming $\alpha 1$ subunits in Area X and HVC suggests that high levels of both these subunits are required. Finally, evidence that CACNA2D3 participates in neurexin-mediated retrograde signaling [269] suggests Area X might utilize a $\alpha 2\delta$-dependent, inhibitory synaptic feedback mechanism that is unique among song nuclei. Most γ (CACNG) subunits are transmembrane AMPA receptor (AMPAR) regulatory proteins, or TARPs, which modulate gating and synaptic targeting of AMPARs [270, 271]. A sparse population of Area X cells that resemble the large DLM-projecting neurons in Area X [147] showed enhanced expression of CACNG5, a TARP unique in its ability to increase AMPAR desensitization and deactivation rates [271]. Intriguingly, a population of sparse, large cells in Area X also expresses GluR4, the AMPAR subunit with the fastest kinetics [272], further suggesting that temporally precise signaling through AMPARs is particularly important for Area X projection neurons. In contrast, CACNG4 and CACNG8 are the most effective TARPs in slowing the desensitization, deactivation, and mEPSC decay rates of AMPARs [273]. The lower expression of CACNG4 in

HVC, Area X, and LMAN and lack of a functional CACNG8 gene suggest that these nuclei rely on alternate mechanisms to elicit slow AMPA kinetics, such as differential splicing of AMPA subunits into their "flip" or "flop" forms [272]. CACNG7 selectively shuttles to the plasma membrane and boosts currents of calcium-permeable AMPARs while inhibiting membrane expression of calcium-impermeable ones [274, 275]. Thus, biasing AMPAR pools toward calcium permeability and enhancing calcium flow through AMPARs might be a shared specialization in RA, HVC, and Area X. In addition, CACNG7 can dampen CACNA1B (Cav2.2) expression in heterologous expression systems, but not in sympathetic neurons [276]. Accordingly, CACNA1B was not lower in any nuclei that showed higher CACNG7 expression. Finally, the non-TARP CACNG1 and CACNG6 decrease calcium currents by interacting with voltage-gated calcium channels. Birds lack CACNG6, but CACNG1 could potentially compensate for this gene loss. The high expression of multiple intracellular calcium channels suggests that mobilization of internal calcium stores is important for HVC. While the role of TPCNs in neural processing is unknown, inositol 1,2,5-trisphosphate (IP3) receptors (ITPRs) and ryanodine receptors (RYRs) are implicated in plasticity, learning, and memory [277]. The higher expression of RYR2 and CACNA1C in Area X is also intriguing, given that RYR2 interacts with CACNA1C in muscle cells to coordinate excitation-contraction coupling [278]. Area X cells might thus funnel calcium ions through plasma membrane-bound CACNA1C to ER-bound RYR channels as a way to amplify calcium signaling. Lastly, ITPRs and RYRs do not overlap in location or direction of expression, suggesting the recruitment of distinct intracellular calcium stores and signaling pathways across song nuclei [279].

Chloride channels

Of the gene families studied here, chloride channels are the least characterized and had a low incidence of differential expression. Considering their role in stabilizing the resting potential [163, 280], the higher expression of chloride channels in HVC and RA might help the membrane potential to reset despite large voltage fluctuations. Passeriformes appear to lack CLCA genes. In mammals, these calcium-activated proteases are expressed predominantly in intestine and airway epithelium, and a only few are expressed in brain [202]. The absence of CLCAs suggests that songbirds rely on other mechanisms to regulate chloride transport in respiratory, digestive, and excretory tissues. Some CLCAs are expressed in olfactory sensory neurons (OSNs) in mammals, where they modulate chloride currents involved in olfactory signaling [281, 282]. Contrary to previous notions, birds use olfactory cues [283–285] and have large repertoires of olfactory receptor genes [39, 286–288], but downstream signal transduction mechanisms are unknown. In mammals, 90% of the transduction current in OSNs is carried by the calcium-sensitive chloride channel ANO2 (TMEM16B) [289–291]. Because ANO2 is present in zebra finch and other avian species, birds appear to have the necessary machinery for olfactory transduction. Moreover, BEST2 - once the strongest candidate for transduction in OSNs [292] - is missing from zebra finch, consistent with the conclusion that BEST2 is not required for olfaction [293]. In sum, while the main carrier of olfactory transduction current (ANO2) may be conserved between mammals and birds, the lack of CLCAs suggests that regulation of this current may be markedly different in Passeriformes.

Conclusions

We report here on the genomic identity and song system expression of three major ion channel families. The majority of these genes are conserved between birds and mammals, and the expression data paint a picture of abundant differential patterns, especially for sodium and calcium channel genes, in circuitry that supports the acquisition and production of learned vocalizations. We note that while changes in synaptic and intrinsic properties during the song learning period have been reported [144, 159, 234, 235], further studies of developmental regulation of ion channel genes in song nuclei are needed [294, 295]. Finally, this investigation establishes a foundation and framework for future studies to test the contribution of specific ion channel genes to distinct excitability properties of vocal nuclei in songbirds.

Declarations

Acknowledgements: We wish to thank Henrique Von Gersdorff and Benjamin Zemel for proofreading the manuscript and providing feedback. We also wish to thank Alexa Buckner for preparing and uploading high-resolution scans of *in situ* data to ZEBrA, and Alison Thomas for her help with gene model evaluation. Finally, we would like to thank Wes Warren and Erich Jarvis for providing us the chicken and zebra finch PacBio genomes before they became available on NCBI.

Funding: This research was supported by the National Institutes of Health (R24_GM120464 and R21_DC014432) and by the National Science Foundation (NSF-143602 and Graduate Research Fellowship DGE-1448072). These funding bodies played no role in the design

of the study, collection, analysis, or interpretation of data, nor in writing or editing the manuscript.

Availability of data and materials: The datasets supporting the conclusions of this article are included within the article and Additional files 1-7. A GitHub repository for the sequence recovery analysis is available from https://github.com/samifriedrich/seq-recovery. Complete microarray datasets are available from [176] and details regarding curation methods can be found in [177]. High-resolution images of most of the *in situ* data presented here are publicly available on ZEBrA .

Author contributions: SRF, CVM, PVL: Conceptual and experimental design of the study. TMK, SRF: riboprobe selection and preparation, *in situ* hybridizations, and gene expression analysis. SRF: genomics and alignments, synteny analysis, model improvement, dN/dS and data analysis, figure preparation, and manuscript drafting and editing. SRF, PVL, CVM, TMK: discussion and interpretation of the data, and manuscript editing.

Ethics approval and consent to participate: All procedures involving animals conformed to NIH guidelines for the use and care of animals in research and were approved by OHSU's Institutional Animal Care Use Committee (IACUC).

Chapter 3

Emergence of sex-specific transcriptomes in a sexually dimorphic brain nucleus

At the time of this dissertation's completion, the following chapter was being edited and prepared as a manuscript to submit for publication. Expression data, analysis code, and up-to-date publication info can be found at `https://github.com/samifriedrich/zebrafinchRA`.

3.1 Introduction

The study of sex differences in the brain is a critical area of research for its broad impacts, ethical implications, and exploratory power. A vast number of sex differences in the brain have been reported that range in biological scale, but relatively few gross neuroanatomical sex differences have been documented thus far. One of the most drastic neuroanatomical

sex differences in vertebrates is that of song control regions in songbird brains, which grow several times larger in males than females [48]. A vast body of research has demonstrated the pivotal role sex steroids hormones play in sexual differentiation of neural tissue, including the songbird brain [296, 297]. However, the genetic and molecular dynamics that establish sex differences in the developing brain have only recently come under investigation.

Songbirds provide fertile ground to address questions of sex differences in the brain, as they exhibit marked sexual dimorphism in both singing behavior and underlying brain circuitry. Song is an example of vocal learning, the ability to learn sounds through imitation, which is a rare trait observed in a small number of mammals (humans, cetaceans, pinnipeds, and possibly elephants and bats,) and three groups of birds (songbirds, parrots, and hummingbirds) [16]. The degree of sexual dimorphism in singing behavior varies widely across songbird species, with vocal duetting between sexes at one end of the spectrum, and complete absence of song in one sex at the other [298]. Zebra finches (*Taeniopygia guttata*) are a songbird species in which this behavioral dimorphism is binary. Both males and females produce various types of calls, but only males produce complex song [21]. This pronounced sex difference is accompanied by conspicuous sexual dimorphism in the neural circuitry that drives song [48]. The song system is a network of pallial, basal ganglia, and thalamic components (Figure 1.1), comprising two interconnected circuits; the direct vocal-motor pathway, necessary for song production [28, 29], and the anterior pathway, necessary for song learning and adult song plasticity [14, 30–32]. When the song nuclei of males and females were first characterized [48], neuroscience had rarely seen a more striking sex difference in gross neuroanatomy. Among these dimorphic song nuclei is the robust nucleus of the arcopallium (RA), which is over five times larger adult males compared to females

[53]. RA is the main output nucleus of the telencephalic song system, and lesions of RA severely disrupt song [28]. In RA, signals from the anterior pathway converge with those of the direct vocal-motor pathway, and outputs are sent to brainstem regions that innervate the avian vocal organ (syrinx) and coordinate respiration [35]. In terms of behavioral function, RA neurons are active during song production and are thought to encode the acoustic properties of song syllables [236, 252, 299].

RA undergoes major sex-specific morphological changes during the critical period for song learning (Figures 3.1 and 3.2). In contrast to the striking sex dimorphism seen in adulthood, RA appears monomorphic in young zebra finches (Figure 3.1, left). Over the first three weeks post-hatch, RA grows equally in volume in both sexes [53]. Around 20 DPH, before males have begun producing their first song-like vocalizations, RA's growth trajectory begins to diverge; male RA begins increasing in volume, and female RA begins decreasing in volume. By 50 DPH, about the time when males begin singing rudimentary song, male and female RA are extremely dimorphic (Figure 3.1, right), approximating adult RA volumes.

Over this 20-50 DPH window of development, there are sex-specific shifts in RA's cytoarchitecture that drive the observed volumetric growth in males, and regression in females (Figure 3.2). In males, the expanding volume of RA is driven by increases in cell size and decreases in cell density [54]. In females, the shrinking volume of RA is driven by the loss of neurons [60]. Due to these cellular changes, by 50 DPH, male RA is characterized by more numerous, large, widely spaced cells, and female RA is characterized by fewer, small, tightly packed cells (Figure 3.1, right). In tandem with morphological sex dimorphism, RA develops sex differences in innervation from afferents [52, 60, 300–302], cell viability

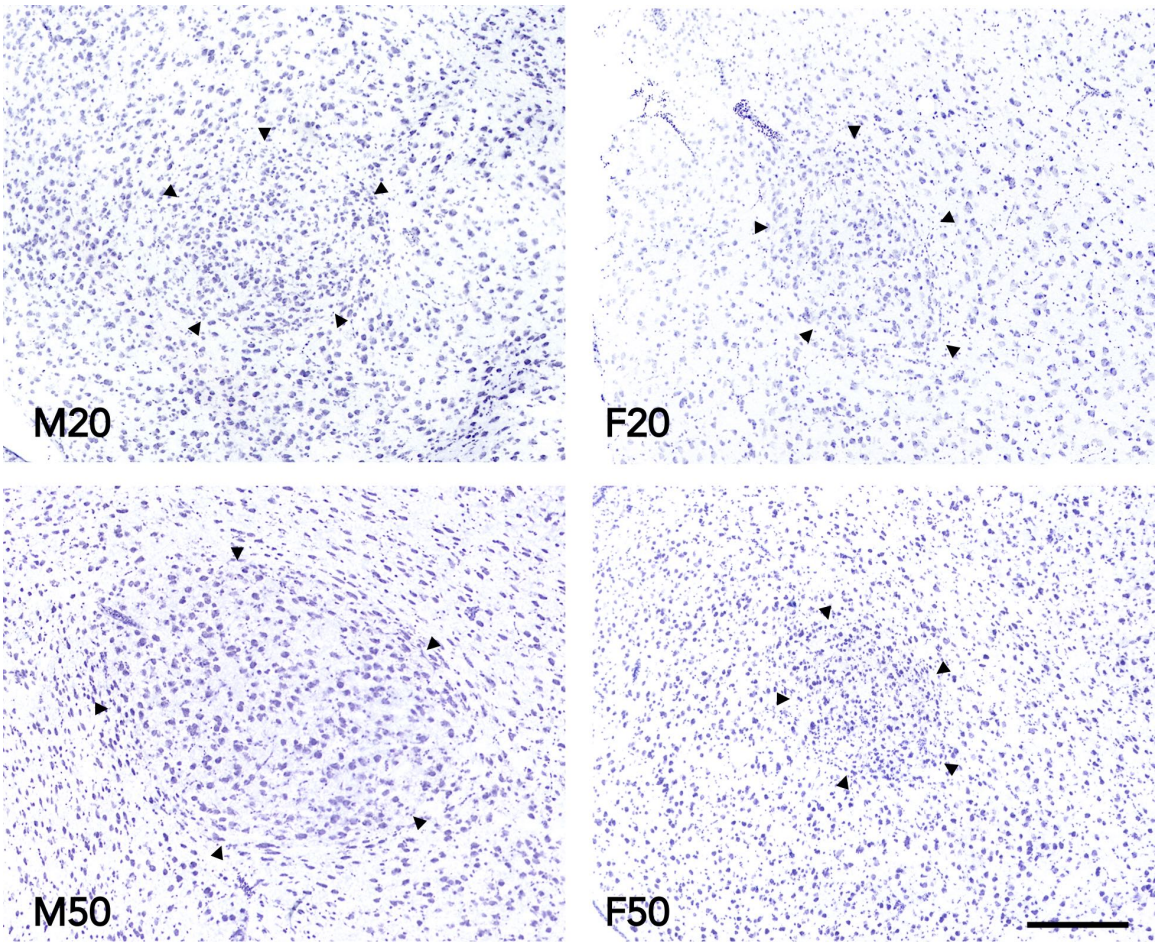

Figure 3.1: The morphological divergence of RA in developing males and females. Nissl stains of sagittal $10\,\mu\mathrm{m}$ brain sections showing RA (indicated by arrowheads) and surrounding arcopallium. At 20 DPH, male and female RA have comparable volume, cell density, and cell size. At 50 DPH, male RA is larger in volume, and is characterized by larger cells that are more spread out than female RA. Scale bar = $250\,\mu\mathrm{m}$

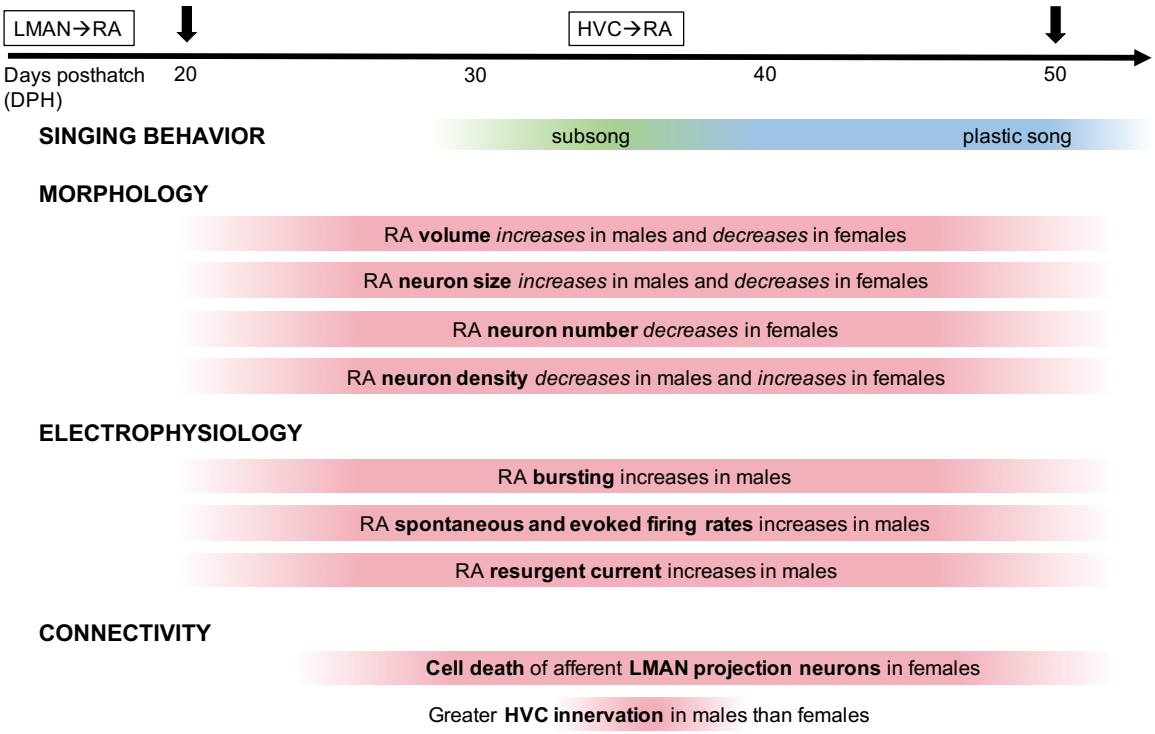

Figure 3.2: Developmental timeline of sex differences in RA. Text boxes (top) denote approximate timing of afferent innervation from RA's main afferents; the lateral magnocellular nucleus of the anterior neostriatum (LMAN), and nucleus HVC (proper name). Arrows denote ages appearing in Figure 3.1, and ages used to generate RNA-seq data for this study. Information summarized from [50, 52–54, 56, 59, 60, 234, 235, 300–303]

[56], and excitability properties [234, 235, 303] (summarized in Figure 3.2). Additionally, developmental sex differences in RA expression levels have been characterized for several genes [303–307]. It is also during this developmental window that males begin practicing their songs, initially producing highly variable vocalizations called subsong as early as ∼30 DPH, and progressing to plastic song characterized by discernible syllables by ∼50 DPH [308].

Considering the multifaceted and rapid nature of sex differentiation in RA (Figure 3.2), we reasoned that many genes spanning a wide array of functional networks must be recruited to orchestrate sex-specific developmental programs. We also hypothesized that the transcriptional profile of RA would mirror that of its sexually dimorphic growth trajectory,

with males and females showing more similar transcriptomes at early ages. To test these ideas, we characterized developmental changes and sex differences in the transcriptomic landscape of RA. We used laser capture microdissection and bulk RNA-sequencing to assay the male and female transcriptomes of RA at the outset (20 DPH) and tail end (50 DPH) of its divergent growth trajectory. The results show that male and female RA start out with similar transcriptomes, where sex differences in gene expression are mostly due to sex-linked genes, and then undergo two massively gene-rich and functionally distinct sex-linked developmental programs.

3.2 Methods

3.2.1 Animals and tissue preparation

All procedures involving live birds were approved by the OHSU Institutional Animal Care and Use Committee, and are in accordance with NIH guidelines. Zebra finches were obtained from our colony or purchased from a commercial supplier. All birds were kept under a 12:12 light/dark cycle and supplied daily with seed, millet spray, water, egg food, cuttle bone, soluble grit, and kale ad libitum. Juveniles were raised by both parents in single family breeding cages, where they remained until the target age (20 or 50 DPH) was reached. Captive zebra finch clutches often hatch over a period of several days, so to minimize age variability within groups, we devised a method to track the exact age of each juvenile. We used nontoxic food coloring to dye down feather patches in distinctive patterns (e.g. red head, green flanks) on hatch day, then transitioned to leg banding around 10 DPH. To min-

Sex	Age Group (DPH)	Exact Age (DPH)	n
Female	20	20±0	5
Male	20	20±0	5
Female	50	47-50	7
Male	50	46-50	5

Table 3.1: RA sample groups for RNA-seq. Additional samples were included in the 50 DPH female group as insurance against the possibility of cDNA library failure, however all samples succeeded and thus were included in the study.

imize relatedness as a confound, juveniles from 11 different breeding pairs were assigned pseudorandomly to groups, such that main contrasts (Table 3.2) did not compare siblings. To minimize the confounds of circadian rhythms and behavioral state (including song-induced gene expression), all juveniles were sacrificed by decapitation within 20 minutes of lights-on, and no singing was observed for any juvenile in this window. Sex was determined around 10 DPH using the highly reliable and economical PCR sexing protocol described in [309], and confirmed postmortem by gonad inspection. Brains were rapidly dissected into hemispheres, blocked in TissueTek OCT (Sakura Finetek USA, Inc.; Torrance, CA), and flash frozen by placing brains into a slurry of pulverized dry ice and isopropanol. Once frozen, brains were transferred to -80 °C freezer for storage until cryosectioning.

3.2.2 Laser capture microdissection

Several methodological precautions were taken to limit the RNA degradation by ribonucleases (RNases), including the use of RNase-free materials, cleaning equipment and work areas with RNase Away (Molecular BioProducts), and frequently changing gloves and staining solutions. Fresh frozen brains were cryosectioned on a Leica CM1850 cryostat at $12\,\mu\mathrm{m}$ thickness. As sectioning advanced through the brain, Nissl staining of tissue mounted on

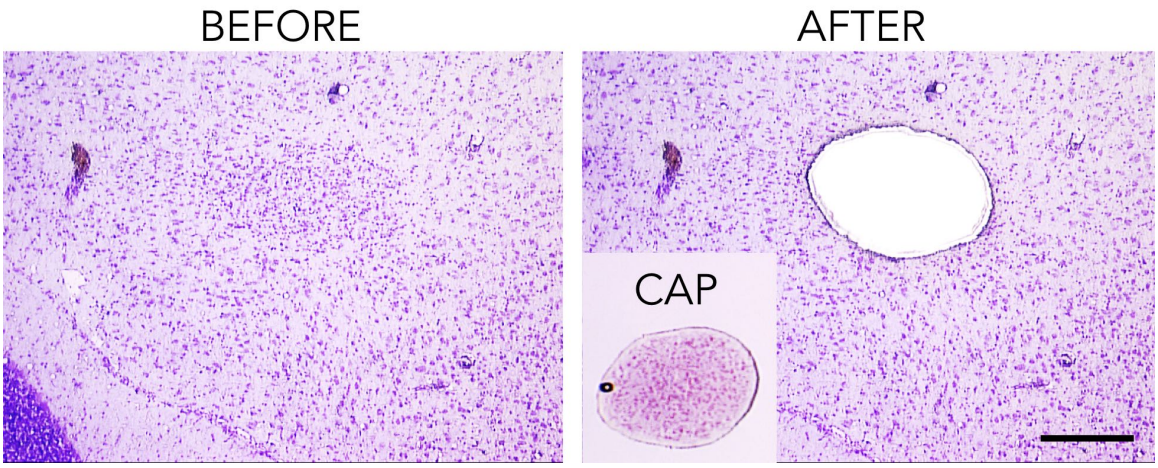

Figure 3.3: Laser capture microdissection of RA. Images were taken using the Leica LMD 6500 and show a sagittal 12 µm section from a 50 DPH female. Tissue is shown before (left) and after (right) laser capture microdissection was performed. Inset shows RA microdissectant in the collection tube cap. Scale bar = 250 µm

regular glass slides was used to assess brain anatomy until the medial edge of RA was visible. PEN membrane glass slides (Leica, No. 11505158) were labeled then UV treated for 15 min on a TFX-20M transilluminator (Life Technologies). Brain sections containing RA were mounted onto UV-treated PEN slides, with the exception of every 12th or 16th section, which was mounted on a frosted glass slide and Nissl stained to assess the level of RA. To avoid freeze-thaw cycles between the successive mounting of multiple sections onto each slide, four sections at a time were cut and arranged on the cryostage using RNase-free paintbrushes, then mounted simultaneously onto a room temperature PEN slide. As soon as sections had fully adhered, slides were transferred to 50 ml Falcon tubes of chilled 100% ethanol stored within the cryostat. Slides remained in chilled 100% ethanol until staining. Sectioning continued as described until the extent of RA was collected. Slides were then stained at room temperature, one at a time, using a series of ethanolic solutions prepared from RNase-free ethanol, cresyl violet acetate, and NanoPure water in 50 ml Falcon tubes.

Ethanolic solutions were used to minimize hydration-activated RNase activity during staining. Slides were immersed for 30 sec in each the following: 100% ethanol, 95% ethanol, 75% ethanol, 4% cresyl violet in 75% ethanol, 75% ethanol, 95% ethanol, 100% ethanol, and again in 100% ethanol. Xylenes were omitted from our staining protocol because we found that 100% ethanol was sufficient to fully dehydrate the tissue. Ethanol series solutions were changed out every 4-6 slides, and the cresyl violet staining solution was pipetted onto each slide to avoid contaminating the stock. Laser capture was performed immediately after staining. To minimize RNA degradation, staining and laser capture were performed in batches of 2-4 slides so that RA tissue was microdissected and immersed in RNA-stabilizing solution within 1 hour after staining.

Laser capture microdissection was performed on a Leica LMD 6500. The surrounding work area and equipment were wiped down with RNase Away before beginning laser capture each day. Tissue was collected into 0.5 ml tube caps containing 40-70 μm RLT Buffer (Qiagen) and 2-mercaptoethanol. The laser path around RA was conservatively drawn around the core of RA, and we confirmed successful capture by inspecting collection tube caps (Figure 3.3). Once laser capture for 2-4 slides was complete, collection tubes were carefully closed and removed from the collection device, vortexed for 30 sec, then immediately placed on dry ice. This procedure was repeated in batches of 2-4 slides until the whole of RA was captured, then collection tubes were transferred to a -80 $^{\circ}$C freezer until RNA isolation.

3.2.3 RNA isolation and RNA-seq

Sample tubes were thawed in a gloved hand until no particulate was visible in the solution, then vortexed for 30 sec. RNA was isolated using the RNeasy Micro Kit (Qiagen) with on-column DNase digestion. RNA isolation was performed in randomized batches of 4-5 samples and according to kit instructions with two exceptions: 1) an additional 80% ethanol wash was performed immediately after the first, and 2) the RNase-free water used to elute the RNA was incubated on the column for 10 min prior to centrifuging to increase RNA yield. Isolated RNA samples were stored at -80 °C until submission to the OHSU Massively Parallel Sequencing Shared Resource for RNA quality assessment, cDNA synthesis, library preparation, and sequencing. Sample size per group was no less than n=5 (see Table 3.1). Because total tissue and RNA yields were lowest for the 50 DPH female group, we prepared additional (n=7) samples in case library preparation failed for one or two samples. Fortunately, all 50 DPH female samples passed quality assessments and library preparation, thus all were sequenced and included in our analysis. RNA quality was assessed on a Bioanalyzer 2100 using the high sensitivity RNA 6000 pico assay (Agilent). The median RIN for all samples was 8.6, and all but one sample (1204R, RIN=6) had a RIN exceeding 7. cDNA libraries were generated using the SmartSeq v4 PLUS kit (Takara Bio USA). Paired end sequencing (2 x 100 bp) was performed on the NovaSeq 6000 S4 flow cell (Illumina) to a target depth of 50M reads per sample.

Quality control and trimming was performed prior to genome alignment using trimmomatic (v0.36), and no issues were detected from FastQC (v0.11.9) reports. Splice-aware STAR (v2.6.1) was used to align reads and generate read counts per gene based on the

bTaeGut1_v1.p zebra finch assembly (GCF_003957565.1) and associated genome features from the NCBI *Taeniopygia guttata* Annotation Release 104.

3.2.4 Differential gene expression analysis

All code and custom functions used for RNA-seq analyses were written in R using RStudio and various Bioconductor packages, and can be found at `https://github.com/samifriedrich/zebrafinchRA`. To summarize, STAR output tables were used to create a sample-by-gene count matrix. This count matrix was used as input to DESeq2 (v1.30.1), which performed filtering, normalization, and regularized log transformation. A sample PCA was generated based on variance transformed values. To determine significantly differentially expressed genes (DEGs), a negative binomial generalized linear model was fit to the data with sex and age as main factors with a sex+age interaction. Wald tests were performed on user-specified contrasts (Table 3.2) to determine: developmentally-regulated genes within each sex; sex-biased genes within each age; and genes significant for a sex+age interaction. To improve detection and diminish the multiple testing problem, independent filtering for each test was performed using the mean of normalized counts as a filter statistic. Genes with a Benjamini-Hochberg-based false discovery rate (FDR) < 0.01 were considered significant, and are referred to as DEGs. Because none of the juveniles sang in the 20 min window between lights-on and sacrifice, we did not remove singing-regulated genes from our result sets.

Result set name	Groups contrasted	DEG type
Female development	20 DPH females vs 50 DPH females	Developmentally regulated
Male development	20 DPH males vs 50 DPH males	Developmentally regulated
20 DPH sex contrast	20 DPH females vs 20 DPH males	Sex-biased
50 DPH sex contrast	50 DPH females vs 50 DPH males	Sex-biased
Sex+age interaction	All four groups	Developmentally regulated in a sex-dependent manner

Table 3.2: Differential expression analysis design

3.2.5 Hierarchical clustering analysis

To identify groups of genes that showed similar expression across sex and age, we performed hierarchical clustering using the degPattern() function from clusterProfiler (v3.18.1). Only DEGs were considered and used as input for clustering analyses. From the regularized log transformed count matrix of relevant DEGs, the degPattern() function composes a distance matrix based on correlations between group means of gene expression, then constructs a hierarchy of clusterings based on that distance matrix.

3.2.6 Functional analyses

To identify gene ontology (GO) terms, specifically biological processes and molecular functions, that were significantly enriched in our DEG sets, we used functions from clusterProfiler (v3.18.1) to perform over-representation analysis (ORA) as well as gene set enrichment analysis (GSEA). Because these functional analysis tools are based on human data, zebra finch genes were mapped to their corresponding human orthologs based on HGNC symbol. For over-representation analyses, DEG sets were compared against a background of

all assessed genes with human orthologs (n=11,541). Only enrichment terms with adjusted $p < 0.05$ and supported by at least 5 DEGs were considered.

3.2.7 *In situ* hybridization

We performed *in situ* hybridization on developmental RA sections to characterize the expression patterns of select DEGs in more detail. These experiments provided validation of the RNA-seq data, as well as arcopallial and cell population expression information. When choosing genes for *in situ* hybridization, we looked for DEGs that a) showed high absolute $\log_2$ fold changes in relevant contrasts, b) were known markers of adult RA, c) were located on chromosome Z, d) were representative of an expression pattern cluster, e) had functional annotations of interest, or some combination thereof. Digoxigenin (DIG)-labeled riboprobe synthesis and *in situ* hybridization was performed as described in [172]. cDNA clones from the ESTIMA collection [173] were selected based on their alignment to and specificity for the target locus. Where possible, we further maximized specificity by choosing clones from the 3'-untranslated region of each gene. Sagittal sections for *in situ* hybridization were derived from fresh frozen brains, cryosectioned at $10\,\mu\mathrm{m}$ onto charged glass slides (Superfrost plus; Fisher Scientific).

3.3 Results

3.3.1 Transcriptional profiling of RA using RNA-seq

To characterize the molecular dynamics underlying sexual dimorphism of the song system, we evaluated genome-wide sex differences and developmental regulation within song nucleus RA. We collected brain tissue from RA of male and female zebra finches at 20 DPH, when RA is largely monomorphic, and at 50 DPH, when RA reaches its peak morphological sex dimorphism [53]. Juveniles remained in their family breeding cages until they reached the desired age. We used juveniles from 11 different breeding pairs to ensure genetic diversity within and between experimental groups. To minimize the confound of relatedness, male and female sibling pairs were assigned to groups such that they would not be directly contrasted (Table 3.2), i.e. a 20 DPH male and a 50 DPH female, or a 20 DPH female and a 50 DPH male. Sensorimotor and social experiences such as singing, hearing song, or being socially isolated are known to induce changes in gene expression within the brain [40, 42, 45, 310, 311]. To minimize the effects of variability in behavioral, sensory, and social states, we removed birds from the aviary just after lights on, monitoring them to verify that none of the 50 DPH males sang, and collected brains within 20 min. We used laser capture microdissection to extract RA from $12\,\mu\mathrm{m}$-thick sagittal, ethanol-fixed, Nissl-stained brain sections spanning the mediolateral extent of RA (see Figure 3.3 and Methods for details). We isolated high quality total RNA from 5-7 RA microdissectants per group (Table 3.1), opting not to pool samples, and thus retaining information about individual sample variability while maximizing statistical power. We prepared and sequenced cDNA libraries using the Illumina Novaseq platform, which produced 100 bp paired end reads to an average depth

of ∼50M reads per library. After quality control filtering and trimming, we aligned reads to the zebra finch assembly (bTaeGut1_v1.p, GCF_003957565.1) using the STAR aligner (v2.6.1), and then used DESeq2 (v1.30.1) to perform normalization, statistical modeling, and differential gene testing for n=21,955 genes. We found no evidence of outliers or batch effects based on hemisphere, RNA isolation batch, read depth, or sequencing lane.

3.3.2 Male and female RA transcriptomes are similar at 20 DPH and divergent at 50 DPH

To visualize the sample-to-sample variation and high-dimensional structure in our data, we performed a principal component analysis (PCA) using the top 500 genes that showed the greatest variance across all samples. The PCA revealed overall sample structure in line with our hypothesis that RA transcriptome would parallel its morphological divergence. When plotting the first two principal components, we observed that samples fell into three distinct clusters; the 20 DPH males and females intermixed within a single cluster, while the 50 DPH animals separated into male and female clusters (Figure 3.4). Even when all assessed genes (n=21,955) were used to generate a PCA plot, the 20 DPH groups remained closely clustered, but could be bisected into male and female groups by a diagonal line through the cluster (Figure S3.1). This clustering pattern provides a strong correlate to the morphological states of RA; at 20 DPH when male and female RA are mostly monomorphic, their transcriptome signatures closely resemble one another; at 50 DPH when male and female RA have become dimorphic, transcriptome signatures separate into sex-specific clusters.

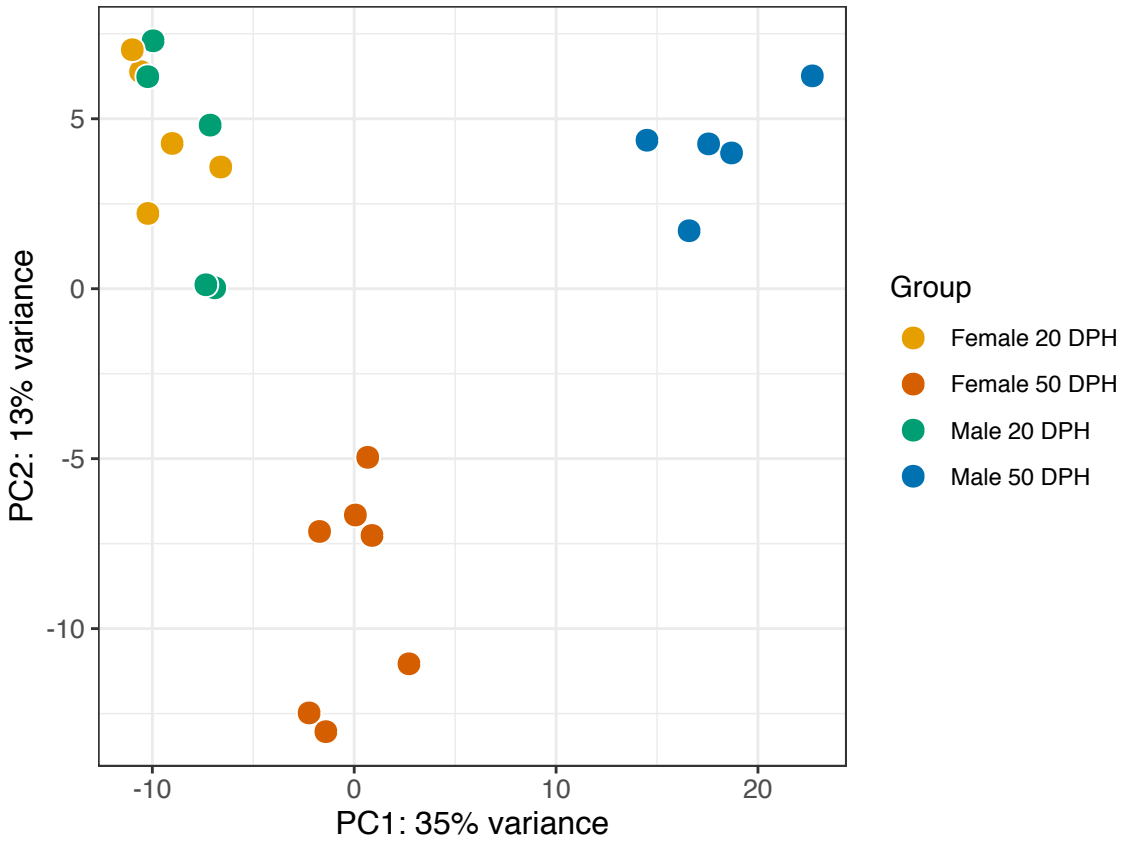

Figure 3.4: PCA plot of all RNA-seq samples. The 500 most variant genes were used to calculate principal components. Sample group is indicated by color. 20 DPH male (green) and female (yellow) samples cluster together, while 50 DPH samples cluster by sex (female=orange, male=blue).

3.3.3 Differential gene expression in RA

To determine statistically significant (adjusted p-value < 0.01) differentially expressed genes (DEGs), we built a model with sex and age as main factors, plus an interaction coefficient of sex+age. Paired contrasts of specified groups from this model (Table 3.2) yielded four sets of DEGs; 3,394 developmentally regulated DEGs in males, 1,803 developmentally regulated DEGs in females, 339 sex-biased DEGs at 20 DPH, and 4,262 sex-biased DEGs at 50 DPH. In addition, we found 1,446 DEGs that showed a sex+age interaction, i.e. genes whose developmental trajectories were significantly sex-dependent. One notable finding of this DEG analysis was how few genes were sex-differential at 20 DPH relative to 50 DPH. This result is consistent with our hypothesis that male and female RA would express similar genes when RA is monomorphic, and explains the tight clustering of 20 DPH male and female samples in the PCA plots (Figure 3.4 and Figure S3.1).

Validation of RNA-seq data

Before performing further analyses, we validated our DEG analysis by comparing differential expression results for several genes against published mRNA and/or protein expression patterns in developmental RA. Due to variability across studies in quantification technique and exact age assessed, we evaluated the relative trends for each gene. We found that sex differences and/or developmental changes were consistent between our RNA-seq data and published data for SCN3B and SCN4B [303], SCAMP1 [304], VIM [312], PVALB [313], ROBO1, and SLIT1 [305]. Additionally, we analyzed the set of known RA markers published by our lab on the Zebra Finch Brain Expression Atlas, ZEBrA (`http://www.`

zebrafinchatlas.org) that appeared in the DEG set for male development. RA markers are defined as genes whose expression within adult male RA contrasts with expression in the surrounding arcopallium, such that the boundaries of RA are clearly evident in the *in situ* hybridization pattern. Positive and negative markers show increased and decreased mRNA expression, respectively, within RA relative to the surrounding arcopallium. We found that the vast majority of developmentally regulated DEGs in males changed in the direction consistent with their adult male RA marker type. Specifically, of the 73 RA marker genes that were DEGs in male development, 27 out of 32 (84%) positive marker genes increased with age, and 41 out of 41 (100%) negative marker genes decreased with age. Assuming that most RA marker genes emerge or are intensified over the course of song learning, the congruence between adult marker type and developmental $\log_2$ fold change direction provides further validation of the RNA-seq data.

Male RA undergoes more drastic transcriptional changes than female RA

Massive sex differences were immediately apparent from the summary data for the DEG analysis. The MA plots of the four main contrasts are shown in Figure 3.5, with DEGs indicated by blue dots. In male and female development contrasts, DEGs were evenly distributed between up- and down- regulated genes: there were 870 up- and 933 down- regulated genes whose expression changed over development in females, and 1,686 up- and 1,709 down-regulated genes whose expression changed over development in males. Notably, many more genes shift in their expression levels over development in male RA compared to female RA. Additionally, the mean and median absolute $\log_2$fold changes of developmentally regulated DEGs were larger in males (1.06 mean; 0.78 median) than females (0.87 mean;

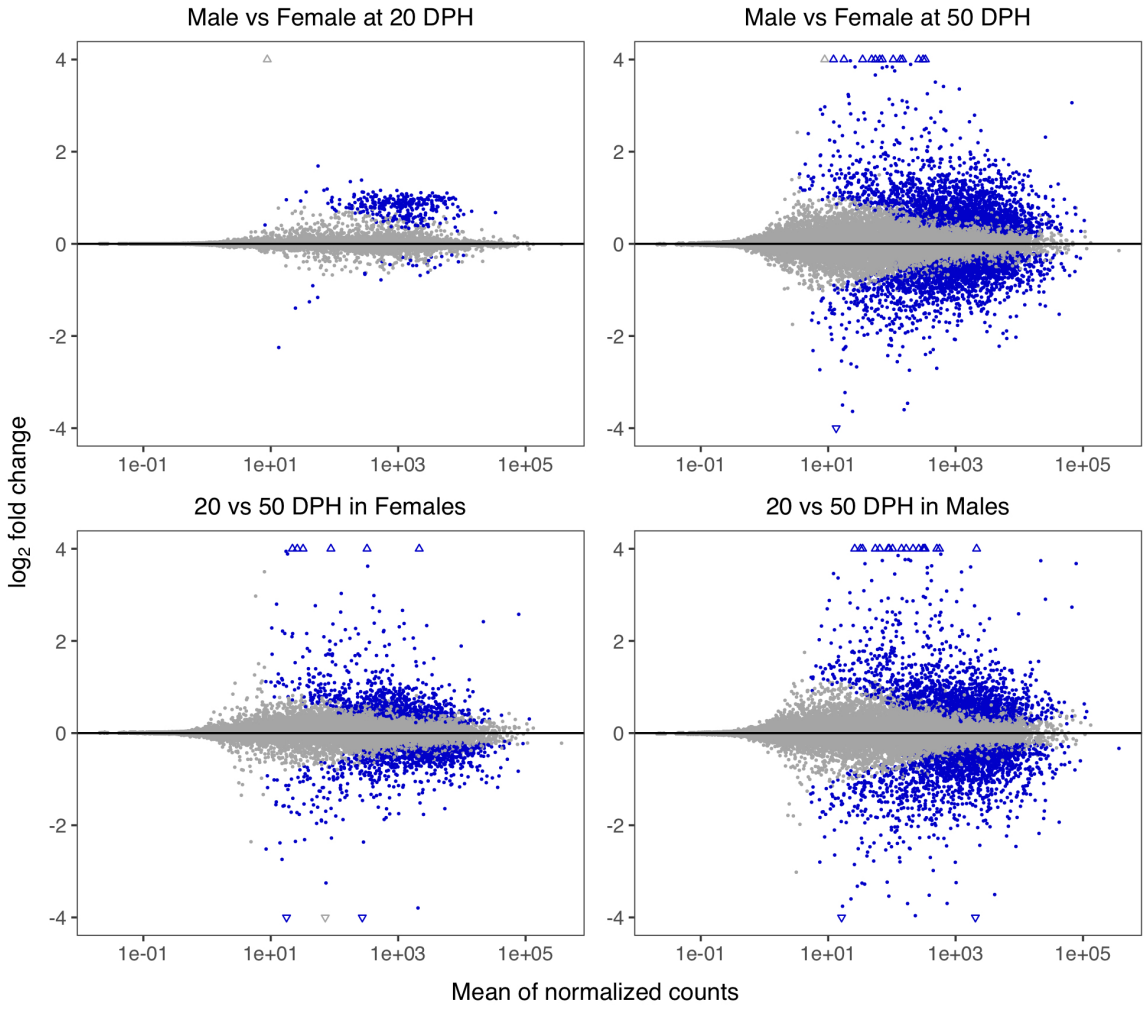

Figure 3.5: MA plots of DEGs for sex and age contrasts. Positive $\log_2$ fold change values indicate higher expression in males for sex contrasts (top), and higher expression at 50 DPH in age contrasts (bottom). Blue and grey points represent differential and nondifferential genes, respectively. Triangles represent genes with log2 fold changes > |4|.

0.63 median), indicating the magnitude of changes in expression levels were also greater in males. Together, these data strongly suggest that normal RA development in males recruits a broader gene network and more drastic expression level shifts. Consequently, 50 DPH male RA is the most transcriptionally distinct from a 20 DPH RA, a finding echoed in the remoteness of the 50 DPH male cluster in the PCA plot (Figure 3.4).

Developmentally regulated genes are predominantly sex-specific

To better understand the degree of shared versus sex-specific changes in gene expression, we looked at how many genes were developmentally regulated in one versus both sexes. Sex-specific developmentally regulated genes (n=978 in females; n=2,569 in males) outweighed shared ones (n=825), adding further support to the idea that male and female RA undergo distinct developmental programs. Among the 825 DEGs that showed developmental changes in both sexes, 760 (92%) of them changed in the same direction. Of these 760 DEGs that were directionally congruent, only 70 (9%) were significant for an interaction between sex and age. Indeed, the majority (n=690) of DEGs common to male and female development changed in the same direction and by comparable relative magnitudes, suggesting these genes may be part of a sex-neutral developmental program. Collectively, these findings indicated that sex-specific development of RA is coordinated by largely nonoverlapping gene networks unique to each sex.

Male-biased expression of chromosome Z genes dominates early transcriptional sex differences in RA

A defining feature of the 20 DPH sex contrast is the uneven distribution of DEGs toward male-biased expression. As shown by the MA plot in Figure 3.5 (top left), the majority of sex differential genes have positive $\log_2$ fold change values, indicating greater expression in males than females. Given that males are the homogametic (ZZ) sex, and that zebra finches lack global dosage compensation [136, 138], we suspected that many of the male-biased genes would be located on the Z sex chromosome. Indeed, we found that 87% (n=295)

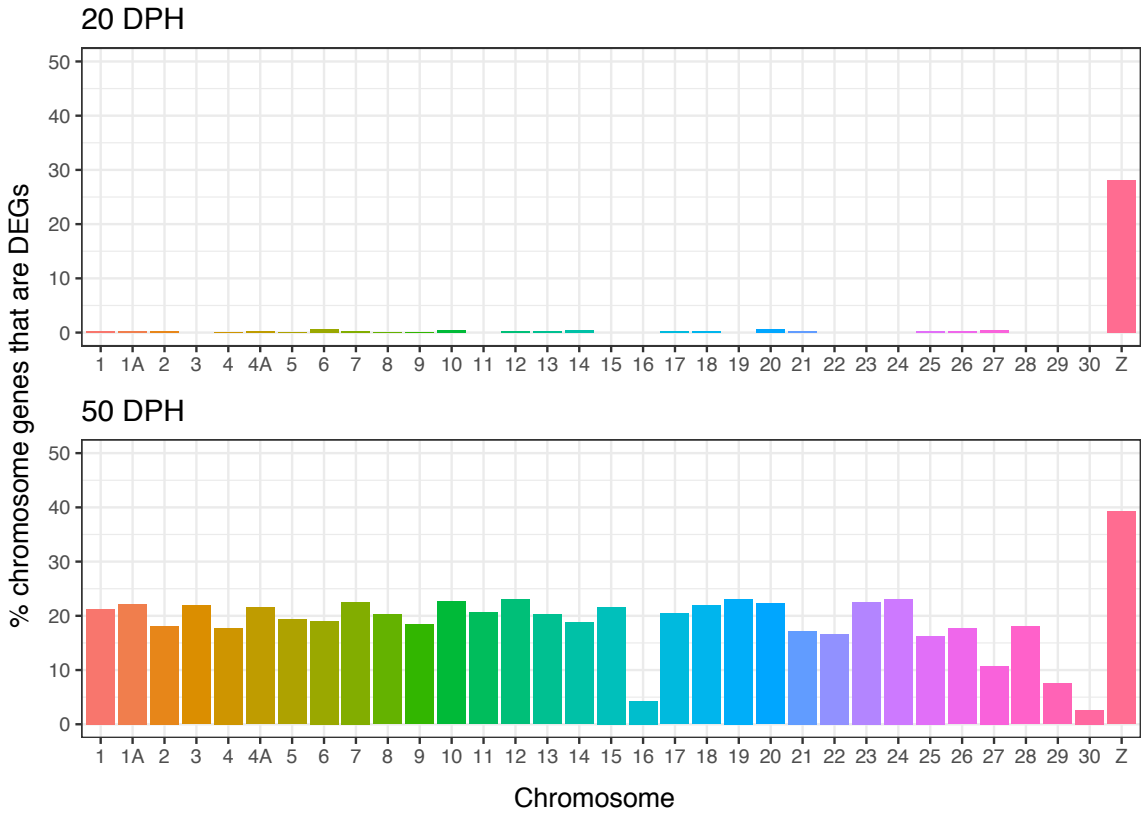

Figure 3.6: Sex-biased genes by chromosome at 20 and 50 DPH. Number of DEGs per chromosome was normalized to the total number of genes on each chromosome to account for differences in chromosome length and gene density.

of the DEGs from the 20 DPH sex contrast were located on the Z chromosome, and all of them were male-biased. Conversely, only 10% (n=413) of all DEGs from the 50 DPH sex contrast were Z chromosome genes, of which 94% (n=388) were male-biased. This developmental shift in the proportion of Z-linked-to-autosomal DEGs is quantified in Figure 3.6, which clearly shows the overrepresentation of Z-linked genes among 20 DPH sex-biased genes. Thus, transcriptional sex differences are dominated by sex chromosome genes early in RA development, and shift to being driven more by autosomal genes once RA is sexually dimorphic.

3.3.4 Z chromosome DEGs cluster into distinct expression patterns

Sex chromosome genes are well-situated to stage the development of sex differences [63], especially in species like zebra finches where there is no known mechanism for global dosage compensation [136, 138]. We ran a hierarchical clustering analysis on all Z chromosome genes appearing in at least one DEG set (n=509) to group Z-linked genes into shared expression patterns. We found that most Z-linked DEGs (n=431 from Groups 1, 2, and 3) appear to be expressed at higher levels in males at both ages (Figure 3.7). A small number of Z-linked DEGs was higher in females, some showing developmental increases in females and decreases in males, which could reflect gene-specific dosage compensation. Functional analyses of the genes from each expression pattern group did not identify any significant enrichments. However, *in situ* hybridization experiments revealed striking expression patterns for two Z chromosome genes implicated in neural development; LPL and CTSL.

LPL was a representative Z-linked gene from Group 1 that showed developmental increases in both male and female RA, yet was not significantly male-biased at either time point. The *in situ* hybridization data shows relatively flat expression throughout the arcopallium at 20 DPH in males and females (Figure 3.8). By 50 DPH, there is an increase in LPL expression within RA relative to the arcopallial surround in both males and females. In adult male, LPL is a highly discrete positive marker of multiple song nuclei including RA (Supplementary Figure S3.2). LPL codes for lipoprotein lipase, an enzyme integral to metabolising and transporting lipids. In vitro studies point to a role for LPL in neuronal differentiation and neurite extension [314]. In rodents, LPL is highly expressed in a number of brain regions and cell types, including prominent expression in primary motor cortex and

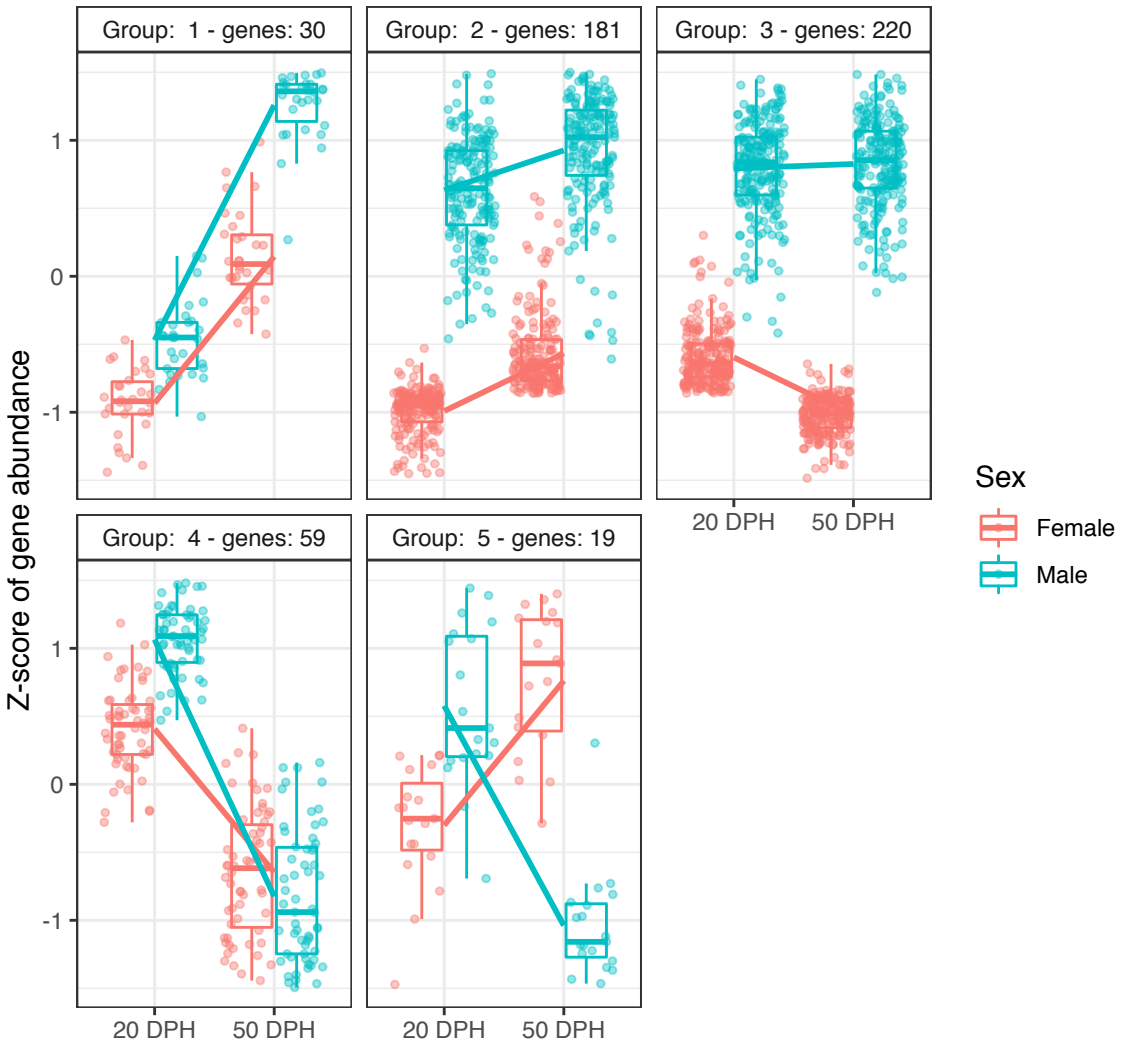

Figure 3.7: Expression pattern clustering for all Z chromosome DEGs. Number of genes per group is displayed above each plot.

layer II-VI cortical cells [315]. Considering that RA shares transcriptional convergence with mammalian motor cortical regions [19], LPL expression may represent a shared molecular specialization between birds and mammals.

Cathepsin L (CTSL) was a representative Z-linked gene from Group 3, which showed sex-specific developmental regulation, decreasing only in females to become male-biased at 50 DPH. We confirmed this regulatory pattern via *in situ* hybridization, which also revealed CTSL to be a strong positive RA marker in males (Figure 3.8). Although RA is visible among CTSL mRNA-expressing cells in both sexes at 20 DPH, the contrast between RA and its surround is most intense in 50 DPH male brain, seemingly due to developmental decreases in CTSL expression in the surrounding arcopallium. In contrast, CTSL expression in females appears to decrease throughout both the arcopallium and RA. Cathepsin L and its close homolog cathepsin B (CTSB) are two lysosomal cysteine proteases that have been linked to a wide array of functions in the brain, including extracellular matrix remodeling, neuropeptide synthesis, and apoptosis [316–319]. These cathepsins may play a role in synapse formation [319, 320] and extracellular cathepsin L has been shown to directly stimulate axon growth in vitro [321]. As detailed above, CTSL decreased in female RA, and our RNA-seq data indicates that CTSB increases more with age in males compared to females. If cathepsin function is conserved in vertebrate brain development, perhaps the decrease of CTSL in female RA leaves neurons more susceptible to lysosomally-mediated apoptosis, while higher levels of both CTSB and CTSL in males provide neuroprotection from cell death, and support synapse organization and axon growth.

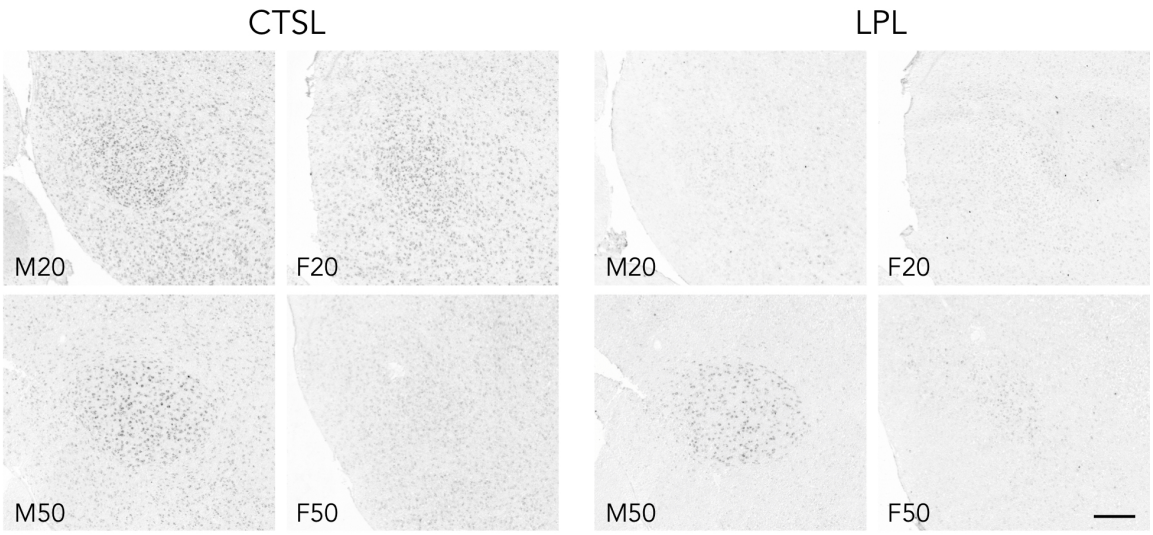

Figure 3.8: Expression of sex differential chromosome Z genes in developing RA. *In situ* hybridization photomicrographs show sagittal $10\,\mu\mathrm{m}$ sections at the core of RA. Scale bar = $250\,\mu\mathrm{m}$

3.3.5 Functional enrichments in RA development are highly sex-specific

To gain insight into the biological processes and molecular pathways of sex-differential RA development, we performed both competitive and noncompetitive functional analyses. Competitive, overrepresentation analysis (ORA) was performed to find enriched pathways in each of the DEG result sets. Overall, we found that functional enrichments for developmentally-regulated DEG sets were quite different between sexes with very little overlap 3.3 3.4. Functional themes that were significant and unique to female development include response to steroid hormone, establishment and regulation of cell polarity, negative regulation of cellular component movement, and differentiation of glia and oligodendrocytes. The functional themes associated with DEGs in male development include axon/projection development, axon insulation (oligodendrocyte development, axon ensheathment, myelin maintenance), cell morphogenesis and growth, metabolic and energetic processes, synapse organization, neurotransmission (including several glutamatergic, GABAer-

GO Enrichments in Female RA Development	
Cell movement	
GO:0051271	negative regulation of cellular component movement
GO:0030336	negative regulation of cell migration
Regulation of membrane potential	
GO:1903817	negative regulation of voltage-gated potassium channel activity
GO:1902260	negative regulation of delayed rectifier potassium channel activity
Cell differentiation	
GO:0010001	glial cell differentiation
GO:0048709	oligodendrocyte differentiation
GO:0045666	positive regulation of neuron differentiation
GO:0045165	cell fate commitment
Transcriptional regulation	
GO:0001217	DNA-binding transcription repressor activity
GO:0035195	gene silencing by miRNA
GO:0150100	RNA binding involved in posttranscriptional gene silencing
GO:0001216	DNA-binding transcription activator activity
Hormone signaling	
GO:0048545	response to steroid hormone
GO:0009755	hormone-mediated signaling pathway

Table 3.3: Summary of GO enrichments for female RA development.

gic and peptidergic receptors), cell junction assembly, regulation of membrane potential, and voltage-gated ion channel activity.

In testing for overrepresented GO terms associated with sex differences, we found no significant enrichments among the 339 DEGs that were sex-biased at 20 DPH. However, many of the sex-specific developmental enrichments mentioned above were similarly enriched among DEGs that were sex-biased at 50 DPH, including most of the functional themes listed above for male development. Several additional functional categories unique to the 50 DPH sex contrast appeared, including histone binding, transcription corepressor and coregulator activity, mRNA processing, response to monoamines, response to catecholamines, cell-cell signaling involved in cardiac conduction, and cerebral cortex GABAergic interneuron dif-

GO Enrichments in Male RA Development	
Cell movement	
GO:0042330	taxis
Regulation of membrane potential	
GO:0042391	regulation of membrane potential
GO:0034765	regulation of ion transmembrane transport
GO:0005244	voltage-gated ion channel activity
GO:0046873	metal ion transmembrane transporter activity
GO:0017080	sodium channel regulator activity
Axon and projection development	
GO:0061564	axon development
GO:0014003	oligodendrocyte development
GO:0031346	positive regulation of cell projection organization
GO:0032291	axon ensheathment in central nervous system
GO:0043217	myelin maintenance
GO:1990138	neuron projection extension
Synaptic assembly, organization, and function	
GO:0050808	synapse organization
GO:0051963	regulation of synapse assembly
GO:0050803	regulation of synapse structure or activity
GO:0099560	synaptic membrane adhesion
GO:0099177	regulation of trans-synaptic signaling
GO:0051937	catecholamine transport
GO:0099601	regulation of neurotransmitter receptor activity
GO:1900449	regulation of glutamate receptor signaling pathway
GO:0099003	vesicle-mediated transport in synapse
GO:0099645	neurotransmitter receptor localization to postsynaptic specialization membrane
Cell growth and morphogenesis	
GO:0022604	regulation of cell morphogenesis
GO:0060560	developmental growth involved in morphogenesis
GO:0061387	regulation of extent of cell growth
GO:0048588	developmental cell growth
Cell energetics and metabolism	
GO:0006734	NADH metabolic process
GO:0009150	purine ribonucleotide metabolic process
GO:0006091	generation of precursor metabolites and energy
GO:0006090	pyruvate metabolic process
GO:0046034	ATP metabolic process
GO:0061718	glucose catabolic process to pyruvate
GO:0019693	ribose phosphate metabolic process
GO:0044282	small molecule catabolic process
GO:0010563	negative regulation of phosphorus metabolic process
GO:0016052	carbohydrate catabolic process

Table 3.4: Summary of GO enrichments for male RA development.

ferentiation. For all of these functional enrichments unique to the 50 DPH sex contrast, females expressed most of the associated genes at higher levels than males. Female-biased expression was observed for 57 out of 70 (81%) DEGs associated with histone binding; 43 out of 60 (72%) DEGs associated with transcriptional corepressor activity; 103 out of 144 (72%) DEGs associated with transcription coregulator activity; 130 out of 155 (84%) DEGs associated with mRNA processing; 29 out of 35 (83%) DEGs associated with response to monoamines; 31 out of 35 (89%) DEGs associated with response to catecholamines; 10 out of 15 (67%) DEGs associated with cell-cell signaling involved in cardiac conduction; and 8 out of 9 (89%) DEGs associated with cerebral cortex GABAergic interneuron differentiation. Functional enrichments for the sex+age interaction DEGs contained many of the same themes as those for the four contrasts. However, a few unique functions emerged, including beta-catenin binding, and insulin-like growth factor binding.

In addition to the ORA, we also performed a non-competitive gene set enrichment analysis (GSEA) for each of the DEG result sets. Unlike ORA, GSEA does not require delineation of DEGs from non-differential genes. Instead, GSEA ranks the log fold changes of all assessed genes to test for significantly coordinated shifts in gene pathways [322]. For age contrasts within each sex, we again observed sex-specific pathways, many of which overlapped with the ORA results for males. Functional enrichments specific to female development included hormone-mediated signaling, DNA-binding transcription repressor activity, oligodendrocyte differentiation, negative regulation of voltage-gated potassium channel activity, and negative regulation of delayed rectifier potassium channel activity. We also observed female-specific enrichments for cytokine production and regulation of cytokine production, lymphocyte mediated immunity, and mRNA binding involved in posttranscrip-

tional gene silencing. These particular functional enrichments are intriguing in light of emerging evidence that neuroimmune signaling and microRNAs (miRNAs) may influence sex-differentiation in the brain [323, 324]. miRNAs are particularly promising given their ability to influence transcriptional networks, with relative concentrations of miRNAs to their target mRNAs determining whether mRNA is translated to protein or translationally suppressed. Our study found two miRNA genes with significant sex-bias in RA. MIR2954, a chromosome Z gene, showed male-biased expression at both 20 DPH and 50 DPH. This miRNA gene is unique to birds, and shows considerable sex-biased expression across several tissues in adult zebra finch, including the brain [325]. This gene is also regulated in response to song, as upon exposure to song playbacks, expression levels of MIR2954 increase slightly in males, and decrease in females [311]. The other miRNA gene for which we found sex-biased expression was MIR9-1, which showed no sex difference at 20 DPH, but was significantly higher in males by 50 DPH. MIR9-1 is a variant of MIR9, which is known to regulate a suite of genes in the developing vertebrate brain, in turn effecting neuronal proliferation, migration, differentiation, and axon development [326].

For male development, the familiar themes of axonogenesis, synapse organization/assembly, and cell morphogenesis turned up in the GSEA results. The 20 DPH sex contrast was associated only weakly with a type 1 interferon pathway. Functional pathways enriched among 50 DPH sex-biased genes included synapse organization/assembly, axon guidance and neuron projection, RNA splicing, membrane depolarization during action potential, regulation of hormone levels and hormone transport, regulation of neurogenesis, histone binding, chromatin binding, and mitochondrial respiration. For the sex+age interaction, the most significant enrichment from this GSEA was cellular respiration, accompanied by functions related

to posttranscriptional gene silencing, voltage-gated calcium channels, synapse organization, and axonogenesis.

Taken together, a few overarching motifs emerge from these functional results. The first is that developmental pathways invoked in RA development are highly sex specific. While the DEG sets for male and female development contained many hundreds of sex-specific genes, it was possible that those gene sets would converge on similar functions. However, we did not find evidence of functional convergence; not only were developmentally regulated genes mostly unique between males and females, the functional enrichments they represent were also highly sex-specific. Broadly, female development was associated with regulation of genes involved in gene silencing, hormone signaling and response, immune signaling, cell polarity, and cell differentiation. In contrast, male development was associated with the regulation of genes that participate in the growth and organization of neuronal projections and synapses, cell morphogenesis, neurotransmission, cellular metabolism and energy, and voltage-gated ion channels. Many of these functional enrichment terms associated with male or female development reappeared in the 50 DPH sex contrast and sex+age interaction results, further supporting the idea that transcriptional shifts in RA reflect functional divergence between sexes. Additionally, no significant functional enrichments were found for the 20 DPH sex contrast, which may reflect a true lack of functional sex differences at this age, or alternatively, may be due to fewer DEGs, human orthologs, and/or functional annotations for this Z chromosome-dominated DEG set. All together, these results demonstrate that sex-specific and functionally-discrete gene networks are regulated over the course of RA development.

3.3.6 Sex+age interaction DEGs cluster into expression pattern groups with distinct functional enrichments

The set of genes significant for an interaction between sex and age were quite heterogeneous in their developmental dynamics and sex differences. To identify groups of genes with similar patterns of sex-dependent developmental regulation, we performed hierarchical clustering on all sex+age interaction DEGs (n=1,446). Hierarchical clustering yielded 9 unique expression pattern groups, providing a visual representation of the diversity of regulatory motifs in this gene set (Figure 3.9). For followup analyses, we focused on the first three expression pattern groups, as together they contained 1,006 (70%) of all sex+age interaction DEGs. Representative examples of genes from each group were assessed by *in situ* hybridization (Figure 3.10). To test whether unique expression patterns were associated with specific functional pathways, we performed an over-representation analysis (ORA) on each group's DEG set. The smaller clusters (groups 4-9) did not produce any enriched terms that met our criteria (see Methods). However, we found that the largest three groups (Groups 1-3) were uniquely enriched for different biological processes, demonstrating that directionally coordinated shifts in gene expression were associated with distinct functional networks.

Group 1 comprised 470 genes that became male-biased over development, mostly through an increase in males and/or a decrease in females. The functional enrichments for Group 1 were largely metabolic and mitochondrial processes. One such gene, SLC4A4, was linked to ATP metabolic process. SLC4A4 codes for a sodium bicarbonate cotransporter and has been implicated in activity-dependent metabolic coordination between astrocytes and neu-

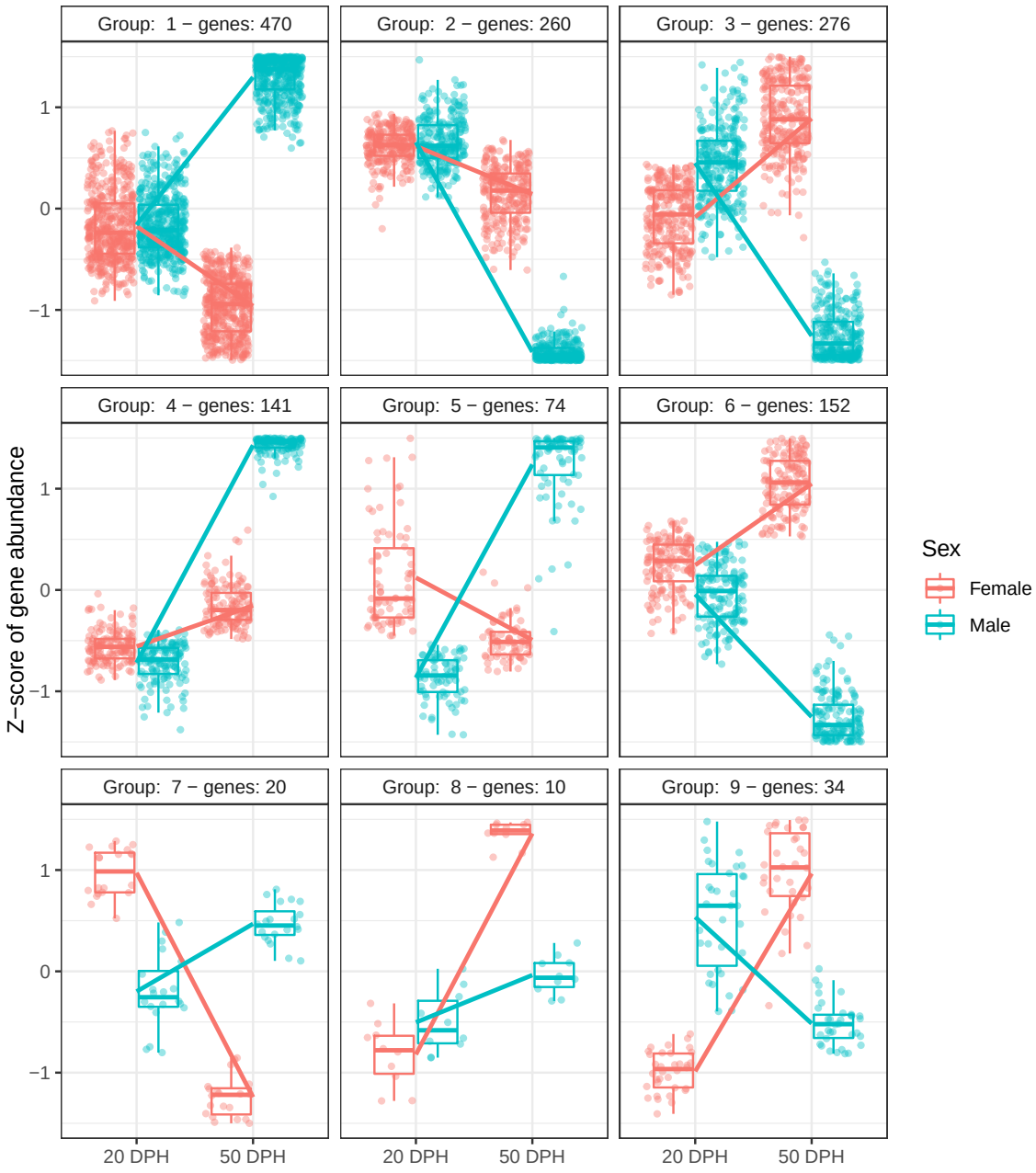

Figure 3.9: Expression pattern clustering for genes that show an interaction between sex and age. Number of genes in each group is displayed above each plot.

rons [327]. RNA-seq data indicated that SLC4A4 was expressed at similar levels in 20 DPH and increased developmentally only in males. SLC4A4 mRNA expression assessed via *in situ* hybridization corroborated this observation of a male-specific increase (Figure 3.10). SLC4A4 mRNA showed widespread expression in arcopallium at 20 DPH, with RA clearly visible in males and females by its high cell density. The level of SLC4A4 expression in the arcopallium surrounding RA decreased over development in both males and females, so that by 50 DPH, SLC4A4 was a pronounced positive RA marker in males, but just barely a positive marker in females. The increased expression of SLC4A4 in male development appears to be part of a larger gene network of enriched cellular energetics pathways that evolves to support the energy demands of fast spiking in large male RA neurons [234].

Group 1 also encompassed other genes that while not part of a significant enrichment set, may be crucial to growth and development, such as growth factors. Pleiotrophin, the gene product of PTN, is a secreted cytokine that acts as a growth factor. It is required for the proper development of dendrites in newborn hippocampal neurons [328], and is implicated in neuronal differentiation, axon growth, and synapse formation [329]. Our DEG analyses revealed that PTN was developmentally regulated in a sex-dependent manner, which we verified using *in situ* hybridization (Figure 3.10). At 20 DPH, mRNA expression looked similar between males and females, and was not markedly different within RA versus its surround. At 50 DPH, PTN is a striking positive marker of male but not female RA. The diffuse expression pattern between darkly-stained cell nuclei suggests PTN mRNA may be present in neurites, where it may act locally in supporting the growth of axons or dendrites, potentially contributing to the greater dendritic arborization of RA neurons in males compared to females [89].

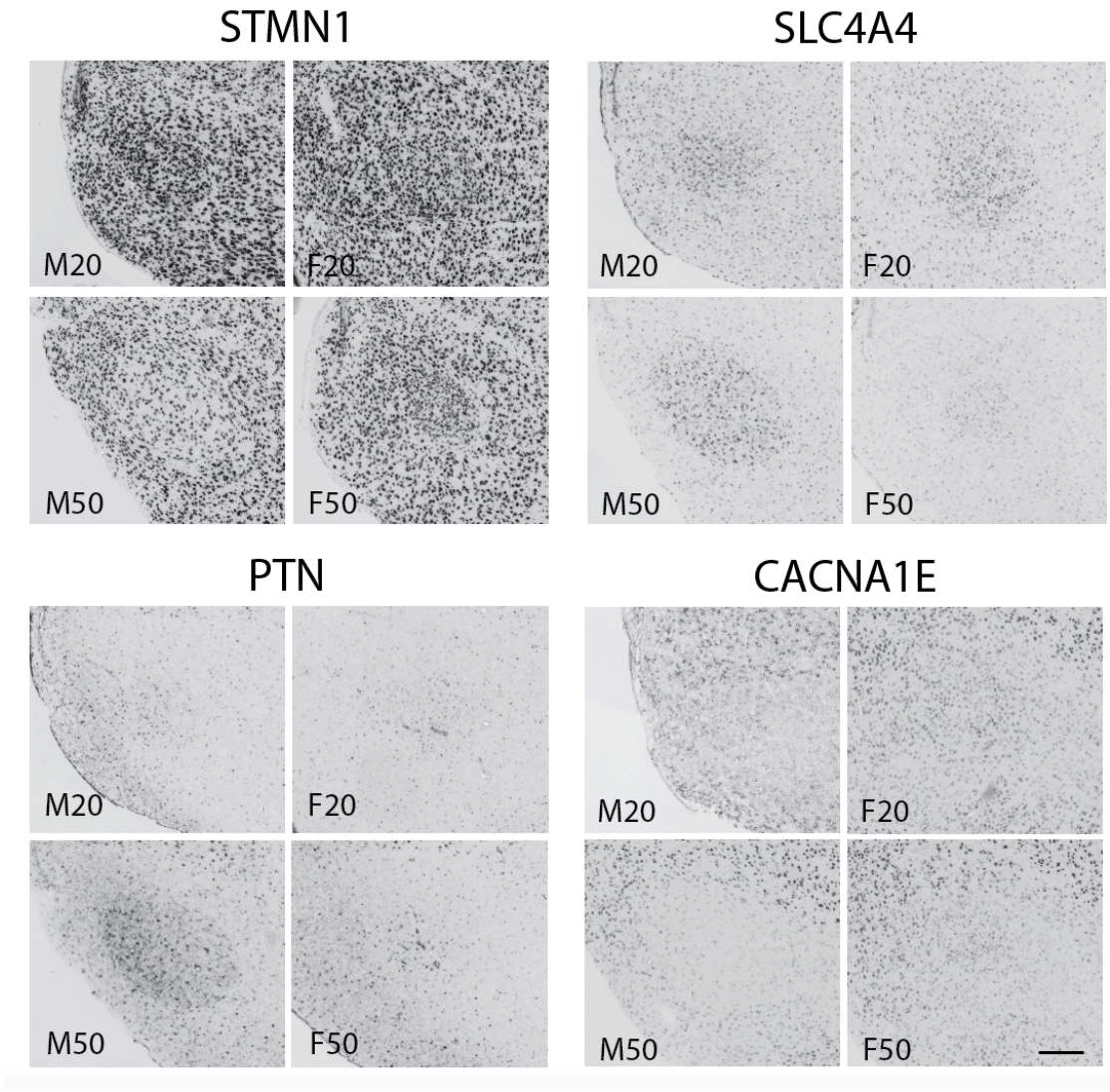

Figure 3.10: Expression of genes significant for an interaction between sex and age. *In situ* hybridization photomicrographs show sagittal $10\,\mu\mathrm{m}$ sections at the core of RA. Top row of Nissl-stained sections shows cytoarchitecture of RA and surrounding arcopallium. Scale bar = $250\,\mu\mathrm{m}$

Group 2 contained 260 genes that became female-biased over development through marked decreases in males. This group showed enrichments in GO terms related to axon development, synapse assembly and organization, neurotransmission, potassium channels, and sodium channel regulators. STMN1, which decreased substantially in male development, was one gene in the enrichment set for axonogenesis. The gene product of STMN1, stathmin 1, is a cytosolic phosoprotein that destabilizes microtubules [330]. Microtubule network regulation is a key aspect of axon and dendrite development, and *in vitro* studies demonstrate that developmental downregulation of stathmin 1 activity is necessary for normal dendritic arborization in cerebellar Purkinje cells [331], and axon formation in hippocampal cells [332]. mRNA expression patterns confirm the male-specific developmental decrease in RA (Figure 3.10). STMN1 is highly expressed within RA and surrounding arcopallium at 20 DPH in both sexes. At 50 DPH, female RA continues to express high levels of STMN1. In contrast, the overall expression within male RA at 50 DPH decreased substantially from 20 DPH levels, and this decrease continues to adulthood, as STMN is an exquisitely high-contrast negative marker of adult RA (`http://www.zebrafinchatlas.org`). Given the neuromorphogenic effects of stathmin 1 suppression in mammalian neurons, downregulation of STMN1 in male RA may encourage the elaboration of axons and/or dendrites, resulting in greater arborization in adult males [89].

Group 3 contained genes that became female-biased through increases in females and/or decreases in males. This group was associated with GO terms including negative chemotaxis, voltage-gated ion channels (including several calcium channels), transcription cofactor binding, and synapse organization. Chemotaxis is a key part of neural circuit development that involves directing the growth of cells and neurites through both attractive and

repellent factors [333, 334]. There were 6 DEGs in the enrichment set associated with negative chemotaxis; 5 genes (SEMA3F, SLIT1, NRG3, FLRT2, and SEMA4D) decreased over male development but were static in females, and 1 gene (SEMA5A) increased over female development but was static in males. The sex-specific developmental regulation of these chemorepulsive cues provide a channel through which sex differences in RA afferents may be established. Likewise, 15 out of 20 (75%) of the DEGs in the enrichment set for synapse organization exhibited developmental decreases in males but no developmental shifts in females. Combined with the predominance of synapse and axon development-related enrichments in male but not female development, these findings suggest that genes involved in orchestrating connectivity are more widely regulated in males.

Voltage-gated calcium channels were significantly enriched in Group 3, including alpha-1 subunits CACNA1H, CACNA1D, CACNA1B, and CACNA1I. Another calcium channel alpha-1 subunit, CACNA1E, was in Group 6, a group whose overall expression pattern closely resembled Group 3 (Figure 3.9). Consistent with the RNA-seq data, CACNA1E showed similar expression between males and females at 20 DPH, but was selectively downregulated in RA over male development (Figure 3.10). The CACNA1E gene codes for an R-type voltage-gated calcium channel that has been shown to limit depolarization in mammalian hippocampus [262, 263]. This raises the possibility that developmental downregulation of CACNA1E in males contributes to the male-specific increases in action potential amplitude observed in developing RA neurons [303].

3.3.7 Differential expression in gene families implicated in sexually dimorphic brain development

Based on previous literature describing RA's multifaceted sexually dimorphic development (Figure 3.2), we hypothesized that several key gene families and functional themes would show transcriptional regulation, namely transcription factors, growth factors, and apoptosis regulators. In addition, because sex steroid hormones have an established role in song system development [61], we were curious about developmental expression levels of related receptors and enzymes. Also, given sex differences and developmental changes in the firing properties of RA neurons [234, 235, 303, 335], we expected to find sex-specific developmental regulation of voltage-gated ion channels. In line with these predictions, we found several indications of these gene families in the results of our enrichments analyses reported above. However, considering that most gene ontology annotations encompass a variety of gene families and molecule types, we decided to perform more directed analyses of relevant genes. To avoid limiting our analyses to genes with human orthologs or human-based functional annotations, we instead identified relevant genes using strict term searches (e.g "growth" or "neurotrophic" for growth factors) of zebra finch gene descriptions. Using this approach, we found a substantial number of sex-biased and developmentally regulated genes across these gene groups, and highlight specific examples below.

Transcription factors

Bearing in mind their established role in development and ability to regulate multiple genes, transcription factors are poised to modulate gene networks and induce widespread

changes in transcriptome dynamics. We identified over 100 DEGs that contained the phrase "transcription factor" in their gene description. Of note were four transcription factor genes, RFX3, BDP1, GTF2H2, and BTF3, that were more highly expressed in males at 20 DPH, and all but RFX3 were also male-biased at 50 DPH. Interestingly, all four of these transcription factor genes are located on the Z chromosome, suggesting their male-biased expression likely result from a lack of dosage compensation. Eight Sry-box (SOX) transcription factor genes were sex differential at 50 DPH, 6 of which were female-biased, either due to developmental decreases in males (n=4), or developmental increases in females (n=2). Transcription factors ASCL1, MITF, and POU2F1 increased over development in females, resulting in significant female-biased expression at 50 DPH. Many transcription factor genes exhibited male-specific decreases over development, including MAFB, HES4, and SP9, and several others showed male-biased expression at 50 DPH, including ETV4, ERG, and SP5.

Growth factors

Functional analyses of male development revealed several growth-related enrichment terms that included a variety of molecule types. We focus here on growth factors, which can have distributed effects as secreted molecules. Of the 10 fibroblast growth factor (FGF) genes in our DEG set, 7 were sex differential at 50 DPH, 5 of which were higher in males, including FGF9 and FGF2. Interestingly, infusion of glial mitogen FGF2 into juvenile female RA increased cell proliferation and decreased pyknotic cells [336]. When taken with the higher number of non-neuronal cell types in male RA prior to RA sexual dimorphism [337], these studies raise the possibility that glia provide sex differential neurotrophic support. In contrast to fibroblast growth factors, insulin-like growth factor-associated genes, (IGF1R,

IGF2BP2, and IGF2BP3,) showed female-biased expression at 50 DPH due to developmental decreases in males. Additionally, LOC100221052, which encodes transforming growth factor beta activator LRRC32-like, increased many-fold in males over development, producing a pronounced sex difference at 50 DPH, and KDR (also known as VEGFR2) was expressed at higher levels in males at 50 DPH as a consequence of developmental decreases in females. We also found several cases of sex-biased expression for neurotrophic factors and their receptors, predominantly arising from developmental regulation in males. These genes were of particular interest, as infusion of neurotrophins have been shown to prevent apoptosis in deafferented RA [338]. In our data, we observed male-specific increases in GDNF (a Z-linked gene), NENF, and NDNF, as well as male-specific decreases in CNTFR, NTRK3, NGF, PDGFA, and BDNF. Of these, BDNF and its receptor, NTRK2, have been implicated in sexually dimorphic song system development. BDNF released from HVC projections may influence the formation of afferent connections with RA neurons [105, 338, 339]. NTRK2, also known as tyrosine receptor kinase B (trkB), is a chromosome Z gene that was not developmentally regulated in either sex, but showed higher expression in males at both ages. Studies of NTRK2 indicate it is more highly expressed in male zebra finch brain from a very young age, particularly in HVC [340], and our data strongly suggest this BDNF receptor is also male-biased in juvenile RA. Intriguingly, two sex differential neurotrophic genes showed opposite directions of developmental regulation between males and females; PDGFD decreased in females and increased in males, while HDGFL3 increased in females and decreased in males. These opposing patterns of regulation make PDGFD and HDGFL3 particularly interesting targets for follow-up studies.

Apoptosis regulators

Female RA undergoes marked cell loss during the same time that male RA is growing, and is characterized by higher rates of pyknosis, strongly indicating that cell death drives female cell loss [52, 56]. In line with this putative sex difference in cell death, we found many sex-biased genes associated with cell death and apoptotic processes. We observed female-biased expression at 50 DPH for several genes that promote apoptosis, including EVA1A, AATK, CCAR1, PPP1R13B, ANKDD1A, MADD, PDCD11, and DIDO1. In contrast, males showed increased expression for multiple genes that have been linked to anti-apoptotic and protective functions, including CFLAR, DDIAS, NIBAN1, and Z-linked CAAP1. Many of these sex-differential genes were also developmentally regulated. For example, two apoptosis-promoting genes that showed sex-specific developmental changes are EVA1A, which decreased in males, and DIDO1, which increased in females. In conjunction, apoptosis-suppressing genes CFLAR, DDIAS, and NIBAN1 increased over male development. Furthermore, the substantial male-specific increase in FAS (Fas cell surface death receptor) is curious, as this gene has paradoxically been linked both to neuronal death and cell survival [341].

Sex steroid receptors and enzymes

Sex differentiation of the song system has classically been studied through the lens of sex hormones. Although manipulations of sex hormone levels have a long and convoluted history in the zebra finch [reviewed in 61], it is undeniable that sex hormone action influences the development of song nuclei, including RA. Consistent with previous studies

[71–73], we found relatively low levels of expression and no significant sex differences in the genes encoding aromatase (CYP19A1) or estrogen receptors (ESR1 and ESR2). Somewhat surprisingly, androgen receptor (AR) showed a developmental increase in females, resulting in female-biased expression at 50 DPH. Sex differences and developmental regulation were observed for several genes that encode other enzymes involved in steroid metabolism and biosynthesis. Hydroxysteroid 17-β-dehydrogenase genes HSD17B7 and HSD17B12 were male-biased at 50 DPH, and Z-linked HSD17B4 was male-biased at both ages. These enzymes catalyze redox reactions of estrogens and androgens, thus their transcriptional regulation can alter the cellular potency of sex steroids. In mammals, HSD17B4 and HSD17B7 are generally considered estrogenic, converting estrone to the more active estradiol [342]. Another hydroxysteroid dehydrogenase gene, HSDL2, was male-biased at both ages and showed a developmental increase in males. Similarly, steroid 5 α-reductases SRD5A2 and SRD5A3 were male-biased at 50 DPH, with SRD5A2 increasing over male development. Steroid 5 α-reductases convert testosterone into 5-α-dihydrotestosterone, a non-aromatizable form of testosterone. Administration of a 5 α-reductase inhibitor to zebra finch hatchlings decreased the number and density of RA neurons only in males, although this effect may also have resulted from nonspecific inhibition of aromatase and 5 β-reductase [343]. In summary, sex-biased gene expression of sex steroid enzymes was heavily male-biased at 50 DPH, suggesting higher levels of sex steroid biosynthesis and metabolism in male RA, offering indirect support to theories of steroid-induced song system masculinization.

Voltage-gated ion channels and auxiliary subunits

The excitable properties of RA are integral to its function in song production. Over the song learning period, neurons in male RA progressively fire faster, more precisely, and generate more bursts [234, 235, 303]. The small number of studies that have examined sex differences in RA excitability have found that male and female RA neurons fire similarly around 20 DPH, and sex differences in spontaneous activity, high frequency spiking, and sodium currents emerge over the course of RA maturation [234, 303]. Consistent with these previous studies, no voltage-gated ion channels in our data showed sex-biased expression at 20 DPH. By 50 DPH, 45 voltage-gated ion channel and auxiliary subunit genes showed sex differences in expression. Interestingly, the majority (n=37) of these ion channel genes showed higher expression in females, largely due to developmental decreases in males, including KCNQ5, SCN3B, CACNA1E, and KCNA6. Males expressed higher levels of 8 voltage-gated ion channel genes, including KCNS1, SCN4B, CLCN2, and KCNQ1-like, due to developmental increases in expression. As a family, calcium voltage-gated channel genes tended to decrease developmentally in males, with the single exception of CACNG3. This observation is consistent with the functional enrichment of voltage-gated calcium channels in Group 3 of the sex+age interaction clusters (Figure 3.9) and the male-specific decrease of CACNA1E (Figure 3.10). Also, three out of the four genes that make up the family of sodium channel beta subunits were sex-biased at 50 DPH. Consistent with previous *in situ* hybridizations from our lab, SCN3B and SCN4B decreased and increased, respectively, in male development [303]. SCN2B was female-biased at 50 DPH due to a female-specific increase over development. The fourth member, SCN1B, is present in the zebra finch genome

[344], but not annotated in zebra finch assembly used for this study, and thus was not assessed. However, given that a) SCN1B is a striking positive marker of several adult male song nuclei including RA [344], and b) positive RA marker genes tend to increase over development, we suspect that SCN1B expression increases with age in males.

3.4 Discussion

Understanding how sex differences in the brain manifest requires that we understand the molecular factors orchestrating their development. Using RNA-seq to assay gene expression in laser capture microdissected tissue, we observed large-scale sex differences and developmental shifts in the transcriptional landscape of sexually dimorphic nucleus RA during a critical window of neural sex differentiation and song development. We found evidence that wide-ranging, sex-specific gene networks orchestrate sexually dimorphic developmental pathways. In line with our initial hypothesis, the transcriptional landscape of RA followed its morphological divergence. Less than 400 genes were sex-biased at 20 DPH, and over 4,000 genes were sex-biased at 50 DPH - more than a tenfold increase over this developmental window. We also discovered age-dependent contributions of autosomal versus sex chromosome genes to these genome-wide sex differences; chromosome Z genes made up the vast majority of all sex-biased genes at 20 DPH but not 50 DPH, consistent with modern theories that early sex bias in sex chromosome gene expression may set the stage for subsequent sexual differentiation [63].

Our study puts forth solid evidence that RA undergoes two distinct, sex-specific developmental programs carried out by largely nonoverlapping gene networks. For one, most

developmentally regulated genes were specific to one sex. The majority of genes that were common to both male and female development showed little difference in direction or magnitude of change across age, suggesting these genes may be involved in basal developmental processes necessary for both sexes. Furthermore, we did not find evidence of functional convergence, as there was little to no overlap in the enriched pathways indicated for male and female development. Indeed, we found that RA development was characterized by highly sex-specific functional enrichments. The developmental program in male RA appears to recruit functional networks involved in cellular energetics, cell morphogenesis and growth, axon formation and myelination, voltage gated ion channels, and multiple synaptic processes including assembly, organization, and neurotransmission. In contrast, female development was characterized by enrichments in hormone response and signaling pathways, negative regulation of cellular movement, establishment of cell polarity, glial cell differentiation, immune signaling, and gene silencing. More focused analyses of specific gene families and functions revealed developmental and sex-biased regulation of many genes encoding transcription factors, growth factors, apoptosis regulators, sex steroid enzymes, and voltage gated ion channels. In summary, these findings identify molecular players and functional pathways that differentiate male from female RA, and that may serve as the molecular substrate of RA sexual dimorphism. In addition to identifying genes linked to sexually dimorphic processes previously described in the literature, we identify novel sex differences in gene expression and functional networks whose roles are less well established in songbird brain development.

Relatively little is known about sex differences in developmental gene expression of the song system. A few studies have assessed developmentally regulated genes in male RA [44,

294, 345, 346], and HVC [294, 347]. One recent study aimed at understanding genomic responses to estrogen manipulation reported sex differences in song nuclei transcriptomes of treated and untreated 30 DPH male and female zebra finches [106]. While these studies provide some insight into genes involved in the masculinization and hormone sensitivity of song nuclei, they assess developmental changes only in male song nuclei that are already sexually dimorphic, or they assess sex differences at a single time point, leaving open the question of how developmental dynamics in gene expression may give rise to sexually dimorphic properties. To our knowledge, ours is the first study to assess genome-wide, developmental gene regulation in a female song nucleus, and to compare it with that of developmental regulation in the corresponding male song nucleus. Through this approach, we were able to assess the combined effects of sex and age in RA.

Many of RA's sexually dimorphic features demonstrate sensitivity to sex steroid hormones, particularly estrogen [reviewed in 61]. Most notably, the administration of estradiol to young female zebra finches prompts the development of masculinized song nuclei and singing in female zebra finches [82–88]. However, multiple lines of evidence imply that sex steroids alone are insufficient to fully determine sex differences in the song system. For one, estrogen-induced masculinization of females is only partial, as their song nuclei are still smaller than males [82, 83, 86, 88]. Also, efforts to block masculinization of the male song system have been mostly unsuccessful, producing only modest effects [78, 100, 101, 106]. Then, there is the case of the spontaneously arising gynandromorph, a singing zebra finch who was genetically male on one side of its body and female on the other [108]. The song nuclei on the genetically female side of the brain were smaller than those on the male side, demonstrating the insufficiency of circulating hormones to fully masculinize the song

system. Specifically for RA, recent work seems to suggest that early RA gene expression may be largely unaffected by estrogen manipulation [106]. Taken together, these studies imply that song system sex differences are also determined by hormone-independent and brain cell-autonomous mechanisms. One such theory that has gained traction is the influence of a cell's genetic sex via differential expression of sex-linked genes. In our study, sex differential genes at the outset of RA's divergent growth trajectory were overwhelmingly Z-linked. Thus, sex differences in Z-linked gene expression precede the development of gross morphological sex differences. This observation could be interpreted in support of the idea that differences in sex chromosome gene expression prime the developmental processes that orchestrate RA's sexually dimorphic transformation. However, we must also consider external factors that could initiate sexual dimorphism in RA, including the influence of cells outside of RA.

Some of the differential expression we observed may reflect transcriptional regulation in neurons that project into RA, as a substantial body of work demonstrates that RA afferents exert presynaptic influences on various aspects of RA development. Around 30-35 DPH, male RA is innervated by premotor song nucleus HVC [52, 302, 348], but whether this same projection forms in females and to what extent is a matter of debate. Although commonly described in the literature as absent, tract tracing [51, 89] and optical imaging of neural activity [349] seem to indicate that the HVC-RA projection forms in females. However, this HVC-RA projection is likely less robust in females, if only due to the fact that female HVC has many fewer cells than male HVC [52, 302, 348]. Lesions of HVC in 20 DPH males blocked subsequent increases in volume and soma size in RA [350], and prevented estrogen-induced masculinization of female RA [351]. This suggests HVC afferents may

encourage masculinization of RA. The other major input to RA is from LMAN, the output nucleus of the anterior pathway. Around 20 DPH, the LMAN-RA projection is comparable between sexes, but over vocal development there is a sexually dimorphic loss of neurons in females that ultimately results in a weaker projection [300]. Lesions of LMAN in 20 DPH males blocked subsequent increases in volume and cell number in RA [350, 352], and there is convincing evidence that neurotrophins transported from LMAN modulate cell survival in RA [338]. Importantly, however, lesions of HVC and LMAN do not entirely eliminate sexual dimorphism in RA, as the RA of lesioned males is still larger than that of unlesioned females [353]. Thus, afferent factors appear to influence RA, but are just one of many multifaceted processes driving RA development. As a bulk RNA-seq study, our results likely encompass transcriptomic signatures of factors both endogenous and exogenous to RA, and one challenge going forward will be to distinguish between them.

The direct assay of song nucleus tissue is a major advantage of this study. A few high-throughput studies of developmental gene expression in the zebra finch brain have included both males and females [44, 354, 355]. However, these studies utilized tissue from the whole brain or telencephalon, which produces a "brain average" expression level for each gene, at the expense of assessing the nuanced heterogeneity of gene expression in different brain regions. While some genes from these studies were individually screened for expression in the song system using histochemical methods, our approach of quantifying gene expression directly from microdissected song nucleus tissue is considerably more efficient and sensitive in detecting genes relevant to song system development. Another strength of our study is the precision with which the target nucleus was extracted. Instead of relying on separate reference slides, we captured RA directly from Nissl-stained sections in ethanol-fixed tis-

sue. This ensured that the boundaries of RA were clearly visible and that only RA cells were captured, even when tissue warping or large inter-slide morphology changes were apparent. We also note that this RNA-seq dataset was derived from high quality RNA and sequencing data. All samples were sequenced to sufficient read depth, and there were no batch effects or outlier samples. Furthermore, we did not pool our samples, which preserved information regarding interindividual variation for the genes assayed. Our study was carefully designed to minimize several confounds that could impact gene expression, including behavioral state, circadian rhythms, age variability, and genetic relatedness. Finally, our study enriches previous studies of gene expression in RA by extending expression profiles to females and/or additional developmental time points, while providing quantitative measures of gene expression at the transcript level.

By investigating the transcriptome at two time points along the development of a major sexual dimorphism, we have identified candidate genes and pathways potentially involved in establishing the observed sex differences. We acknowledge that not all genes and pathways identified in this study necessarily contribute directly to sexually dimorphic properties in RA, and some sex-biased genes may actually serve to prevent sex differences [356], thus further experimentation is required to evaluate candidate genes. Moreover, the fact that this was a bulk RNA-seq experiment, and that there are complex cytoarchitectural changes in RA (e.g. cell size, number, and density) limits our ability to draw conclusions about expression per cell or cell type. In the future, this could be overcome through the use of single-cell sequencing. Nonetheless, marked sex differences in developmental gene expression are a prominent feature of RA, and several cell type-specific enrichments were identified in our functional analysis, including oligodendrocyte differentiation in male and female

development, and GABAergic interneuron differentiation in the 50 DPH sex contrast. The observation that glial cell differentiation was enriched in female development is intriguing considering that early sex differences in non-neuronal RA cells have been hypothesized to contribute to sexual differentiation of RA [337].

Because we aligned to a male zebra finch genome assembly, we cannot evaluate the expression levels of W chromosome genes. It is likely that many reads from female samples which did not align to the genome originated from W chromosome genes. Another source of potentially ambiguous read mapping are the pseudoautosomal regions of the W chromosome, which contain genes homologous to Z chromosome genes. Presumably, Z/W genes that are pseudoautosomal would show lower male-to-female expression ratios than those that are Z-specific. Even with this caveat, the vast majority of Z chromosome genes showed male-biased expression, consistent with a lack of global dosage compensation in this species [136, 138].

Lastly, it is important to consider some limitations of our functional analyses. For one, genes were excluded that could not be assigned to a human gene, either due to differing gene symbols, or because there is in fact no ortholog in the human genome. Thus, many zebra finch-specific genes are missing from these functional analyses. In addition, not all genes have known functions, as many genes are lacking in functional annotations, or could have entirely different functions in zebra finches compared to mammals. Another thing worth noting is the relatively small number of genes driving the significant functional enrichments. Of the 6,201 total DEGs from all contrasts and the sex+age interaction, only 2,305 (37%) appeared in at least one enrichment of the over-representation results. Because relative gene ratios determine statistical significance, these enrichment analyses are somewhat

biased toward functional terms supported by the differential expression of many associated genes. This bias leaves open the possibility that some biological processes disproportionately affected by only a few key players are not represented in the functional results. Taking all this into consideration, it could be that a much wider array of biological processes is driving RA's development and sex differentiation. Evaluating this possibility would require more sensitive measures of a gene's functional impact, and major expansion of functional annotations for the zebra finch genome.

Author contributions

SRF wrote the manuscript. SRF was responsible for the conception and design of experiments, zebra finch colony management, tissue collection, laser capture microdissection, RNA isolation, data management and preprocessing, statistical analyses, and functional enrichment analyses. SRF and CVM interpreted the results. AN synthesized probe and performed in situ hybridizations. SRF and AN prepared figures. SRF and CVM acquired funding.

Acknowledgements

We wish to thank Denesa Lockwood for her instruction on laser capture microscopy; Peter V. Lovell for his help in brain dissections and postmortem sexing; Kristina Vartanian, Amy Carlos, Robert Searles, and Chris Harrington from the Oregon Health and Science University Massively Parallel Sequencing and Gene Profiling Shared Resources for their

guidance on RNA quality and sequencing; and Brett Davis for his instruction on RNA-seq analysis pipelines and statistics.

Chapter 4

Discussion

The goal of this dissertation was to elucidate the molecular bases of excitability and sexual dimorphism of the song system. I achieved this by creating detailed transcriptional profiles of the genes and gene networks implicated in these biological processes. Functional themes emerged from these data that yield novel insights into song nuclei specializations and sex-specific development. In addition, these large-scale efforts produced comprehensive and high quality data sets that I hope will be an asset to future studies. In this final chapter, I briefly summarize the major findings of my work, propose some future experiments, and discuss how studying female songbirds will radically enrich a classically male-oriented field.

4.1 Summary of major findings

4.1.1 Song system circuit elements tune their firing properties through ion channel gene expression

The song system is a discrete sensorimotor circuit that controls the complex processes of song learning and song production. Each song nucleus has a unique role in singing behavior, and exhibits distinct electrophysiological properties that are largely influenced by ion channels. Complementing an earlier study from our lab on potassium channels [160], we evaluated the genomics and song system expression of three major families of ion channels - sodium, calcium, and chloride. We found that the majority of sodium and calcium but few chloride channels showed differential expression in the song system, illustrating that song nuclei are electrophysiologically specialized relative to their surrounding brain region. For several ion channel genes, we noted a coordinated pattern of expression across multiple song nuclei, which might explain some of the firing characteristics shared between nuclei. In several cases, we observed sparse expression in only a subset of cells, which seems to correlate with the unique electrophysiological signatures of distinct cell populations within a given song nucleus. Finally, we found gene regulation of several ion channels that likely support high-frequency and burst firing in song nuclei. In summary, the electrophysiological properties that characterize song nuclei are reflected in unique configurations of expressed ion channel genes.

4.1.2 Extensive sex differences in gene expression and function during the development of a sexually dimorphic song nucleus

Singing behavior and song nuclei in zebra finches are highly sexually dimorphic. Over the course of song learning, song nucleus RA undergoes drastic developmental changes, including the emergence of sex differences in volume, cell size, cell density, cell number, firing properties, and connectivity (see Figure 3.2 for summary and references). To begin to understand the developmental dynamics in gene expression orchestrating these processes, we generated male and female RA transcriptomes for two developmental time points, before (20 DPH) and after (50 DPH) RA's major morphological sexual dimorphism has manifested. Mirroring the timeline of cytoarchitectural changes, we found that the transcriptional landscape of RA showed few sex differences in gene expression at 20 DPH, but an abundance of sex differential genes at 50 DPH. Most of the sex differential genes at 20 DPH were male-biased chromosome Z genes, reflecting the lack of global dosage compensation in this species, and raising the possibility that sex chromosome genes may disproportionately influence the initiation of sex differentiation processes in RA. Particularly compelling was the finding that male and female RA undergo two distinct developmental programs, as most of the affected genes and associated functional enrichments were unique to each sex. Intriguing male-specific pathways included metabolism, voltage-gated ion channels, cell growth and morphogenesis, axon development, and synapse organization. Female-specific enrichments were associated with establishing cell polarity, hormone signaling and response pathways, immune signaling, gene silencing, glial cell differentiation, and negative regulation of cellular movement. In addition, we found sex differences in several genes encoding transcription

factors, growth factors, apoptosis regulators, and sex steroid enzymes. Overall, these efforts identified transcriptomic dynamics that could feasibly explain the molecular basis of previously reported sex differences in RA, and in addition, revealed novel sex differences in genes and pathways underlying RA's development.

4.2 Future directions

4.2.1 In-depth studies of gene function

The studies described in this dissertation lay the groundwork for genetic and pharmacological manipulations to determine how ion channel, sex-biased, and developmentally regulated genes individually and cooperatively give rise to neuronal excitability and sexually dimorphic properties of vocal learning systems. Our work identified many promising candidate genes for followup studies to evaluate their cell type expression, subcellular localization, and function within the context of the zebra finch song system. Already, our lab has performed in-depth followup studies of sodium channel beta subunit gene SCN4B, establishing its role in generating resurgent sodium currents within RA projection neurons [303]. The *in situ* hybridization patterns and neural recordings from this study (Figure 4.1) are well complemented by the quantitative RNA-seq data discussed in Chapter 3, cohesively indicating that SCN4B is upregulated significantly in male but not female RA during song development, resulting in increasing resurgent currents in males. Neural recordings in juvenile RA brought to light sex differences in other firing properties, and the timing of their emergence tracked with the morphological and transcriptomic trajectory of RA's sexually

dimorphic development. These sex differences in firing properties that emerge over development likely reflect sex-dependent shifts in the complement of voltage-gated ion channels in RA neurons, and this idea is strongly supported by the RNA-seq data showing widespread developmental and sex-specific changes in voltage-gated ion channel gene expression.

Some of the most intriguing candidate genes are those that are definitive markers of song nuclei, as they illustrate a molecular specialization of a song circuit element relative to its surround. The analysis of markers in Chapter 3 found that many adult RA marker genes showed sex differences and developmental regulation during the song learning period. However, we do not yet know the extent to which these markers may show similar expression patterns in female RA. When evaluating select genes using *in situ* hybridization, we found evidence that some adult male RA marker genes, such as SLC4A4 and LPL, are RA markers in both males and females during development, prompting a need for additional experiments to determine whether their female marker status persists into adulthood. Genes that are markers of RA in both sexes may hint at shared properties of this song nucleus. In contrast, RA markers that are male-specific may provide further insights into the neural mechanisms of vocal learning, while those that are female-specific may provide clues to the elusive function of RA in non-singing female zebra finches. Performing a comparison of transcription factor binding sites for these genes would be useful in identifying potential "master regulators" of sex-specific gene regulation, and in evaluating the role of sex steroids to influence these genes (see next section).

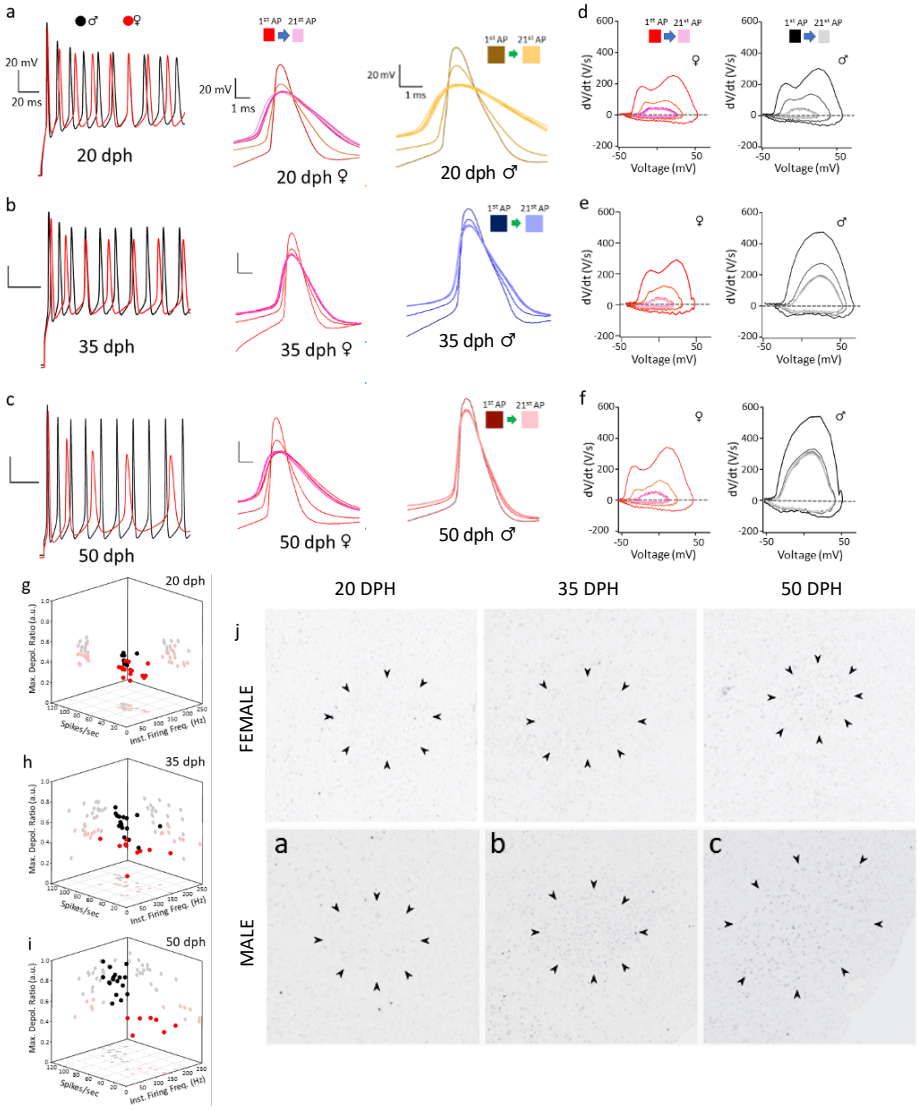

Figure 4.1: Sex-dependent developmental changes in intrinsic excitable properties of RA projection neurons (RAPNs). **a-c**. Male and female RAPNs show developmental decreases and increases, respectively, in action potential (AP) widths during a spike train. Left: Representative AP trains elicited by a 500 pA current injection in RA projection neurons in males (black) and females (red) across ages. Right: APs #1, 2 and 16-21 from the traces on the left aligned at the peaks for each age group in females and males. **d-f**. Phase plane plots from APs #1, 2, and 16-21 plotted at the same scale for all age groups for females (left) and males (right). **g-i**. 3D dot plots showing the instantaneous firing frequency, number of spikes per second and the fold-change in maximum depolarization rate between the 2nd and 1st APs during a 1 sec 500 pA current injection in male (black) and female (red) RA projection neurons. **j**. Developmental SCN4B mRNA expression pattern in female (top) and male (bottom) RA (indicated by arrowheads) in $10\,\mu\mathrm{m}$ sagittal brain sections. Figure adapted from Figures 6 and 10 of [303]

4.2.2 The intersection of transcriptomics and hormone action

The RNA-seq study of developmental sex differences in gene expression found an abundance of sex-biased and developmentally regulated genes, but the question remains to what extent those transcriptional metamorphoses are hormone-mediated. Hormone receptors can alter gene expression by acting directly on the genome, or through non-genomic mechanisms that do not involve DNA binding. One feasible way to investigate the genomic interaction between sex steroid hormones and gene expression is to examine hormone response elements (HREs), for example androgen and estrogen response elements (AREs and EREs). HREs are DNA binding motifs typically composed of inverted repeats separated by three spacer nucleotides [357]. Once activated, nuclear hormone receptor complexes exert direct genomic effects by binding to HREs in the genome, and regulating transcription. Although known HRE sequences may be easy to locate in the genome, the relationship between hormones, HREs, and gene expression is far from direct due to several factors [reviewed in 358]. For one, the ultimate effect of any given HRE on gene expression depends upon the interplay of many coactivators and intermediary transcription factors that make up the hormone receptor complex. Added complexity is introduced through variations in HRE sequences, which affect hormone receptor binding affinity. Additionally, genomic effects of hormone receptors are not limited to HREs, as evidenced by the fact that over one third of human genes regulated by estrogen receptors do not contain EREs [359]. Hormone receptors can exert indirect genomic effects by binding to transcription factors that target other DNA binding motifs. Still, it may be worthwhile to adopt a simplified approach and evaluate which zebra finch genes contain conserved AREs and EREs within a prescribed distance

of transcription start sites [360]. This response element analysis would identify the subset of estrogen- and androgen- sensitive genes that are subject to direct genomic effects. One method to widen the net to genes regulated by indirect genomic and non-genomic effects of hormones would be to compare the song nucleus transcriptomes of hormone-treated versus control animals. Considering the age-dependent effects of estrogen treatment on the zebra finch song system [85], ideally this proposed study would include several developmental time points. Together, these experiments would define a suite of hormone-sensitive genes, and delineate those modulated through direct HRE binding effects from those modulated through indirect mechanisms. The proportion of sex-biased genes that display hormone sensitivity would provide a relative measure of the extent to which hormones influence sex-dependent gene expression. For example, a large proportion might indicate that sex differences arise mainly from hormone-mediated gene regulation. In contrast, a small proportion could mean that sex differential processes proceed in a mostly hormone-insensitive fashion via genomic and/or other mechanisms. So far, the evidence for RA seems to suggest that estrogen has only moderate effects on specialized gene expression during development, as the transcriptomes of 30 DPH male and female zebra finches treated with estradiol or an estrogen-inhibitor were not remarkably different from untreated animals [106].

4.3 Towards a new, sex-inclusive era of songbird research

Research efforts aimed at understanding the behavioral role and neural basis of female song are relatively recent, as historically, the songbird field has focused on male songbirds. In the classic songbird paradigm, females are often circumscribed as recipients or evalu-

ators of male song, thus female song and song systems has received comparatively little attention. This male bias in songbird research can likely be attributed to a confluence of factors. For one, research in the songbird field has been dominated by extensive study of a few, mostly temperate species in which females do not sing [361, 362]. The most commonly used songbird models - zebra finches, canaries, and Bengalese finches - are species in which the females do not sing, a fact which has biased the study of vocal learning mechanisms toward male songbirds. Similarly, classic field studies have predominantly focused on North American songbird species where song is absent in females. Compounding the issue of male-focused field studies is the challenge of sex identification, as species where both males and females sing tend to be less sexually dimorphic in plumage [363]. It may also be the case that females generally sing less conspicuously than males, for example less frequently or obscured in the nest [364, 365]. Another contributing factor may be that only relatively recently have granting institutions implemented policy changes that require major justification for the exclusion of female subjects from studies. "Only males sing" may be sufficient justification for some behavioral studies, but nonetheless, designing studies to include females even when female song is absent for a species can offer considerable explanatory power and valuable experimental controls. Case in point, female zebra finch RA expresses lower levels of SCN4B, providing a natural contrast to males in recent work from our lab exploring the role of SCN4B in RA projection neurons [303]. Though scarcely acknowledged in the literature, decades of songbird research has in fact produced a detailed model of male vocal learning, with little knowledge of whether its principles generalize to females in species with female song. In addition, this myopic scope has fostered the perception that song-less females are the norm for songbirds, a view that has recently been

challenged by comparative studies.

4.3.1 Female song as the ancestral state

In 2014, Odom et al. [366] surveyed the presence or absence of female song in 34 songbird families, and concluded that female song is likely the ancestral state in songbirds (Figure 4.2). This publication marked a pivotal moment for the songbird field, prompting a reexamination of the long-held dogma that female song was a rare oddity. It is important to note that while the authors' conclusion is highly compelling, the assessments for most species included in the study were based not on detailed descriptions or recordings of female song, but somewhat anecdotal descriptions in published fieldguides. Many species' fieldguide descriptions lacked any mention of the presence or absence of female song at all. Despite these limitations, the phylogenetic distribution of species that ostensibly possess female song strongly indicates that male and female song was present in the ancestor of all songbirds. Notably, several other phylogenetic studies support this finding [363, 367–370]. Taken together, these studies paint a picture in which female song was present in the songbird ancestor, and progressively lost in some lineages, especially those evolved to occupy temperate niches and/or migrate.

In the *Estrildidae* family of songbirds, home to the zebra finch, female song has been documented for several species [371]. In general, detailed characterizations of song are lacking for estrildid species, however there are exceptions. One such species is the blue-capped cordon-bleu, for which complex, learned song is well established for males and females [372, 373]. During courtship displays, both sexes of this species sing while producing

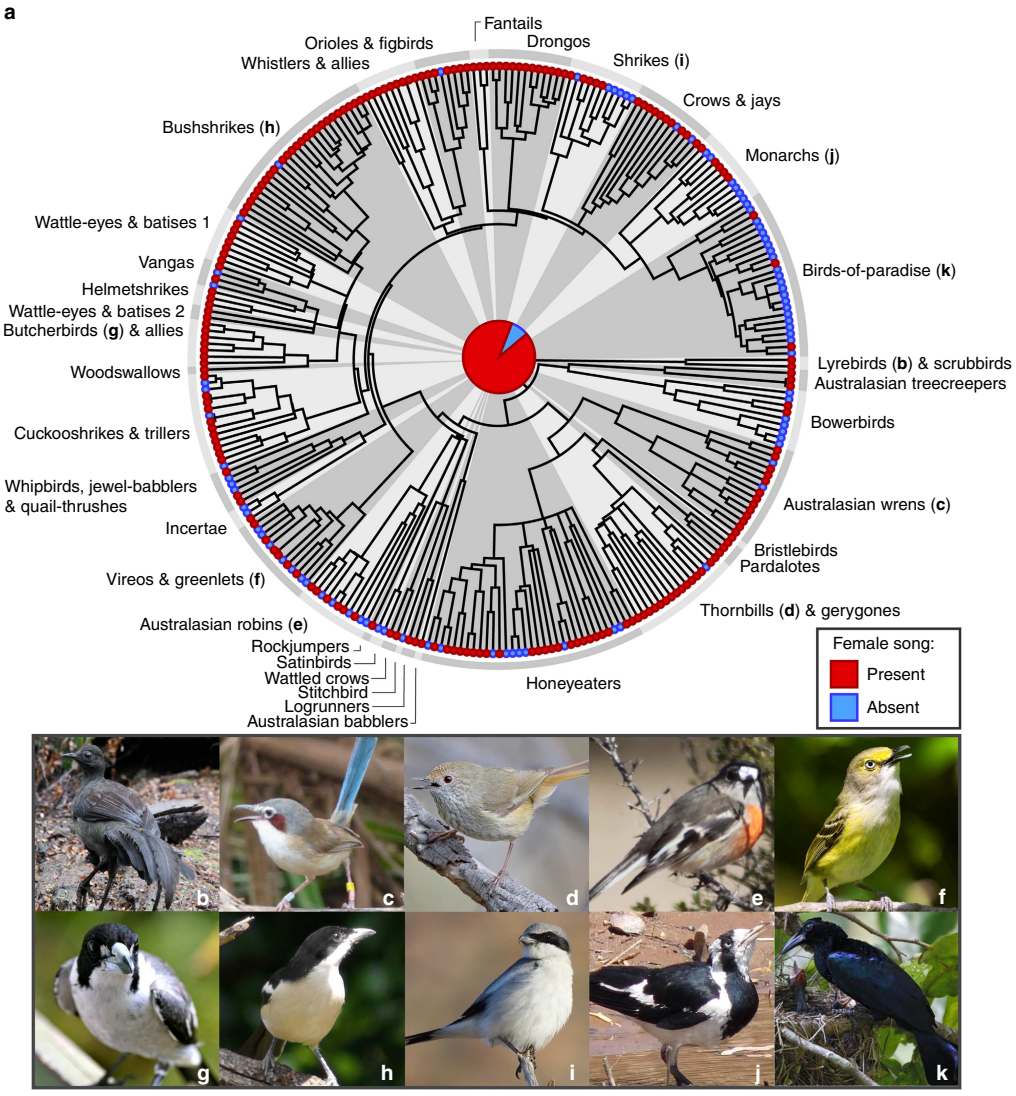

Figure 4.2: Ancestral state reconstruction of female song on a phylogenetic tree of songbirds. The tree (**a**) includes all species for which female song could be scored as present or absent (323/1,141 species from 34/44 songbird families). Female song was present in 229 species (32 families; red terminal nodes) and female song was absent in 94 species (19 families; blue terminal nodes). The pie chart in the centre shows that female song is reconstructed as present (red) in the common ancestor of modern songbirds (92% maximum-likelihood probability strongly supported by a likelihood decision threshold of 2.0). Pictures show females of the following species with female song from families throughout the phylogeny; (**b**) superb lyrebird (*Menura novaehollandiae*; (**c**) purple-crowned fairywren (*Malurus coronatus*; (**d**) brown thornbill (*Acanthiza pusilla*; (**e**) scarlet robin (*Petroica boodang*; (**f**) white-eyed vireo (*Vireo griseus*; (**g**) grey butcherbird (*Cracticus torquatus*; (**h**) tropical boubou (*Laniarius aethiopicus*; (**i**) loggerhead shrike (*Lanius ludovicianus*; (**j**) magpie-lark (*Grallina cyanoleuca*; (**k**) curl-crested manucode (*Manucodia comrii*). Figure adapted from [366]

.

rhythmic foot taps, making for an impressive multimodal display [374]. With a sequenced genome and captive colony, blue-capped cordon-bleus are emerging as a promising songbird model to investigate shared versus sex-specific features of vocal learning [375].

The distribution of female song throughout the estrildid family shows a strong phylogenetic signal, as the presence of female song tends to be clustered within branches containing closely related species [376]. The zebra finch lies within an early branch of the Estrildid tree, surrounded exclusively by related species for which there is no evidence that females sing. Parsimony would suggest female song was lost in the common ancestor to this particular branch containing zebra finches. Given that zebra finches lack a phylogenetic neighbor with female song, a more compelling comparative study would focus on pairs of estrildid species from mixed branches where female song was lost in only one of the pair. Comparing the genomic and transcriptomic properties that distinguish female singers from nonsingers could reveal genomic signatures of female song loss versus retention, and including multiple pairs could increase the signal to noise ratio of genomic signatures specifically related to female song. In particular, finding consistent genomic signatures across several pairs would suggest conserved evolutionary mechanisms for the loss or retention of female song.

4.3.2 Characteristics of female song

There is considerable variance across songbird species in the nature and extent of differences between male and female song. Studies of acoustic properties have observed a number of differences in select species; compared to male song, female song can be shorter, lower in amplitude, less frequent, less complex, or in some cases more frequent [364, 365, 377–

382]. While it is tempting to speculate that a widely shared feature of female song is that it is less robust than male song, evaluating this possibility requires concerted and collaborative efforts to significantly expand the library of female song recordings.

One trait that seems to correlate highly with female song is whether the species inhabits a tropical or temperate zone. In temperate species, it is commonly the case that males sing and females are mostly songless [362, 383, 384]. Robust female song has been observed in several temperate species, such as the streak-backed oriole [379], the house wren [365], and the eastern bluebird [380, 385]. Because the study of female song is nascent, there are probably many more temperate species with singing females yet unrecognized. Compared to temperate species, the females of tropical species are more likely to display elaborate singing abilities [362, 379, 386]. In many tropical species, males and females perform intertwined duets, singing in a temporally precise and coordinated fashion [reviewed in 383, 387, 388].

The function of song varies between sexes and across species. A common function of male song is to attract mates and defend territory [361, 389]. Male zebra finches diverge from this pattern somewhat in that they do not sing in defense of territory, but rather to attract mates, uphold pair bonds, and maintain auditory contact [21]. While females of some species use song for mate attraction and territory defense [378, 390], females of other species sing to defend resources [390, 391], confront other females [378], deter predators [392], and communicate with mates, including to maintain pair bonds [389]. Duets produced by tropical species function in territory defense, mate-guarding, solicitation of copulation, and coordination of reproductive behaviors between mates [383, 387, 388].

4.3.3 Female song systems

The neuroanatomy of the female song system has only been characterized for a handful of songbird species [reviewed in 393]. Overall, these studies have found that female song nuclei are smaller in volume than male song nuclei. Early in the study of the song system, it was hypothesized that the degree of song system sexual dimorphism may determine the extent of sex differences in singing behavior. Though compelling, this ostensibly direct correlation between neuroantomical sex differences in song nuclei and singing has not consistently held up when a variety of songbird species are surveyed. For example, some studies found correlations between female song repertoire size and the volume of song nuclei [393, 394], while others found no correlation [395, 396]. Of particular note is the streak-backed oriole, a species where females sing more than males, yet the female song system is markedly smaller than that of males [397]. On the other hand, a few studies that have attempted to control for phylogenetic history support the idea that sex differences in the song system and singing behavior coevolved [393, 398]. Given the large radiation of songbirds and limited number surveyed for female song or neuroanatomy, additional studies need to be carried out to evaluate which features of sexual dimorphism may predict sex differences in specific measures of song. Of course, we are still left with the confounding fact that some female songbirds possess song nuclei, yet do not sing at all.

When I learned that nonsinging female zebra finches have song systems, I was baffled and struck by a deep curiosity. Even if we assume that zebra finch female song regions are "leftovers" from an evolutionary past when both sexes sang, the current function of that female song system is a tantalizing mystery. Is the female zebra finch song system vestigial,

slowly evolving away until it disappears, like the eyes of a cave dwelling salamander, or is it evolving to stick around and serve a novel as-yet-unknown function? In the case of RA, there is evidence that female RA receives projections from HVC [51, 89, 349], and sends projections to nXIIts [51, 306]. The only study to my knowledge that has demonstrated a direct role of zebra finch RA in female vocal production showed that intact RA is necessary for the precise timing of rhythmic calling between birds [399]. A few studies suggest song nuclei in female zebra finches may be functioning in the evaluation of song; female zebra finches may not learn to produce song, but they do learn to discriminate between different males' songs [400–402].

Further studies are necessary to determine the function of the song system in song-less females. For one, much could be learned from additional studies of connectivity to determine the afferents and efferents of female song nuclei. We also have yet to determine what kind of stimuli or behaviors activate female song nuclei, a question that could be answered with neural recordings of female song nuclei in awake behaving birds. One final question to consider is what happens to the "empty space" left by a regressing song system? Simply due to vicinity, it seems logical that the sexually dimorphic volumes of song nuclei impose sex differences on surrounding brain regions, potentially affecting cell number, size, or density. For example, RA sits within the arcopallium, a highly interconnected brain region that outputs many descending sensory and motor projections, and is composed of several distinct subdomains [403]. A recent study from the Mello lab found that female zebra finches share at least one of these subdomains, but the rest of the female arcopallium remains to be characterized [404]. Interestingly, the camera lucida drawings from this study (Figure 4.3E) define a female arcopallium (blue outlines) that appears considerably smaller than that of

males. More rigorous anatomical quantification is needed to confirm this sex difference, but assuming this sex difference is robust, size differences in the arcopallium might reflect ripple effects of the sexually dimorphic evolution of song nucleus RA. The functional implications of song nuclei-adjacent regions "rearranging" due to growth or shrinkage of song nuclei are entirely unknown and ripe for investigation.

4.3.4 Broader implications of sex-inclusive research

It is imperative that we investigate the mechanisms and functions of female song if we are to form a complete, evolutionary picture of vocal communication in songbirds. A crucial piece of this puzzle is characterizing female song systems in songbird species both with and without female song, as each can provide distinct insights into the evolution of this trait. Turning to females to investigate behaviors that have traditionally been studied in males will lead to novel insights on the evolution and mechanisms of sexual dimorphism, as well as expand our understanding of how complex behaviors may serve different functions in males and females of the same species. In a wider and more clinical context, there are striking sex biases in neurodegenerative diseases, autism, anxiety disorders, and speech disorders, and we will overlook crucial insights into their mechanisms and potential treatment if we only carry out investigations in one sex. Finally, understanding sex differences in the brain as a source of neurodiversity has deep and sweeping impacts on societal systems, scientific reproducability and applicability, and fundamental principles of biology and behavior.

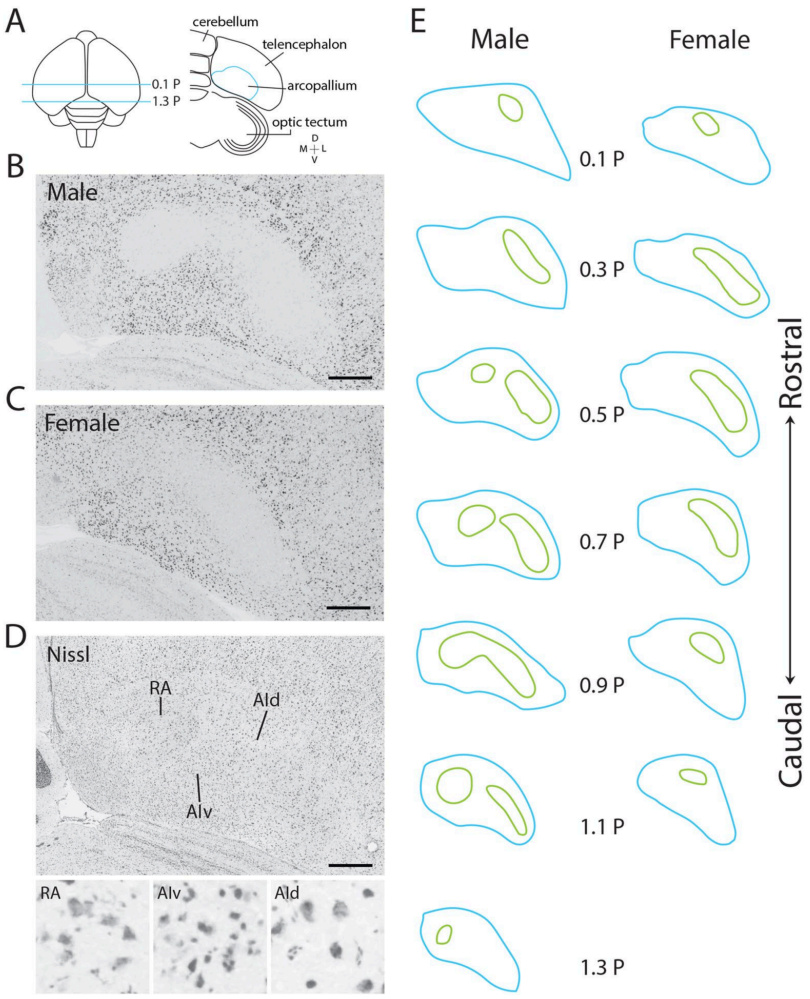

Figure 4.3: Potential sexual dimorphism in the size of zebra finch arcopallium. Molecular definition of RA and AId in adult zebra finches. (**A**) Top left: Top-down view of a schematic drawing of the zebra finch brain; blue lines indicate the range of frontal sections examined. Top right: Drawing of a frontal section at 0.7P; blue line indicates the boundaries of the arcopallium, seen under Nissl staining. (**B,C**) SCN3B in situ hybridization images from a male and a female. RA and AId appear continuous in the male, and RA is indistinguishable in the female. (**D**) Nissl-stained frontal section through arcopallium at the center of RA in a male; RA, but not AId, has clear cytoarchitectonic boundaries. Small panels show high power views (100×100 µm images) within RA, AIv, and AId. (**E**) Drawings depicting SCN3B expression boundaries (green) in serial frontal sections through the arcopallium (blue) of adult male (lef) and female (right) zebra fnches. *AId* dorsal intermediate arcopallium, *AIr* rostral intermediate arcopallium, *AIv* ventral intermediate arcopallium, *RA* robust nucleus of the arcopallium. Scale bar: $400\,\mu\mathrm{m}$ for all images. Figure adapted from [404]

Supplementary Figures

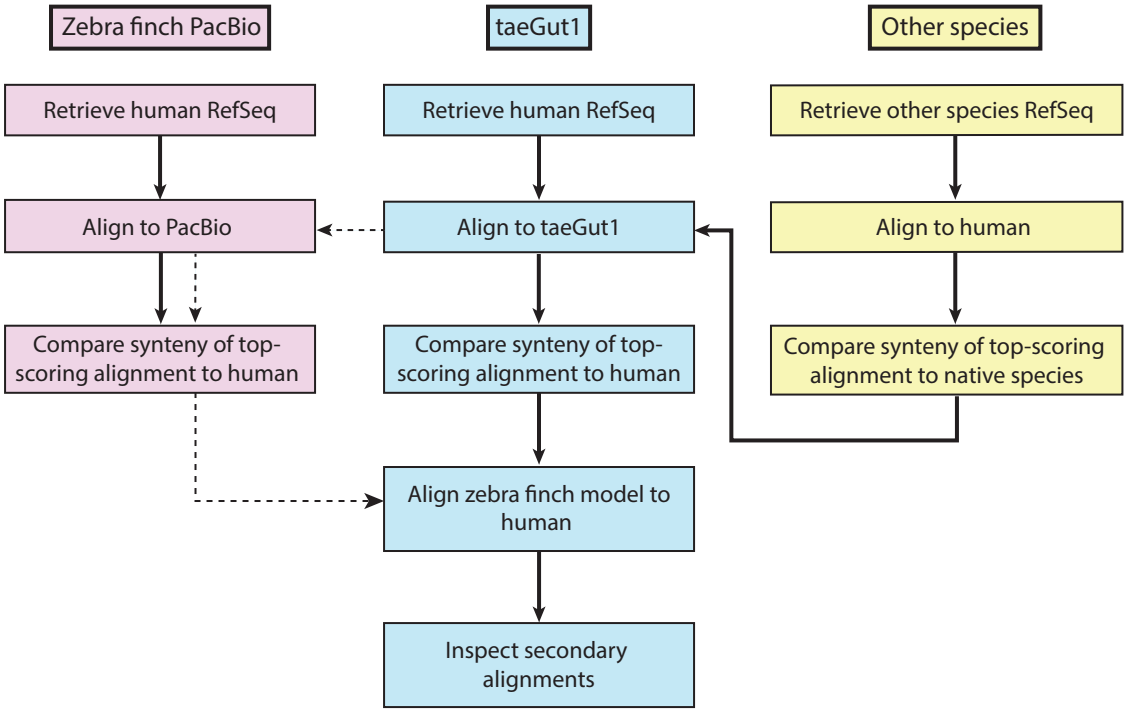

Supplementary Figure S2.1: Overview of ortholog identification pipeline. Each box represents a step toward identifying an ortholog in zebra finch. Arrows connecting boxes indicate the most common workflows. Details of main pipeline (blue) and all variations (Cases 1-6), including the use of zebra finch PacBio (pink) and other species (yellow), can be found in the Methods section of Chapter 2. Dotted line indicates Case 4, where there is limited synteny information in taeGut1 and PacBio is required for verification.

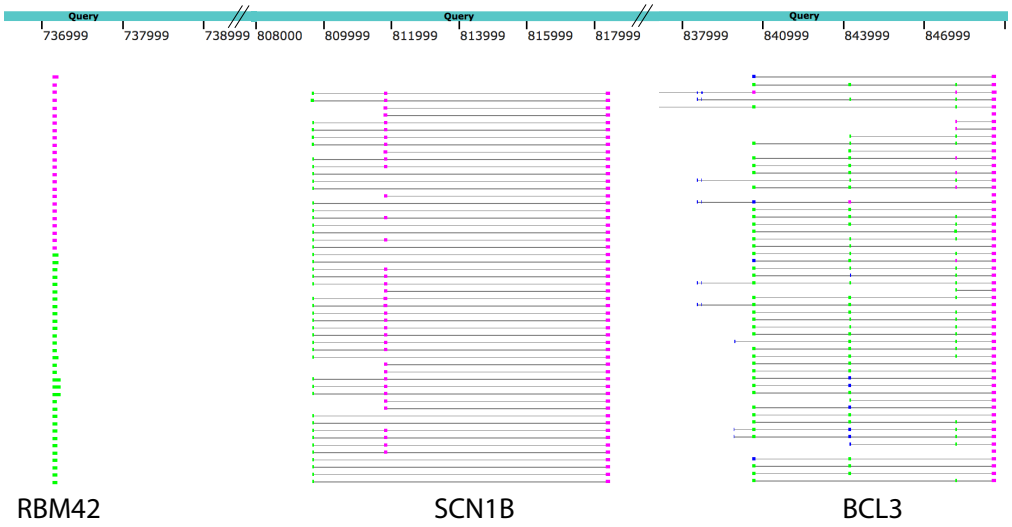

Supplementary Figure S2.2: Confirming orthology in the PacBio assembly using BLAST. Graphic summary of BLAST results demonstrating that SCN1B is present on gap-less PacBio scaffold MUGN01000920.1 with conserved exon structure and the conserved syntenic genes BCL3 and a fragment of RMB42 (see Figure 2.2). Numbers indicate location (bases) along the scaffold. All alignments shown are non-avian RefSeqs. Double dashes indicate additional contracted sequence between selected regions shown.

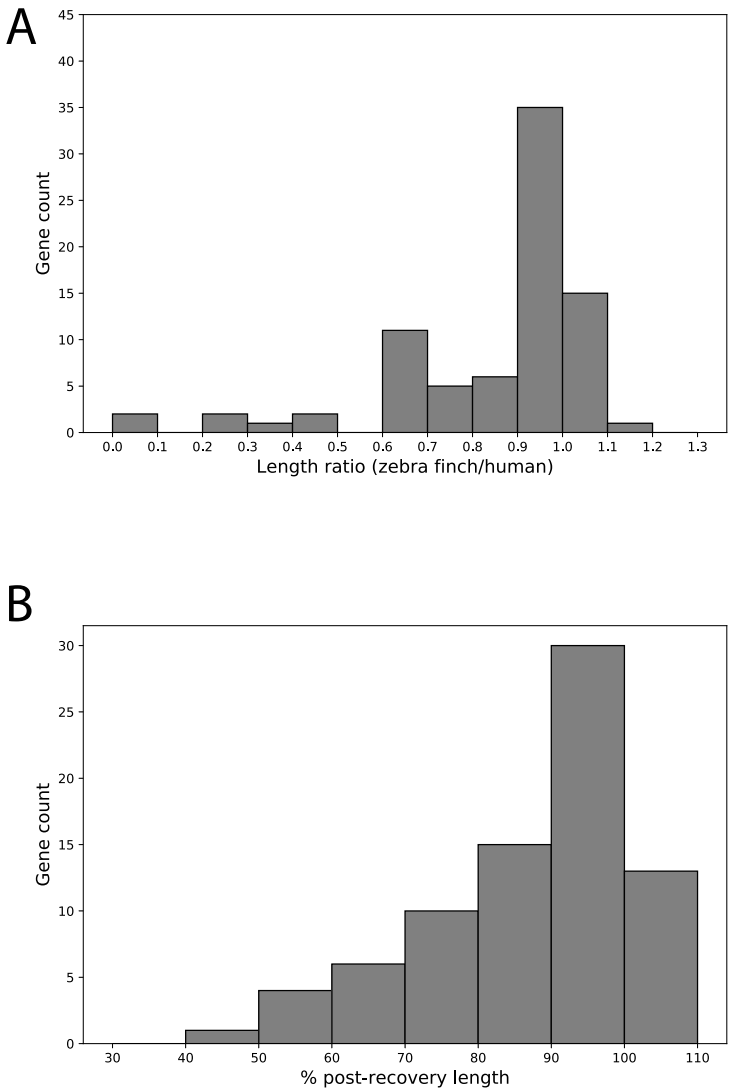

Supplementary Figure S2.3: Quantitative analysis of zebra finch model completeness. A) Frequency histogram of genes by zebra finch/human model length ratio. B) Frequency histogram of genes by percent of post-recovery length.

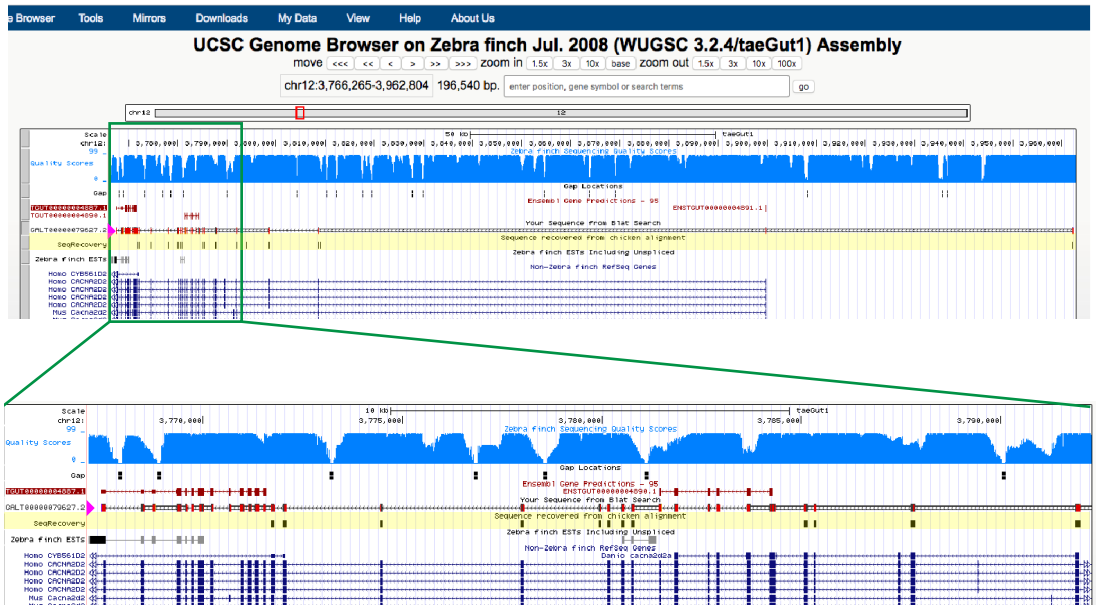

Supplementary Figure S2.4: Visualization of sequence recovery for a gene with split models. The zebra finch gene, CACNA2D2, is displayed using the UCSC Genome Browser. A zoomed-in region from within the green rectangle is shown in the bottom panel to highlight the detailed structure of alignments. This gene has three partial zebra finch Ensembl models (dark red track) in a region with numerous gaps (black Gap tack). Note the dips in sequence quality scores (light blue track) surrounding the gaps. Alignment of a more complete chicken model (magenta arrowheads) reveals additional sequence blocks that are missing from the zebra finch model, displayed in the SeqRecovery BED track highlighted in yellow. Non-zebra finch RefSeqs (dark blue tracks) provide further support for blocks of additional sequence recovered through alignments of the chicken model.

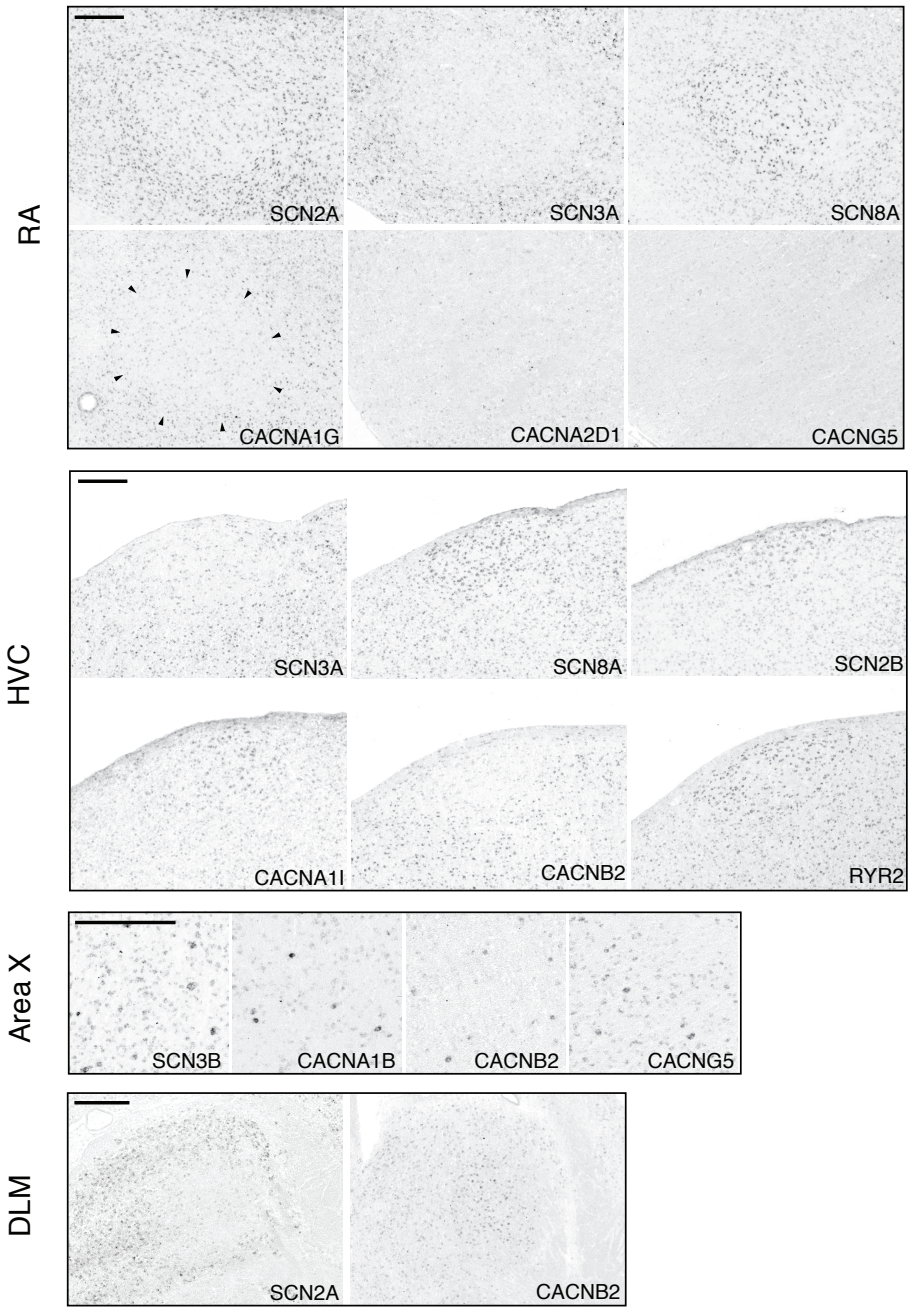

Supplementary Figure S2.5: Additional *in situ* hybridization photomicrographs of select ion channel genes in song nuclei RA, HVC, Area X, and DLM. All genes are differentially expressed except for CACNA2D1 and CACNG5 in RA, which appear to label sparse populations of cells. Area X panels show select genes with enhanced expression in sparse populations of cells. Camera lucida drawings indicating the location of these nuclei can be found in Figure 2.5a for RA, Figure 2.6a for HVC, Figure 2.7a for Area X, and Figure 2.8a for DLM. Gene abbreviations are given in Table 2.1. All scale bars = $500\,\mu\mathrm{m}$.

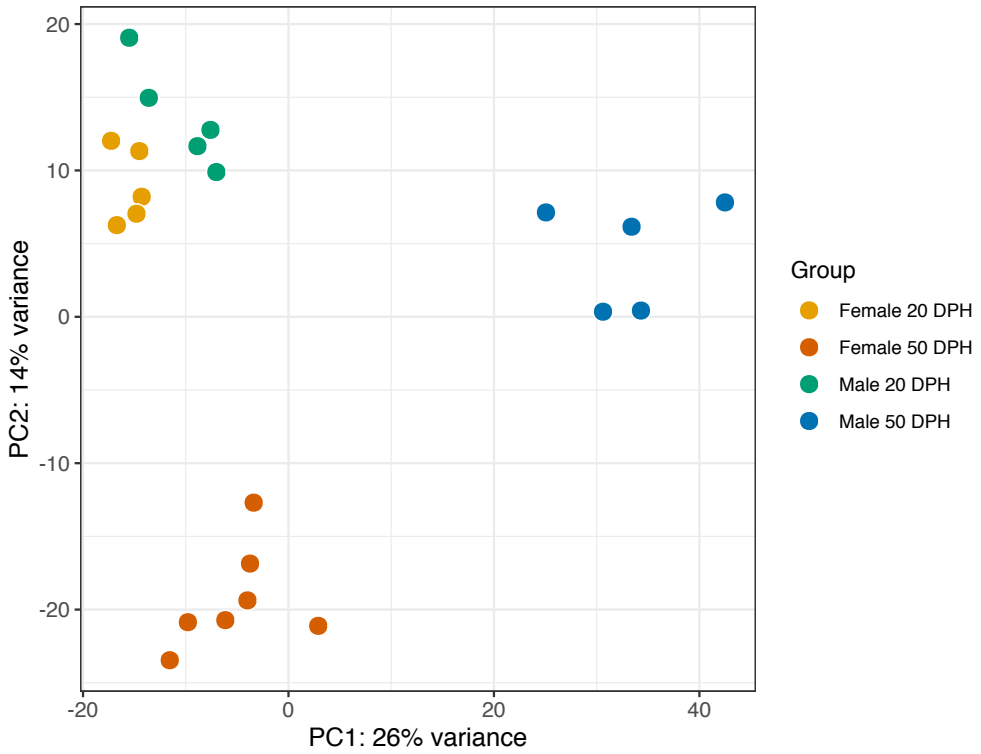

Supplementary Figure S3.1: PCA plot of all RNA-seq samples based on all assessed genes (n=21,955). Sample group is indicated by color. 20 DPH male (green) and female (yellow) samples cluster together, but can be bisected by a diagonal line through the cluster.

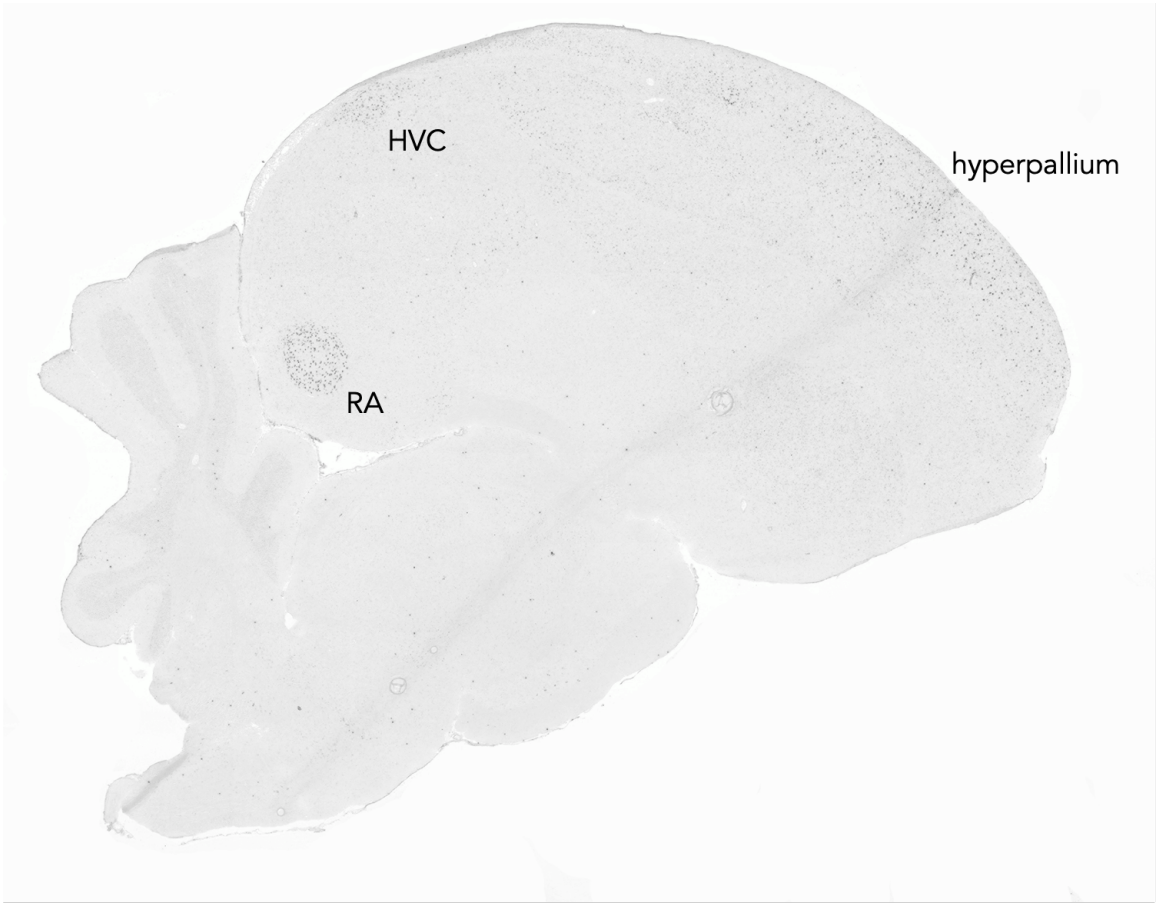

Supplementary Figure S3.2: LPL expression in adult song system. *In situ* hybridization of LPL in a parasagittal section of an adult male zebra finch. LPL expression is high in hyperpallium, and in song nuclei RA and HVC.

References

1. Griffith, S. C. & Buchanan, K. L. The Zebra Finch: The Ultimate Australian Supermodel. *Emu - Austral Ornithology* **110,** v–xii (2010).

2. Haesler, S. *et al.* Incomplete and Inaccurate Vocal Imitation after Knockdown of FoxP2 in Songbird Basal Ganglia Nucleus Area X. *PLoS Biology* **5,** e321 (2007).

3. Winograd, C., Clayton, D. & Ceman, S. Expression of Fragile X Mental Retardation Protein within the Vocal Control System of Developing and Adult Male Zebra Finches. *Neuroscience* **157,** 132–142 (2008).

4. Tanaka, M., Alvarado, J. S., Murugan, M. & Mooney, R. Focal Expression of Mutant Huntingtin in the Songbird Basal Ganglia Disrupts Cortico-Basal Ganglia Networks and Vocal Sequences. *Proceedings of the National Academy of Sciences* **113,** E1720–E1727 (2016).

5. George, J. M., Jin, H., Woods, W. S. & Clayton, D. F. Characterization of a Novel Protein Regulated during the Critical Period for Song Learning in the Zebra Finch. *Neuron* **15,** 361–372 (1995).

6. Miller, J. E., Hafzalla, G. W., Burkett, Z. D., Fox, C. M. & White, S. A. Reduced Vocal Variability in a Zebra Finch Model of Dopamine Depletion: Implications for Parkinson Disease. *Physiological Reports* **3,** e12599 (2015).

7. Swaddle, J. P. & Cuthill, I. C. Preference for Symmetric Males by Female Zebra Finches. *Nature* **367,** 165–166 (1994).

8. Griffith, S. C. & Buchanan, K. L. Maternal Effects in the Zebra Finch: A Model Mother Reviewed. *Emu - Austral Ornithology* **110,** 251–267 (2010).

9. Birkhead, T. R., Pellatt, E. J., Brekke, P., Yeates, R. & Castillo-Juarez, H. Genetic Effects on Sperm Design in the Zebra Finch. *Nature* **434,** 383–387 (2005).

10. Blount, J. D., Metcalfe, N. B., Birkhead, T. R. & Surai, P. F. Carotenoid Modulation of Immune Function and Sexual Attractiveness in Zebra Finches. *Science* **300,** 125–127 (2003).

11. Mundy, N. I. *et al.* Red Carotenoid Coloration in the Zebra Finch Is Controlled by a Cytochrome P450 Gene Cluster. *Current Biology* **26,** 1435–1440 (2016).

12. Zeigler, H. P. & Marler, P. *Neuroscience of Birdsong* xvii, 550. xvii, 550. ISBN: 978-0-521-86915-7 (Cambridge University Press, New York, NY, US, 2008).

13. Mello, C. V. The Zebra Finch, Taeniopygia Guttata: An Avian Model for Investigating the Neurobiological Basis of Vocal Learning. *Cold Spring Harbor Protocols* **2014,** pdb.emo084574 (2014).

14. Brainard, M. S. & Doupe, A. J. What Songbirds Teach Us about Learning. *Nature* **417,** 351–358 (2002).

15. Petkov, C. I. & Jarvis, E. Birds, Primates, and Spoken Language Origins: Behavioral Phenotypes and Neurobiological Substrates. *Frontiers in Evolutionary Neuroscience* **4** (2012).

16. Jarvis, E. D. Evolution of Vocal Learning and Spoken Language. *Science* **366,** 50–54 (2019).

17. Doupe, A. J. & Kuhl, P. K. Birdong and Human Speech: Common Themes and Mechanisms. *Annual Review of Neuroscience* **22,** 567–631 (1999).

18. Karten, H. J. Neocortical Evolution: Neuronal Circuits Arise Independently of Lamination. *Current Biology* **23,** R12–R15 (2013).

19. Pfenning, A. R. *et al.* Convergent Transcriptional Specializations in the Brains of Humans and Song-Learning Birds. *Science* **346,** 1256846 (2014).

20. Haesler, S. *et al.* FoxP2 Expression in Avian Vocal Learners and Non-Learners. *Journal of Neuroscience* **24,** 3164–3175 (2004).

21. Zann, R. *The Zebra Finch: A Synthesis of Field and Laboratory Studies* 335 pp. ISBN: 978-0-19-854079-3 (Oxford University Press, 1996).

22. Price, P. H. Developmental Determinants of Structure in Zebra Finch Song. *Journal of Comparative and Physiological Psychology* **93,** 260–277 (1979).

23. Geberzahn, N. & Derégnaucourt, S. Individual Vocal Recognition in Zebra Finches Relies on Song Syllable Structure Rather than Song Syllable Order. *Journal of Experimental Biology* **223** (2020).

24. Sossinka, R. & Böhner, J. Song Types in the Zebra Finch Poephila Guttata Castanotis. *Zeitschrift für Tierpsychologie* **53,** 123–132 (1980).

25. Jarvis, E. D., Scharff, C., Grossman, M. R., Ramos, J. A. & Nottebohm, F. For Whom the Bird Sings: Context-Dependent Gene Expression. *Neuron* **21,** 775–788 (1998).

26. Riters, L. V. & Stevenson, S. A. Reward and Vocal Production: Song-Associated Place Preference in Songbirds. *Physiology & Behavior* **106,** 87–94 (2012).

27. Feenders, G. *et al.* Molecular Mapping of Movement-Associated Areas in the Avian Brain: A Motor Theory for Vocal Learning Origin. *PLoS ONE* **3,** e1768 (2008).

28. Nottebohm, F., Stokes, T. M. & Leonard, C. M. Central Control of Song in the Canary, Serinus Canarius. *The Journal of Comparative Neurology* **165,** 457–486 (1976).

29. Nottebohm, F., Kelley, D. B. & Paton, J. A. Connections of Vocal Control Nuclei in the Canary Telencephalon. *The Journal of Comparative Neurology* **207,** 344–357 (1982).

30. Bottjer, S. W., Miesner, E. A. & Arnold, A. P. Forebrain Lesions Disrupt Development but Not Maintenance of Song in Passerine Birds. *Science* **224,** 901–903 (1984).

31. Sohrabji, F., Nordeen, E. J. & Nordeen, K. W. Selective Impairment of Song Learning Following Lesions of a Forebrain Nucleus in the Juvenile Zebra Finch. *Behavioral and Neural Biology* **53,** 51–63 (1990).

32. Scharff, C. & Nottebohm, F. A Comparative Study of the Behavioral Deficits Following Lesions of Various Parts of the Zebra Finch Song System: Implications for Vocal Learning. *Journal of Neuroscience* **11,** 2896–2913 (1991).

33. Cardin, J. A., Raksin, J. N. & Schmidt, M. F. Sensorimotor Nucleus NIf Is Necessary for Auditory Processing but Not Vocal Motor Output in the Avian Song System. *Journal of Neurophysiology* **93,** 2157–2166 (2005).

34. Williams, H. & Vicario, D. S. Temporal Patterning of Song Production: Participation of Nucleus Uvaeformis of the Thalamus. *Journal of Neurobiology* **24,** 903–912 (1993).

35. Vicario, D. S. Organization of the Zebra Finch Song Control System: Functional Organization of Outputs from Nucleus Robustus Archistriatalis. *The Journal of Comparative Neurology* **309,** 486–494 (1991).

36. Bottjer, S. W., Halsema, K. A., Brown, S. A. & Miesner, E. A. Axonal Connections of a Forebrain Nucleus Involved with Vocal Learning in Zebra Finches. *The Journal of Comparative Neurology* **279,** 312–326 (1989).

37. Vates, G. E. & Nottebohm, F. Feedback Circuitry within a Song-Learning Pathway. *Proceedings of the National Academy of Sciences* **92,** 5139–5143 (1995).

38. Johnson, F., Sablan, M. M. & Bottjer, S. W. Topographic Organization of a Forebrain Pathway Involved with Vocal Learning in Zebra Finches. *The Journal of Comparative Neurology* **358,** 260–278 (1995).

39. Warren, W. C. *et al.* The Genome of a Songbird. *Nature* **464,** 757–762 (2010).

40. Mello, C. V., Vicario, D. S. & Clayton, D. F. Song Presentation Induces Gene Expression in the Songbird Forebrain. *Proceedings of the National Academy of Sciences* **89,** 6818–6822 (1992).

41. Mello, C. V. & Clayton, D. F. Song-Induced ZENK Gene Expression in Auditory Pathways of Songbird Brain and Its Relation to the Song Control System. *Journal of Neuroscience* **14,** 6652–6666 (1994).

42. Dong, S. *et al.* Discrete Molecular States in the Brain Accompany Changing Responses to a Vocal Signal. *Proceedings of the National Academy of Sciences* **106,** 11364–11369 (2009).

43. Hilliard, A. T., Miller, J. E., Fraley, E. R., Horvath, S. & White, S. A. Molecular Microcircuitry Underlies Functional Specification in a Basal Ganglia Circuit Dedicated to Vocal Learning. *Neuron* **73,** 537–552 (2012).

44. Wada, K. *et al.* A Molecular Neuroethological Approach for Identifying and Characterizing a Cascade of Behaviorally Regulated Genes. *Proceedings of the National Academy of Sciences* **103,** 15212–15217 (2006).

45. Whitney, O. *et al.* Core and Region-Enriched Networks of Behaviorally Regulated Genes and the Singing Genome. *Science* **346** (2014).

46. McCarthy, M. M. Multifaceted Origins of Sex Differences in the Brain. *Philosophical Transactions of the Royal Society B: Biological Sciences* **371,** 20150106 (2016).

47. Roselli, C. E., Larkin, K., Resko, J. A., Stellflug, J. N. & Stormshak, F. The Volume of a Sexually Dimorphic Nucleus in the Ovine Medial Preoptic Area/Anterior

Hypothalamus Varies with Sexual Partner Preference. *Endocrinology* **145,** 478–483 (2004).

48. Nottebohm, F. & Arnold, A. P. Sexual Dimorphism in Vocal Control Areas of the Songbird Brain. *Science* **194,** 211–213 (1976).

49. Wade, J. & Buhlman, L. Lateralization and Effects of Adult Androgen in a Sexually Dimorphic Neuromuscular System Controlling Song in Zebra Finches. *The Journal of Comparative Neurology* **426,** 154–164 (2000).

50. Bottjer, S. W., Glaessner, S. L., Arthur & Arnold, P. Ontogeny of Brain Nuclei Controlling Song Learning and Behavior in Zebra Finches. *Journal of Neuroscience* **5,** 1556–1562 (1985).

51. Shaughnessy, D. W., Hyson, R. L., Bertram, R., Wu, W. & Johnson, F. Female Zebra Finches Do Not Sing yet Share Neural Pathways Necessary for Singing in Males. *The Journal of Comparative Neurology* **527,** 843–855 (2019).

52. Konishi, M. & Akutagawa, E. Neuronal Growth, Atrophy and Death in a Sexually Dimorphic Song Nucleus in the Zebra Finch Brain. *Nature* **315,** 145–147 (1985).

53. Nixdorf-Bergweiler, B. E. Divergent and Parallel Development in Volume Sizes of Telencephalic Song Nuclei in and Female Zebra Finches. *The Journal of Comparative Neurology* **375,** 445–456 (1996).

54. Bottjer, S. W., Miesner, E. A. & Arnold, A. P. Changes in Neuronal Number, Density and Size Account for Increases in Volume of Song-Control Nuclei during Song Development in Zebra Finches. *Neuroscience Letters* **67,** 263–268 (1986).

55. Alvarez-Buylla, A., Theelen, M. & Nottebohm, F. Birth of Projection Neurons in the Higher Vocal Center of the Canary Forebrain before, during, and after Song Learning. *Proceedings of the National Academy of Sciences* **85,** 8722–8726 (1988).

56. Kirn, J. R. & DeVoogd, T. J. Genesis and Death of Vocal Control Neurons during Sexual Differentiation in the Zebra Finch. *Journal of Neuroscience* **9,** 3176–87 (1989).

57. Scott, B. B. & Lois, C. Developmental Origin and Identity of Song System Neurons Born during Vocal Learning in Songbirds. *The Journal of Comparative Neurology* **502,** 202–214 (2007).

58. Konishi, M. & Akutagawa, E. Growth and Atrophy of Neurons Labeled at Their Birth in a Song Nucleus of the Zebra Finch. *Proceedings of the National Academy of Sciences* **87,** 3538–3541 (1990).

59. Konishi, M. & Akutagawa, E. in *Novartis Foundation Symposia* (eds Bock, G. & O'Connor, M.) 173–185 (John Wiley & Sons, Ltd., Chichester, UK, 1987). ISBN: 978-0-471-91092-3.

60. Nordeen, E. J. & Nordeen, K. W. Sex and Regional Differences in the Incorporation of Neurons Born during Song Learning in Zebra Finches. *Journal of Neuroscience* **8,** 2869–2874 (1988).

61. Wade, J. & Arnold, A. P. Sexual Differentiation of the Zebra Finch Song System. *Annals of the New York Academy of Sciences* **1016,** 540–559 (2004).

62. Phoenix, C. H. Organizing Action of Prenatally Administered Testosterone Propionate on the Tissues Mediating Mating Behavior in the Female Guinea Pig. *Hormones and Behavior* **55,** 566 (2009).

63. Arnold, A. P. The Organizational–Activational Hypothesis as the Foundation for a Unified Theory of Sexual Differentiation of All Mammalian Tissues. *Hormones and Behavior* **55,** 570–578 (2009).

64. Gahr, M. & Metzdorf, R. The Sexually Dimorphic Expression of Androgen Receptors in the Song Nucleus Hyperstriatalis Ventrale Pars Caudale of the Zebra Finch Develops Independently of Gonadal Steroids. *Journal of Neuroscience* **19,** 2628–36 (1999).

65. Kim, Y.-H., Perlman, W. R. & Arnold, A. P. Expression of Androgen Receptor mRNA in Zebra Finch Song System: Developmental Regulation by Estrogen. *The Journal of Comparative Neurology* **469,** 535–547 (2004).

66. Veney, S. L. & Wade, J. Steroid Receptors in the Adult Zebra Finch Syrinx: A Sex Difference in Androgen Receptor mRNA, Minimal Expression of Estrogen Receptor α and Aromatase. *General and Comparative Endocrinology* **136,** 192–199 (2004).

67. Arnold, A. P. & Saltiel, A. Sexual Difference in Pattern of Hormone Accumulation in the Brain of a Songbird. *Science* **205,** 702–705 (1979).

68. Arnold, A. P. Quantitative Analysis of Sex Differences in Hormone Accumulation in the Zebra Finch Brain: Methodological and Theoretical Issues. *The Journal of Comparative Neurology* **189,** 421–436 (1980).

69. Jacobs, E. C., Arnold, A. P. & Campagnoni, A. T. Developmental Regulation of the Distribution of Aromatase- and Estrogen-Receptor- mRNA-Expressing Cells in the Zebra Finch Brain. *Developmental Neuroscience* **21,** 453–72 (1999).

70. Gahr, M. & Konishi, M. Developmental Changes in Estrogen-Sensitive Neurons in the Forebrain of the Zebra Finch. *Proceedings of the National Academy of Sciences* **85,** 7380–7383 (1988).

71. Schlinger, B. A. & Arnold, A. P. Plasma Sex Steroids and Tissue Aromatization in Hatchling Zebra Finches: Implications for the Sexual Differentiation of Singing Behavior. *Endocrinology* **130,** 289–299 (1992).

72. Vockel, A., Pröve, E. & Balthazart, J. Sex- and Age-Related Differences in the Activity of Testosterone-Metabolizing Enzymes in Microdissected Nuclei of the Zebra Finch Brain. *Brain Research* **511,** 291–302 (1990).

73. Wade, J., Schlinger, B. A. & Arnold, A. P. Aromatase and 5β-Reductase Activity in Cultures of Developing Zebra Finch Brain: An Investigation of Sex and Regional Differences. *Journal of Neurobiology* **27,** 240–251 (1995).

74. Adkins-Regan, E., Abdelnabi, M., Mobarak, M. & Ottinger, M. A. Sex Steroid Levels in Developing and Adult Male and Female Zebra Finches (Poephila Guttata). *General and Comparative Endocrinology* **78,** 93–109 (1990).

75. Hutchison, J. B., Wingfield, J. C. & Hutchison, R. E. Sex Differences in Plasma Concentrations of Steroids during the Sensitive Period for Brain Differentiation in the Zebra Finch. *The Journal of Endocrinology* **103,** 363–369 (1984).

76. Arnold, A. P. The Effects of Castration on Song Development in Zebra Finches (Poephila Guttata). *Journal of Experimental Zoology* **191,** 261–277 (1975).

77. Adkins-Regan, E. & Ascenzi, M. Sexual Differentiation of Behavior in the Zebra Finch: Effect of Early Gonadectomy or Androgen Treatment. *Hormones and Behavior* **24,** 114–127 (1990).

78. Wade, J., Swender, D. A. & McElhinny, T. L. Sexual Differentiation of the Zebra Finch Song System Parallels Genetic, Not Gonadal, Sex. *Hormones and Behavior* **36,** 141–152 (1999).

79. Springer, M. L. & Wade, J. The Effects of Testicular Tissue and Prehatching Inhibition of Estrogen Synthesis on the Development of Courtship and Copulatory Behavior in Zebra Finches. *Hormones and Behavior* **32,** 46–59 (1997).

80. Schlinger, B. A. & Arnold, A. P. Androgen Effects on the Development of the Zebra Finch Song System. *Brain Research* **561,** 99–105 (1991).

81. Holloway, C. C. & Clayton, D. F. Estrogen Synthesis in the Male Brain Triggers Development of the Avian Song Control Pathway in Vitro. *Nature Neuroscience* **4,** 170–5 (2001).

82. Gurney, M. E. & Konishi, M. Hormone-Induced Sexual Differentiation of Brain and Behavior in Zebra Finches. *Science* **208,** 1380–1383 (1980).

83. Gurney, M. E. Behavioral Correlates of Sexual Differentiation in the Zebra Finch Song System. *Brain Research* **231,** 153–172 (1982).

84. Pohl-Apel, G. & Sossinka, R. Hormonal Determination of Song Capacity in Females of the Zebra Finch: Critical Phase of Treatment. *Zeitschrift für Tierpsychologie* **64,** 330–336 (1984).

85. Simpson, H. B. & Vicario, D. S. Early Estrogen Treatment Alone Causes Female Zebra Finches to Produce Learned, Male-like Vocalizations. *Journal of Neurobiology* **22,** 755–776 (1991).

86. Simpson, H. B. & Vicario, D. S. Early Estrogen Treatment of Female Zebra Finches Masculinizes the Brain Pathway for Learned Vocalizations. *Journal of Neurobiology* **22,** 777–793 (1991).

87. Adkins-Regan, E. & Ascenzi, M. Social and Sexual Behaviour of Male and Female Zebra Finches Treated with Oestradiol during the Nestling Period. *Animal Behaviour* **35,** 1100–1112 (1987).

88. Adkins-Regan, E., Mansukhani, V., Seiwert, C. & Thompson, R. Sexual Differentiation of Brain and Behavior in the Zebra Finch: Critical Periods for Effects of Early Estrogen Treatment. *Journal of Neurobiology* **25,** 865–877 (1994).

89. Gurney, M. Hormonal Control of Cell Form and Number in the Zebra Finch Song System. *Journal of Neuroscience* **1,** 658–673 (1981).

90. Grisham, W. & Arnold, A. P. A Direct Comparison of the Masculinizing Effects of Testosterone, Androstenedione, Estrogen, and Progesterone on the Development of the Zebra Finch Song System. *Journal of Neurobiology* **26,** 163–170 (1995).

91. Jacobs, E. C., Grisham, W. & Arnold, A. P. Lack of a Synergistic Effect between Estradiol and Dihydrotestosterone in the Masculinization of the Zebra Finch Song System. *Journal of Neurobiology* **27,** 513–519 (1995).

92. Arnold, A. P. Effects of Androgens on Volumes of Sexually Dimorphic Brain Regions in the Zebra Finch. *Brain Research* **185,** 441–444 (1980).

93. Wade, J., Buhlman, L. & Swender, D. Post-Hatching Hormonal Modulation of a Sexually Dimorphic Neuromuscular System Controlling Song in Zebra Finches. *Brain Research* **929,** 191–201 (2002).

94. Nordeen, K. W., Nordeen, E. J. & Arnold, A. P. Estrogen Establishes Sex Differences in Androgen Accumulation in Zebra Finch Brain. *Journal of Neuroscience* **6,** 734–738 (1986).

95. Grisham, W., Lee, J., McCormick, M. E., Yang-Stayner, K. & Arnold, A. P. Antiandrogen Blocks Estrogen-Induced Masculinization of the Song System in Female Zebra Finches. *Journal of Neurobiology* **51,** 1–8 (2002).

96. Perlman, W. R., Ramachandran, B. & Arnold, A. P. Expression of Androgen Receptor mRNA in the Late Embryonic and Early Posthatch Zebra Finch Brain. *The Journal of Comparative Neurology* **455,** 513–530 (2003).

97. London, S. E., Boulter, J. & Schlinger, B. A. Cloning of the Zebra Finch Androgen Synthetic Enzyme CYP17: A Study of Its Neural Expression throughout Posthatch Development. *The Journal of Comparative Neurology* **467,** 496–508 (2003).

98. DeWulf, V. & Bottjer, S. W. Age and Sex Differences in Mitotic Activity within the Zebra Finch Telencephalon. *Journal of Neuroscience* **22,** 4080–4094 (2002).

99. Adkins-Regan, E. Testosterone Increases Singing and Aggression but Not Male-Typical Sexual Partner Preference in Early Estrogen Treated Female Zebra Finches. *Hormones and Behavior* **35,** 63–70 (1999).

100. Merten, M. D. P. & Stocker-Buschina, S. Fadrozole Induces Delayed Effects on Neurons in the Zebra Finch Song System. *Brain Research* **671,** 317–320 (1995).

101. Balthazart, J., Absil, P., Fiasse, V. & Ball, G. F. Effects of the Aromatase Inhibitor R76713 on Sexual Differentiation of Brain and Behavior in Zebra Finches. *Behaviour* **131,** 225–260 (1994).

102. Mathews, G. A. & Arnold, A. P. Antiestrogens Fail to Prevent the Masculine Ontogeny of the Zebra Finch Song System. *General and Comparative Endocrinology* **80,** 48–58 (1990).

103. Mathews, G. A. & Arnold, A. P. Tamoxifen Fails to Block Estradiol Accumulation, yet Is Weakly Accumulated by the Juvenile Zebra Finch Anterior Hypothalamus: An Autoradiographic Study. *Journal of Neurobiology* **22,** 970–975 (1991).

104. Mathews, G. A., Brenowitz, E. A. & Arnold, A. P. Paradoxical Hypermasculinization of the Zebra Finch Song System by an Antiestrogen. *Hormones and Behavior* **22,** 540–551 (1988).

105. Dittrich, F., Feng, Y., Metzdorf, R. & Gahr, M. Estrogen-Inducible, Sex-Specific Expression of Brain-Derived Neurotrophic Factor mRNA in a Forebrain Song Control Nucleus of the Juvenile Zebra Finch. *Proceedings of the National Academy of Sciences* **96,** 8241–8246 (1999).

106. Choe, H. N. *et al.* Estrogen and Sex-Dependent Loss of the Vocal Learning System in Female Zebra Finches. *Hormones and Behavior* **129,** 104911 (2021).

107. Arnold, A. P. Sexual Differentiation of the Zebra Finch Song System: Positive Evidence, Negative Evidence, Null Hypotheses, and a Paradigm Shift. *Journal of Neurobiology* **33,** 572–84 (1997).

108. Agate, R. J. *et al.* Neural, Not Gonadal, Origin of Brain Sex Differences in a Gynandromorphic Finch. *Proceedings of the National Academy of Sciences* **100,** 4873–8 (2003).

109. Bennett-Baker, P. & Mueller, J. L. in *eLS* (ed John Wiley & Sons Ltd) 1–7 (John Wiley & Sons, Ltd, Chichester, UK, 2015). ISBN: 978-0-470-01617-6.

110. Zechner, U. *et al.* A High Density of X-Linked Genes for General Cognitive Ability: A Run-Away Process Shaping Human Evolution? *Trends in Genetics* **17,** 697–701 (2001).

111. Arnold, A. P. Sexual Differentiation of Brain and Other Tissues: Five Questions for the next 50 Years. *Hormones and Behavior* **120,** 104691 (2020).

112. McCarthy, M. M. & Arnold, A. P. Reframing Sexual Differentiation of the Brain. *Nature Neuroscience* **14,** 677–683 (2011).

113. Goodfellow, P. N. & Lovell-Badge, R. SRY and Sex Determination in Mammals. *Annual Review of Genetics* **27,** 71–92 (1993).

114. Capel, B. Vertebrate Sex Determination: Evolutionary Plasticity of a Fundamental Switch. *Nature Reviews. Genetics* **18,** 675–689 (2017).

115. Jost, A. Becoming a Male. *Advances in the Biosciences* **10,** 3–13 (1973).

116. Arnold, A. P. & Breedlove, S. M. Organizational and Activational Effects of Sex Steroids on Brain and Behavior: A Reanalysis. *Hormones and Behavior* **19,** 469–498 (1985).

117. Sangrithi, M. N. *et al.* Non-Canonical and Sexually Dimorphic X Dosage Compensation States in the Mouse and Human Germline. *Developmental Cell* **40,** 289–301.e3 (2017).

118. Dewing, P., Shi, T., Horvath, S. & Vilain, E. Sexually Dimorphic Gene Expression in Mouse Brain Precedes Gonadal Differentiation. *Molecular Brain Research* **118,** 82–90 (2003).

119. Bermejo-Alvarez, P., Rizos, D., Rath, D., Lonergan, P. & Gutierrez-Adan, A. Sex Determines the Expression Level of One Third of the Actively Expressed Genes in Bovine Blastocysts. *Proceedings of the National Academy of Sciences* **107,** 3394–3399 (2010).

120. Lowe, R., Gemma, C., Rakyan, V. K. & Holland, M. L. Sexually Dimorphic Gene Expression Emerges with Embryonic Genome Activation and Is Dynamic throughout Development. *BMC Genomics* **16,** 295 (2015).

121. De Vries, G. J. *et al.* A Model System for Study of Sex Chromosome Effects on Sexually Dimorphic Neural and Behavioral Traits. *Journal of Neuroscience* **22,** 9005–9014 (2002).

122. Corre, C. *et al.* Separate Effects of Sex Hormones and Sex Chromosomes on Brain Structure and Function Revealed by High-Resolution Magnetic Resonance Imaging and Spatial Navigation Assessment of the Four Core Genotype Mouse Model. *Brain Structure and Function* **221,** 997–1016 (2016).

123. Raznahan, A. *et al.* Triangulating the Sexually Dimorphic Brain through High-Resolution Neuroimaging of Murine Sex Chromosome Aneuploidies. *Brain Structure and Function* **220,** 3581–3593 (2015).

124. Vousden, D. A. *et al.* Impact of X/Y Genes and Sex Hormones on Mouse Neuroanatomy. *NeuroImage* **173,** 551–563 (2018).

125. Bachtrog, D. *et al.* Sex Determination: Why So Many Ways of Doing It? *PLoS Biology* **12,** e1001899 (2014).

126. Xu, L. *et al.* Dynamic Evolutionary History and Gene Content of Sex Chromosomes across Diverse Songbirds. *Nature Ecology & Evolution* **3,** 834–844 (2019).

127. Smeds, L. *et al.* Evolutionary Analysis of the Female-Specific Avian W Chromosome. *Nature Communications* **6,** 1–10 (2015).

128. Bellott, D. W. *et al.* Avian W and Mammalian Y Chromosomes Convergently Retained Dosage-Sensitive Regulators. *Nature Genetics* **49,** 387–394 (2017).

129. Fridolfsson, A.-K. *et al.* Evolution of the Avian Sex Chromosomes from an Ancestral Pair of Autosomes. *Proceedings of the National Academy of Sciences* **95,** 8147–8152 (1998).

130. Nanda, I. *et al.* 300 Million Years of Conserved Synteny between Chicken Z and Human Chromosome 9. *Nature Genetics* **21,** 258–259 (1999).

131. Bellott, D. W. *et al.* Convergent Evolution of Chicken Z and Human X Chromosomes by Expansion and Gene Acquisition. *Nature* **466,** 612–616 (2010).

132. Lyon, M. F. X-Chromosome Inactivation. *Current Biology* **9,** R235–R237 (1999).

133. Sado, T. & Ferguson-Smith, A. C. Imprinted X Inactivation and Reprogramming in the Preimplantation Mouse Embryo. *Human Molecular Genetics* **14 Spec No 1,** R59–64 (2005).

134. Disteche, C. M. Escape from X Inactivation in Human and Mouse. *Trends in Genetics* **11,** 17–22 (1995).

135. Carrel, L. & Willard, H. F. Heterogeneous Gene Expression from the Inactive X Chromosome: An X-Linked Gene That Escapes X Inactivation in Some Human Cell Lines but Is Inactivated in Others. *Proceedings of the National Academy of Sciences* **96,** 7364–7369 (1999).

136. Itoh, Y. *et al.* Dosage Compensation Is Less Effective in Birds than in Mammals. *Journal of Biology* **6,** 2 (2007).

137. Mank, J. E., Hultin-Rosenberg, L., Webster, M. T. & Ellegren, H. The Unique Genomic Properties of Sex-Biased Genes: Insights from Avian Microarray Data. *BMC Genomics* **9,** 148 (2008).

138. Itoh, Y. *et al.* Sex Bias and Dosage Compensation in the Zebra Finch versus Chicken Genomes: General and Specialized Patterns among Birds. *Genome Research* **20,** 512–518 (2010).

139. Wolf, J. B. & Bryk, J. General Lack of Global Dosage Compensation in ZZ/ZW Systems? Broadening the Perspective with RNA-Seq. *BMC Genomics* **12,** 91 (2011).

140. Uebbing, S., Künstner, A., Mäkinen, H. & Ellegren, H. Transcriptome Sequencing Reveals the Character of Incomplete Dosage Compensation across Multiple Tissues in Flycatchers. *Genome Biology and Evolution* **5,** 1555–1566 (2013).

141. Mueller, J. C., Kuhl, H., Timmermann, B. & Kempenaers, B. Characterization of the Genome and Transcriptome of the Blue Tit Cyanistes Caeruleus: Polymorphisms, Sex-Biased Expression and Selection Signals. *Molecular Ecology Resources* **16,** 549–561 (2016).

142. Warnefors, M. *et al.* Sex-Biased microRNA Expression in Mammals and Birds Reveals Underlying Regulatory Mechanisms and a Role in Dosage Compensation. *Genome Research* **27,** 1961–1973 (2017).

143. *Behavioral Neurobiology of Birdsong* (eds Zeigler, H. P. & Marler, P.) xvii, 788. xvii, 788. ISBN: 978-1-57331-473-2 (New York Academy of Sciences, New York, NY, US, 2004).

144. Livingston, F. S. & Mooney, R. Development of Intrinsic and Synaptic Properties in a Forebrain Nucleus Essential to Avian Song Learning. *Journal of Neuroscience* **17,** 8997–9009 (1997).

145. Dutar, P., Vu, H. M. & Perkel, D. J. Multiple Cell Types Distinguished by Physiological, Pharmacological, and Anatomic Properties in Nucleus HVc of the Adult Zebra Finch. *Journal of Neurophysiology* **80,** 1828–1838 (1998).

146. Kubota, M. & Taniguchi, I. Electrophysiological Characteristics of Classes of Neuron in the HVc of the Zebra Finch. *Journal of Neurophysiology* **80,** 914–923 (1998).

147. Luo, M. & Perkel, D. J. A GABAergic, Strongly Inhibitory Projection to a Thalamic Nucleus in the Zebra Finch Song System. *Journal of Neuroscience* **19,** 6700–6711 (1999).

148. Spiro, J. E., Dalva, M. B. & Mooney, R. Long-Range Inhibition within the Zebra Finch Song Nucleus RA Can Coordinate the Firing of Multiple Projection Neurons. *Journal of Neurophysiology* **81,** 3007–3020 (1999).

149. Goldberg, J. H. & Fee, M. S. Singing-Related Neural Activity Distinguishes Four Classes of Putative Striatal Neurons in the Songbird Basal Ganglia. *Journal of Neurophysiology* **103,** 2002–2014 (2010).

150. Daou, A., Ross, M. T., Johnson, F., Hyson, R. L. & Bertram, R. Electrophysiological Characterization and Computational Models of HVC Neurons in the Zebra Finch. *Journal of Neurophysiology* **110,** 1227–1245 (2013).

151. Meliza, C. D. *et al.* Estimating Parameters and Predicting Membrane Voltages with Conductance-Based Neuron Models. *Biological Cybernetics* **108,** 495–516 (2014).

152. Kadakia, N. *et al.* Nonlinear Statistical Data Assimilation for HVC Neurons in the Avian Song System. *Biological Cybernetics* **110,** 417–434 (2016).

153. Nogaret, A., Meliza, C. D., Margoliash, D. & Abarbanel, H. D. I. Automatic Construction of Predictive Neuron Models through Large Scale Assimilation of Electrophysiological Data. *Scientific Reports* **6,** 32749 (2016).

154. Hille, B. *Ion Channels of Excitable Membranes* 3rd ed. 814 pp. ISBN: 978-0-87893-321-1 (Sinauer, Sunderland, MA, USA, 2001).

155. Bean, B. P. The Action Potential in Mammalian Central Neurons. *Nature Reviews. Neuroscience* **8,** 451–465 (2007).

156. *Handbook of Ion Channels* (eds Zheng, J. & Trudeau, M. C.) (CRC Press, 2015).

157. Zhang, W. & Linden, D. J. The Other Side of the Engram: Experience-Driven Changes in Neuronal Intrinsic Excitability. *Nature Reviews. Neuroscience* **4,** 885–900 (2003).

158. Mozzachiodi, R. & Byrne, J. H. More than Synaptic Plasticity: Role of Nonsynaptic Plasticity in Learning and Memory. *Trends in Neurosciences* **33,** 17–26 (2010).

159. Ross, M. T. *et al.* Experience-Dependent Intrinsic Plasticity During Auditory Learning. *Journal of Neuroscience* **39,** 1206–1221 (2019).

160. Lovell, P. V., Carleton, J. B. & Mello, C. V. Genomics Analysis of Potassium Channel Genes in Songbirds Reveals Molecular Specializations of Brain Circuits for the Maintenance and Production of Learned Vocalizations. *BMC Genomics* **14,** 470 (2013).

161. Yu, F. H. & Catterall, W. A. Overview of the Voltage-Gated Sodium Channel Family. *Genome Biology* **4,** 207 (2003).

162. Catterall, W. A. Voltage-Gated Calcium Channels. *Cold Spring Harbor Perspectives in Biology* **3,** a003947 (2011).

163. Jentsch, T. J., Stein, V., Weinreich, F. & Zdebik, A. A. Molecular Structure and Physiological Function of Chloride Channels. *Physiological Reviews* **82,** 503–568 (2002).

164. Yates, B. *et al.* Genenames.Org: The HGNC and VGNC Resources in 2017. *Nucleic Acids Research* **45,** D619–D625 (2017).

165. Fagerberg, L. *et al.* Analysis of the Human Tissue-Specific Expression by Genome-Wide Integration of Transcriptomics and Antibody-Based Proteomics. *Molecular & Cellular Proteomics: MCP* **13,** 397–406 (2014).

166. Yue, F. *et al.* A Comparative Encyclopedia of DNA Elements in the Mouse Genome. *Nature* **515,** 355–364 (2014).

167. Uhlén, M. *et al.* Proteomics. Tissue-Based Map of the Human Proteome. *Science* **347,** 1260419 (2015).

168. Kent, W. J. BLAT–the BLAST-like Alignment Tool. *Genome Research* **12,** 656–664 (2002).

169. Zerbino, D. R. *et al.* Ensembl 2018. *Nucleic Acids Research* **46,** D754–D761 (2018).

170. Korlach, J. *et al.* De Novo PacBio Long-Read and Phased Avian Genome Assemblies Correct and Add to Reference Genes Generated with Intermediate and Short Reads. *GigaScience* **6,** 1–16 (2017).

171. Boratyn, G. M. *et al.* BLAST: A More Efficient Report with Usability Improvements. *Nucleic Acids Research* **41,** W29–33 (2013).

172. Carleton, J. B. *et al.* An Optimized Protocol for High-Throughput In Situ Hybridization of Zebra Finch Brain. *Cold Spring Harbor Protocols* **2014,** pdb.prot084582 (2014).

173. Replogle, K. *et al.* The Songbird Neurogenomics (SoNG) Initiative: Community-Based Tools and Strategies for Study of Brain Gene Function and Evolution. *BMC Genomics* **9,** 131 (2008).

174. Lovell, P. V., Clayton, D. F., Replogle, K. L. & Mello, C. V. Birdsong "Transcriptomics": Neurochemical Specializations of the Oscine Song System. *PLoS ONE* **3,** e3440 (2008).

175. Hara, E., Rivas, M. V., Ward, J. M., Okanoya, K. & Jarvis, E. D. Convergent Differential Regulation of Parvalbumin in the Brains of Vocal Learners. *PLoS ONE* **7,** e29457 (2012).

176. Lovell, P. V., Huizinga, N. A., Friedrich, S. R., Wirthlin, M. & Mello, C. V. The Constitutive Differential Transcriptome of a Brain Circuit for Vocal Learning. *BMC Genomics* **19,** 231 (2018).

177. Lovell, P. V. *et al.* Curation of Microarray Oligonucleotides and Corresponding ESTs/cDNAs Used for Gene Expression Analysis in Zebra Finches. *BMC Research Notes* **11,** 309 (2018).

178. Zhu, M. X., Evans, A. M., Ma, J., Parrington, J. & Galione, A. Two-Pore Channels for Integrative Ca Signaling. *Communicative & Integrative Biology* **3,** 12–17 (2010).

179. Goldin, A. L. Evolution of Voltage-Gated Na(+) Channels. *The Journal of Experimental Biology* **205,** 575–584 (2002).

180. Zakon, H. H. Adaptive Evolution of Voltage-Gated Sodium Channels: The First 800 Million Years. *Proceedings of the National Academy of Sciences* **109 Suppl 1,** 10619–10625 (2012).

181. Widmark, J., Sundström, G., Ocampo Daza, D. & Larhammar, D. Differential Evolution of Voltage-Gated Sodium Channels in Tetrapods and Teleost Fishes. *Molecular Biology and Evolution* **28,** 859–871 (2011).

182. Calhoun, J. D. & Isom, L. L. The Role of Non-Pore-Forming β Subunits in Physiology and Pathophysiology of Voltage-Gated Sodium Channels. *Handbook of Experimental Pharmacology* **221,** 51–89 (2014).

183. Warren, W. C. *et al.* A New Chicken Genome Assembly Provides Insight into Avian Genome Structure. *G3 (Bethesda, Md.)* **7,** 109–117 (2017).

184. Lovell, P. V. *et al.* Conserved Syntenic Clusters of Protein Coding Genes Are Missing in Birds. *Genome Biology* **15,** 565 (2014).

185. Zha, X.-m. Acid-Sensing Ion Channels: Trafficking and Synaptic Function. *Molecular Brain* **6,** 1 (2013).

186. Ren, D. Sodium Leak Channels in Neuronal Excitability and Rhythmic Behaviors. *Neuron* **72,** 899–911 (2011).

187. Garty, H. & Palmer, L. G. Epithelial Sodium Channels: Function, Structure, and Regulation. *Physiological Reviews* **77,** 359–396 (1997).

188. Hanukoglu, I. & Hanukoglu, A. Epithelial Sodium Channel (ENaC) Family: Phylogeny, Structure-Function, Tissue Distribution, and Associated Inherited Diseases. *Gene* **579,** 95–132 (2016).

189. Zamponi, G. W., Striessnig, J., Koschak, A. & Dolphin, A. C. The Physiology, Pathology, and Pharmacology of Voltage-Gated Calcium Channels and Their Future Therapeutic Potential. *Pharmacological Reviews* **67,** 821–870 (2015).

190. Dolphin, A. C. The $\alpha 2\delta$ Subunits of Voltage-Gated Calcium Channels. *Biochimica Et Biophysica Acta* **1828,** 1541–1549 (2013).

191. Buraei, Z. & Yang, J. The ß Subunit of Voltage-Gated Ca2+ Channels. *Physiological Reviews* **90,** 1461–1506 (2010).

192. Chen, R.-S., Deng, T.-C., Garcia, T., Sellers, Z. M. & Best, P. M. Calcium Channel Gamma Subunits: A Functionally Diverse Protein Family. *Cell Biochemistry and Biophysics* **47,** 178–186 (2007).

193. Ren, D. & Xia, J. Calcium Signaling through CatSper Channels in Mammalian Fertilization. *Physiology (Bethesda, Md.)* **25,** 165–175 (2010).

194. Chung, J.-J. *et al.* CatSperζ Regulates the Structural Continuity of Sperm Ca2+ Signaling Domains and Is Required for Normal Fertility. *eLife* **6,** e23082 (2017).

195. Cai, X. & Clapham, D. E. Evolutionary Genomics Reveals Lineage-Specific Gene Loss and Rapid Evolution of a Sperm-Specific Ion Channel Complex: CatSpers and CatSperbeta. *PLoS ONE* **3,** e3569 (2008).

196. Chung, J.-J. *et al.* CatSperζ Regulates the Structural Continuity of Sperm Ca2+ Signaling Domains and Is Required for Normal Fertility. *eLife* **6,** e23082 (2017).

197. Berridge, M. J. Inositol Trisphosphate and Calcium Signalling. *Nature* **361,** 315–325 (1993).

198. Berridge, M. J. The Inositol Trisphosphate/Calcium Signaling Pathway in Health and Disease. *Physiological Reviews* **96,** 1261–1296 (2016).

199. Singh, H. Two Decades with Dimorphic Chloride Intracellular Channels (CLICs). *FEBS Letters* **584,** 2112–2121 (2010).

200. Pedemonte, N. & Galietta, L. J. V. Structure and Function of TMEM16 Proteins (Anoctamins). *Physiological Reviews* **94,** 419–459 (2014).

201. Kunzelmann, K. TMEM16, LRRC8A, Bestrophin: Chloride Channels Controlled by Ca(2+) and Cell Volume. *Trends in Biochemical Sciences* **40,** 535–543 (2015).

202. Loewen, M. E. & Forsyth, G. W. Structure and Function of CLCA Proteins. *Physiological Reviews* **85,** 1061–1092 (2005).

203. Voss, F. K. *et al.* Identification of LRRC8 Heteromers as an Essential Component of the Volume-Regulated Anion Channel VRAC. *Science* **344,** 634–638 (2014).

204. Lutter, D., Ullrich, F., Lueck, J. C., Kempa, S. & Jentsch, T. J. Selective Transport of Neurotransmitters and Modulators by Distinct Volume-Regulated LRRC8 Anion Channels. *Journal of Cell Science* **130,** 1122–1133 (2017).

205. Abascal, F. & Zardoya, R. LRRC8 Proteins Share a Common Ancestor with Pannexins, and May Form Hexameric Channels Involved in Cell-Cell Communication. *BioEssays: News and Reviews in Molecular, Cellular and Developmental Biology* **34,** 551–560 (2012).

206. Gadsby, D. C., Vergani, P. & Csanády, L. The ABC Protein Turned Chloride Channel Whose Failure Causes Cystic Fibrosis. *Nature* **440,** 477–483 (2006).

207. Hubert, M. D. *et al.* Modulation of Volume Regulated Anion Current by I(Cln). *Biochimica Et Biophysica Acta* **1466,** 105–114 (2000).

208. Nam, K. *et al.* Molecular Evolution of Genes in Avian Genomes. *Genome Biology* **11,** R68 (2010).

209. Zhang, G. *et al.* Comparative Genomics Reveals Insights into Avian Genome Evolution and Adaptation. *Science* **346,** 1311–1320 (2014).

210. Farries, M. A. & Perkel, D. J. A Telencephalic Nucleus Essential for Song Learning Contains Neurons with Physiological Characteristics of Both Striatum and Globus Pallidus. *Journal of Neuroscience* **22,** 3776–3787 (2002).

211. Goldberg, J. H., Adler, A., Bergman, H. & Fee, M. S. Singing-Related Neural Activity Distinguishes Two Putative Pallidal Cell Types in the Songbird Basal Ganglia: Comparison to the Primate Internal and External Pallidal Segments. *Journal of Neuroscience* **30,** 7088–7098 (2010).

212. Cain, S. M. & Snutch, T. P. Contributions of T-Type Calcium Channel Isoforms to Neuronal Firing. *Channels* **4,** 475–482 (2010).

213. Vacher, H., Mohapatra, D. P. & Trimmer, J. S. Localization and Targeting of Voltage-Dependent Ion Channels in Mammalian Central Neurons. *Physiological Reviews* **88,** 1407–1447 (2008).

214. Yu, F. H. *et al.* Reduced Sodium Current in GABAergic Interneurons in a Mouse Model of Severe Myoclonic Epilepsy in Infancy. *Nature Neuroscience* **9,** 1142–1149 (2006).

215. Kalume, F., Yu, F. H., Westenbroek, R. E., Scheuer, T. & Catterall, W. A. Reduced Sodium Current in Purkinje Neurons from Nav1.1 Mutant Mice: Implications for Ataxia in Severe Myoclonic Epilepsy in Infancy. *Journal of Neuroscience* **27,** 11065–11074 (2007).

216. Ogiwara, I. *et al.* Nav1.1 Localizes to Axons of Parvalbumin-Positive Inhibitory Interneurons: A Circuit Basis for Epileptic Seizures in Mice Carrying an Scn1a Gene Mutation. *Journal of Neuroscience* **27,** 5903–5914 (2007).

217. Boiko, T. *et al.* Compact Myelin Dictates the Differential Targeting of Two Sodium Channel Isoforms in the Same Axon. *Neuron* **30,** 91–104 (2001).

218. Leão, R. N., Naves, M. M., Leão, K. E. & Walmsley, B. Altered Sodium Currents in Auditory Neurons of Congenitally Deaf Mice. *The European Journal of Neuroscience* **24,** 1137–1146 (2006).

219. Hu, W. *et al.* Distinct Contributions of Na(v)1.6 and Na(v)1.2 in Action Potential Initiation and Backpropagation. *Nature Neuroscience* **12,** 996–1002 (2009).

220. Beckh, S., Noda, M., Lübbert, H. & Numa, S. Differential Regulation of Three Sodium Channel Messenger RNAs in the Rat Central Nervous System during Development. *The EMBO Journal* **8,** 3611–3616 (1989).

221. Felts, P. A., Yokoyama, S., Dib-Hajj, S., Black, J. A. & Waxman, S. G. Sodium Channel Alpha-Subunit mRNAs I, II, III, NaG, Na6 and hNE (PN1): Different Expression Patterns in Developing Rat Nervous System. *Brain Research. Molecular Brain Research* **45,** 71–82 (1997).

222. Cheah, C. S. *et al.* Correlations in Timing of Sodium Channel Expression, Epilepsy, and Sudden Death in Dravet Syndrome. *Channels* **7,** 468–472 (2013).

223. Kazarinova-Noyes, K. *et al.* Contactin Associates with Na+ Channels and Increases Their Functional Expression. *Journal of Neuroscience* **21,** 7517–7525 (2001).

224. Kim, D. Y. *et al.* BACE1 Regulates Voltage-Gated Sodium Channels and Neuronal Activity. *Nature Cell Biology* **9,** 755–764 (2007).

225. Brackenbury, W. J. *et al.* Functional Reciprocity between Na+ Channel Nav1.6 and Beta1 Subunits in the Coordinated Regulation of Excitability and Neurite Outgrowth. *Proceedings of the National Academy of Sciences* **107,** 2283–2288 (2010).

226. Deschênes, I. & Tomaselli, G. F. Modulation of Kv4.3 Current by Accessory Subunits. *FEBS Letters* **528,** 183–188 (2002).

227. Marionneau, C. *et al.* The Sodium Channel Accessory Subunit Navβ1 Regulates Neuronal Excitability through Modulation of Repolarizing Voltage-Gated K^+ Channels. *Journal of Neuroscience* **32,** 5716–5727 (2012).

228. Nguyen, H. M. *et al.* Modulation of Voltage-Gated K+ Channels by the Sodium Channel β1 Subunit. *Proceedings of the National Academy of Sciences* **109,** 18577–18582 (2012).

229. Raman, I. M. & Bean, B. P. Resurgent Sodium Current and Action Potential Formation in Dissociated Cerebellar Purkinje Neurons. *Journal of Neuroscience* **17,** 4517–4526 (1997).

230. Grieco, T. M., Malhotra, J. D., Chen, C., Isom, L. L. & Raman, I. M. Open-Channel Block by the Cytoplasmic Tail of Sodium Channel Beta4 as a Mechanism for Resurgent Sodium Current. *Neuron* **45,** 233–244 (2005).

231. Bant, J. S. & Raman, I. M. Control of Transient, Resurgent, and Persistent Current by Open-Channel Block by Na Channel β4 in Cultured Cerebellar Granule Neurons. *Proceedings of the National Academy of Sciences* **107,** 12357–12362 (2010).

232. Kim, J. H., Kushmerick, C. & von Gersdorff, H. Presynaptic Resurgent Na+ Currents Sculpt the Action Potential Waveform and Increase Firing Reliability at a CNS Nerve Terminal. *Journal of Neuroscience* **30,** 15479–15490 (2010).

233. Barbosa, C. *et al.* Navβ4 Regulates Fast Resurgent Sodium Currents and Excitability in Sensory Neurons. *Molecular Pain* **11,** s12990-015-0063–9 (2015).

234. Adret, P. & Margoliash, D. Metabolic and Neural Activity in the Song System Nucleus Robustus Archistriatalis: Effect of Age and Gender. *The Journal of Comparative Neurology* **454,** 409–23 (2002).

235. Ölveczky, B. P., Otchy, T. M., Goldberg, J. H., Aronov, D. & Fee, M. S. Changes in the Neural Control of a Complex Motor Sequence during Learning. *Journal of Neurophysiology* **106,** 386–397 (2011).

236. Hahnloser, R. H. R., Kozhevnikov, A. A. & Fee, M. S. An Ultra-Sparse Code Underlies the Generation of Neural Sequences in a Songbird. *Nature* **419,** 65–70 (2002).

237. Aronov, D., Andalman, A. S. & Fee, M. S. A Specialized Forebrain Circuit for Vocal Babbling in the Juvenile Songbird. *Science* **320,** 630–634 (2008).

238. Hessler, N. A. & Doupe, A. J. Singing-Related Neural Activity in a Dorsal Forebrain-Basal Ganglia Circuit of Adult Zebra Finches. *Journal of Neuroscience* **19,** 10461–10481 (1999).

239. Morgan, K. *et al.* β3: An Additional Auxiliary Subunit of the Voltage-Sensitive Sodium Channel That Modulates Channel Gating with Distinct Kinetics. *Proceedings of the National Academy of Sciences* **97,** 2308–2313 (2000).

240. Cummins, T. R. *et al.* Nav1.3 Sodium Channels: Rapid Repriming and Slow Closed-State Inactivation Display Quantitative Differences after Expression in a Mammalian Cell Line and in Spinal Sensory Neurons. *Journal of Neuroscience* **21,** 5952–5961 (2001).

241. Meadows, L. S., Chen, Y. H., Powell, A. J., Clare, J. J. & Ragsdale, D. S. Functional Modulation of Human Brain Nav1.3 Sodium Channels, Expressed in Mammalian Cells, by Auxiliary β1, β2 and β3 Subunits. *Neuroscience* **114,** 745–753 (2002).

242. Yu, E. J. *et al.* Distinct Domains of the Sodium Channel Beta3-Subunit Modulate Channel-Gating Kinetics and Subcellular Location. *The Biochemical Journal* **392,** 519–526 (2005).

243. Cusdin, F. S. *et al.* The Sodium Channel {beta}3-Subunit Induces Multiphasic Gating in NaV1.3 and Affects Fast Inactivation via Distinct Intracellular Regions. *The Journal of Biological Chemistry* **285,** 33404–33412 (2010).

244. Merrick, E. C. *et al.* The Importance of Serine 161 in the Sodium Channel Beta3 Subunit for Modulation of Na(V)1.2 Gating. *Pflugers Archiv: European Journal of Physiology* **460,** 743–753 (2010).

245. Shah, B. S., Stevens, E. B., Pinnock, R. D., Dixon, A. K. & Lee, K. Developmental Expression of the Novel Voltage-Gated Sodium Channel Auxiliary Subunit β3, in Rat CNS. *The Journal of Physiology* **534,** 763–776 (2001).

246. Lu, B. *et al.* The Neuronal Channel NALCN Contributes Resting Sodium Permeability and Is Required for Normal Respiratory Rhythm. *Cell* **129,** 371–383 (2007).

247. Tsien, R. W., Lipscombe, D., Madison, D. V., Bley, K. R. & Fox, A. P. Multiple Types of Neuronal Calcium Channels and Their Selective Modulation. *Trends in Neurosciences* **11,** 431–438 (1988).

248. Berkefeld, H. *et al.* BKCa-Cav Channel Complexes Mediate Rapid and Localized Ca2+-Activated K+ Signaling. *Science* **314,** 615–620 (2006).

249. Berkefeld, H. & Fakler, B. Repolarizing Responses of BKCa-Cav Complexes Are Distinctly Shaped by Their Cav Subunits. *Journal of Neuroscience* **28,** 8238–8245 (2008).

250. Xu, W. & Lipscombe, D. Neuronal Ca(V)1.3alpha(1) L-Type Channels Activate at Relatively Hyperpolarized Membrane Potentials and Are Incompletely Inhibited by Dihydropyridines. *Journal of Neuroscience* **21,** 5944–5951 (2001).

251. Cain, S. M. & Snutch, T. P. T-Type Calcium Channels in Burst-Firing, Network Synchrony, and Epilepsy. *Biochimica Et Biophysica Acta* **1828,** 1572–1578 (2013).

252. Yu, A. C. & Margoliash, D. Temporal Hierarchical Control of Singing in Birds. *Science* **273,** 1871–1875 (1996).

253. Rudy, B. & McBain, C. J. Kv3 Channels: Voltage-Gated K+ Channels Designed for High-Frequency Repetitive Firing. *Trends in Neurosciences* **24,** 517–526 (2001).

254. Kubota, M. & Saito, N. Sodium- and Calcium-Dependent Conductances of Neurones in the Zebra Finch Hyperstriatum Ventrale Pars Caudale in Vitro. *The Journal of Physiology* **440,** 131–142 (1991).

255. Kozlov, A. S. *et al.* Distinct Kinetics of Cloned T-Type Ca2 + Channels Lead to Differential Ca2 + Entry and Frequency-Dependence during Mock Action Potentials. *The European Journal of Neuroscience* **11,** 4149–4158 (1999).

256. Chemin, J. *et al.* Specific Contribution of Human T-Type Calcium Channel Isotypes (Alpha(1G), Alpha(1H) and Alpha(1I)) to Neuronal Excitability. *The Journal of Physiology* **540,** 3–14 (2002).

257. Stanley, E. F. Presynaptic Calcium Channels and the Transmitter Release Mechanism. *Annals of the New York Academy of Sciences* **681,** 368–372 (1993).

258. Sheng, Z. H., Rettig, J., Takahashi, M. & Catterall, W. A. Identification of a Syntaxin-Binding Site on N-Type Calcium Channels. *Neuron* **13,** 1303–1313 (1994).

259. Wheeler, D. B., Randall, A. & Tsien, R. W. Roles of N-Type and Q-Type Ca2+ Channels in Supporting Hippocampal Synaptic Transmission. *Science* **264,** 107–111 (1994).

260. Weber, A. *et al.* N-Type Ca2+ Channels Carry the Largest Current: Implications for Nanodomains and Transmitter Release. *Nature Neuroscience* **13,** 1348–50 (2010).

261. Simms, B. A. & Zamponi, G. W. Neuronal Voltage-Gated Calcium Channels: Structure, Function, and Dysfunction. *Neuron* **82,** 24–45 (2014).

262. Bloodgood, B. L. & Sabatini, B. L. Nonlinear Regulation of Unitary Synaptic Signals by CaV(2.3) Voltage-Sensitive Calcium Channels Located in Dendritic Spines. *Neuron* **53,** 249–260 (2007).

263. Wang, K., Kelley, M. H., Wu, W. W., Adelman, J. P. & Maylie, J. Apamin Boosting of Synaptic Potentials in CaV2.3 R-Type Ca2+ Channel Null Mice. *PLoS ONE* **10,** e0139332 (2015).

264. Weiergräber, M. *et al.* Altered Seizure Susceptibility in Mice Lacking the Cav2.3 E-Type Ca2+ Channel. *Epilepsia* **47,** 839–850 (2006).

265. Zaman, T. *et al.* CaV2.3 Channels Are Critical for Oscillatory Burst Discharges in the Reticular Thalamus and Absence Epilepsy. *Neuron* **70,** 95–108 (2011).

266. Jarvis, S. E. & Zamponi, G. W. Trafficking and Regulation of Neuronal Voltage-Gated Calcium Channels. *Current Opinion in Cell Biology* **19,** 474–482 (2007).

267. Taylor, C. P. & Garrido, R. Immunostaining of Rat Brain, Spinal Cord, Sensory Neurons and Skeletal Muscle for Calcium Channel Alpha2-Delta (Alpha2-Delta) Type 1 Protein. *Neuroscience* **155,** 510–521 (2008).

268. Hoppa, M. B., Lana, B., Margas, W., Dolphin, A. C. & Ryan, T. A. $\alpha 2\delta$ Expression Sets Presynaptic Calcium Channel Abundance and Release Probability. *Nature* **486,** 122–125 (2012).

269. Tong, X.-J. *et al.* Retrograde Synaptic Inhibition Is Mediated by α-Neurexin Binding to the $\alpha 2\delta$ Subunits of N-Type Calcium Channels. *Neuron* **95,** 326–340.e5 (2017).

270. Kato, A. S., Gill, M. B., Yu, H., Nisenbaum, E. S. & Bredt, D. S. TARPs Differentially Decorate AMPA Receptors to Specify Neuropharmacology. *Trends in Neurosciences* **33,** 241–248 (2010).

271. Jackson, A. C. & Nicoll, R. A. The Expanding Social Network of Ionotropic Glutamate Receptors: TARPs and Other Transmembrane Auxiliary Subunits. *Neuron* **70,** 178–199 (2011).

272. Wada, K., Sakaguchi, H., Jarvis, E. D. & Hagiwara, M. Differential Expression of Glutamate Receptors in Avian Neural Pathways for Learned Vocalization. *The Journal of Comparative Neurology* **476,** 44–64 (2004).

273. Cho, C.-H., St-Gelais, F., Zhang, W., Tomita, S. & Howe, J. R. Two Families of TARP Isoforms That Have Distinct Effects on the Kinetic Properties of AMPA Receptors and Synaptic Currents. *Neuron* **55,** 890–904 (2007).

274. Yamazaki, M. *et al.* TARPs Gamma-2 and Gamma-7 Are Essential for AMPA Receptor Expression in the Cerebellum. *The European Journal of Neuroscience* **31,** 2204–2220 (2010).

275. Studniarczyk, D., Coombs, I., Cull-Candy, S. G. & Farrant, M. TARP γ-7 Selectively Enhances Synaptic Expression of Calcium-Permeable AMPARs. *Nature Neuroscience* **16,** 1266–1274 (2013).

276. Moss, F. J. *et al.* The Novel Product of a Five-Exon Stargazin-Related Gene Abolishes Ca(V)2.2 Calcium Channel Expression. *The EMBO Journal* **21,** 1514–1523 (2002).

277. Baker, K. D., Edwards, T. M. & Rickard, N. S. The Role of Intracellular Calcium Stores in Synaptic Plasticity and Memory Consolidation. *Neuroscience & Biobehavioral Reviews* **37,** 1211–1239 (2013).

278. Mouton, J. *et al.* Skeletal and Cardiac Ryanodine Receptors Bind to the Ca2+-Sensor Region of Dihydropyridine Receptor α1C Subunit. *FEBS Letters* **505,** 441–444 (2001).

279. Walton, P. D. *et al.* Ryanodine and Inositol Trisphosphate Receptors Coexist in Avian Cerebellar Purkinje Neurons. *Journal of Cell Biology* **113,** 1145–1157 (1991).

280. Nilius, B. & Droogmans, G. Amazing Chloride Channels: An Overview. *Acta Physiologica Scandinavica* **177,** 119–147 (2003).

281. Gonzalez-Silva, C. *et al.* Ca2+-Activated Cl- Channels of the ClCa Family Express in the Cilia of a Subset of Rat Olfactory Sensory Neurons. *PLoS ONE* **8,** e69295 (2013).

282. Mura, C. V., Delgado, R., Delgado, M. G., Restrepo, D. & Bacigalupo, J. A CLCA Regulatory Protein Present in the Chemosensory Cilia of Olfactory Sensory Neurons Induces a Ca2+-Activated Cl- Current When Transfected into HEK293. *BMC Neuroscience* **18,** 61 (2017).

283. Petit, C., Hossaert-McKey, M., Perret, P., Blondel, J. & Lambrechts, M. M. Blue Tits Use Selected Plants and Olfaction to Maintain an Aromatic Environment for Nestlings. *Ecology Letters* **5,** 585–589 (2002).

284. Amo, L., Galván, I., Tomás, G. & Sanz, J. J. Predator Odour Recognition and Avoidance in a Songbird. *Functional Ecology* **22,** 289–293 (2008).

285. Krause, E. T. *et al.* in *Advances in the Study of Behavior* (eds Naguib, M. *et al.*) 37–85 (Academic Press, 2018).

286. Steiger, S. S., Fidler, A. E., Valcu, M. & Kempenaers, B. Avian Olfactory Receptor Gene Repertoires: Evidence for a Well-Developed Sense of Smell in Birds? *Proceedings of the Royal Society B: Biological Sciences* **275,** 2309–2317 (2008).

287. Steiger, S. S., Kuryshev, V. Y., Stensmyr, M. C., Kempenaers, B. & Mueller, J. C. A Comparison of Reptilian and Avian Olfactory Receptor Gene Repertoires: Species-Specific Expansion of Group Gamma Genes in Birds. *BMC Genomics* **10,** 446 (2009).

288. Khan, I. *et al.* Olfactory Receptor Subgenomes Linked with Broad Ecological Adaptations in Sauropsida. *Molecular Biology and Evolution* **32,** 2832–2843 (2015).

289. Stephan, A. B. *et al.* ANO2 Is the Cilial Calcium-Activated Chloride Channel That May Mediate Olfactory Amplification. *Proceedings of the National Academy of Sciences* **106,** 11776–11781 (2009).

290. Pifferi, S., Cenedese, V. & Menini, A. Anoctamin 2/TMEM16B: A Calcium-Activated Chloride Channel in Olfactory Transduction. *Experimental Physiology* **97,** 193–199 (2012).

291. Dibattista, M., Pifferi, S., Boccaccio, A., Menini, A. & Reisert, J. The Long Tale of the Calcium Activated Cl- Channels in Olfactory Transduction. *Channels* **11,** 399–414 (2017).

292. Pifferi, S. *et al.* Bestrophin-2 Is a Candidate Calcium-Activated Chloride Channel Involved in Olfactory Transduction. *Proceedings of the National Academy of Sciences* **103,** 12929–12934 (2006).

293. Pifferi, S. *et al.* Calcium-Activated Chloride Currents in Olfactory Sensory Neurons from Mice Lacking Bestrophin-2. *The Journal of Physiology* **587,** 4265–4279 (2009).

294. Mori, C. & Wada, K. Audition-Independent Vocal Crystallization Associated with Intrinsic Developmental Gene Expression Dynamics. *Journal of Neuroscience* **35,** 878–889 (2015).

295. Olson, C. R., Hodges, L. K. & Mello, C. V. Dynamic Gene Expression in the Song System of Zebra Finches during the Song Learning Period. *Developmental Neurobiology* **75,** 1315–1338 (2015).

296. Arnold, A. P. & Gorski, R. A. Gonadal Steroid Induction of Structural Sex Differences in the Central Nervous System. *Annual Review of Neuroscience* **7,** 413–442 (1984).

297. Cooke, B., Hegstrom, C. D., Villeneuve, L. S. & Breedlove, S. M. Sexual Differentiation of the Vertebrate Brain: Principles and Mechanisms. *Frontiers in Neuroendocrinology* **19,** 323–362 (1998).

298. Ball, G. F. Species Variation in the Degree of Sex Differences in Brain and Behaviour Related to Birdsong: Adaptations and Constraints. *Philosophical Transactions of the Royal Society of London. Series B, Biological Sciences* **371,** 20150117 (2016).

299. Leonardo, A. & Fee, M. S. Ensemble Coding of Vocal Control in Birdsong. *Journal of Neuroscience* **25,** 652–661 (2005).

300. Nordeen, E. J., Grace, A., Burek, M. J. & Nordeen, K. W. Sex-Dependent Loss of Projection Neurons Involved in Avian Song Learning. *Journal of Neurobiology* **23,** 671–679 (1992).

301. Mooney, R. & Rao, M. Waiting Periods versus Early Innervation: The Development of Axonal Connections in the Zebra Finch Song System. *Journal of Neuroscience* **14,** 6532–6543 (1994).

302. Burek, M. J., Nordeen, K. W. & Nordeen, E. J. Ontogeny of Sex Differences among Newly-Generated Neurons of the Juvenile Avian Brain. *Brain Research. Developmental Brain Research* **78,** 57–64 (1994).

303. Zemel, B. M. *et al.* Resurgent Na+ Currents Promote Ultrafast Spiking in Projection Neurons That Drive Fine Motor Control. *Nature Communications* **12,** 6762 (2021).

304. Tang, Y. P. & Wade, J. Developmental Changes in the Sexually Dimorphic Expression of Secretory Carrier Membrane Protein 1 and Its Co-Localisation with Androgen Receptor Protein in the Zebra Finch Song System. *Journal of Neuroendocrinology* **23,** 584–590 (2011).

305. Wang, R. *et al.* Convergent Differential Regulation of SLIT-ROBO Axon Guidance Genes in the Brains of Vocal Learners. *The Journal of Comparative Neurology* **523,** 892–906 (2015).

306. Wild, J. M., Williams, M. N. & Suthers, R. A. Parvalbumin-Positive Projection Neurons Characterise the Vocal Premotor Pathway in Male, but Not Female, Zebra Finches. *Brain Research* **917,** 235–52 (2001).

307. Wade, J., Tang, Y. P., Peabody, C. & Tempelman, R. J. Enhanced Gene Expression in the Forebrain of Hatchling and Juvenile Male Zebra Finches. *Journal of Neurobiology* **64,** 224–238 (2005).

308. Bottjer, S. W. Neural Strategies for Learning during Sensitive Periods of Development. *Journal of Comparative Physiology A, Neuroethology, Sensory, Neural, and Behavioral Physiology* **188,** 917–928 (2002).

309. Soderstrom, K., Qin, W. & Leggett, M. H. A Minimally Invasive Procedure for Sexing Young Zebra Finches. *Journal of Neuroscience Methods* **164,** 116–119 (2007).

310. George, J. M. *et al.* Acute Social Isolation Alters Neurogenomic State in Songbird Forebrain. *Proceedings of the National Academy of Sciences,* 201820841 (2019).

311. Gunaratne, P. H. *et al.* Song Exposure Regulates Known and Novel microRNAs in the Zebra Finch Auditory Forebrain. *BMC Genomics* **12,** 277 (2011).

312. Tang, Y. P. & Wade, J. Sex and Age Differences in Brain-Derived Neurotrophic Factor and Vimentin in the Zebra Finch Song System: Relationships to Newly Generated Cells. *The Journal of Comparative Neurology* **524,** 1081–96 (2016).

313. Braun, K., Scheich, H., Heizmann, C. W. & Hunziker, W. Parvalbumin and Calbindin-D28K Immunoreactivity as Developmental Markers of Auditory and Vocal Motor Nuclei of the Zebra Finch. *Neuroscience* **40,** 853–869 (1991).

314. Paradis, E., Julien, P. & Ven Murthy, M. R. Requirement for Enzymatically Active Lipoprotein Lipase in Neuronal Differentiation: A Site-Directed Mutagenesis Study. *Brain Research. Developmental Brain Research* **149,** 29–37 (2004).

315. Wang, H. & Eckel, R. H. Lipoprotein Lipase in the Brain and Nervous System. *Annual Review of Nutrition* **32,** 147–160 (2012).

316. Funkelstein, L., Beinfeld, M., Minokadeh, A., Zadina, J. & Hook, V. Unique Biological Function of Cathepsin L in Secretory Vesicles for Biosynthesis of Neuropeptides. *Neuropeptides* **44,** 457–466 (2010).

317. Hook, V. *et al.* Cysteine Cathepsins in the Secretory Vesicle Produce Active Peptides: Cathepsin L Generates Peptide Neurotransmitters and Cathepsin B Produces Beta-Amyloid of Alzheimer's Disease. *Biochimica Et Biophysica Acta* **1824,** 89–104 (2012).

318. Vidak, E., Javoršek, U., Vizovišek, M. & Turk, B. Cysteine Cathepsins and Their Extracellular Roles: Shaping the Microenvironment. *Cells* **8,** 264 (2019).

319. Felbor, U. *et al.* Neuronal Loss and Brain Atrophy in Mice Lacking Cathepsins B and L. *Proceedings of the National Academy of Sciences* **99,** 7883–7888 (2002).

320. Stahl, S. *et al.* Proteomic Analysis of Cathepsin B and L-Deficient Mouse Brain Lysosomes. *Biochimica Et Biophysica Acta* **1774,** 1237–1246 (2007).

321. Tohda, C. & Tohda, M. Extracellular Cathepsin L Stimulates Axonal Growth in Neurons. *BMC Research Notes* **10,** 613 (2017).

322. Subramanian, A. *et al.* Gene Set Enrichment Analysis: A Knowledge-Based Approach for Interpreting Genome-Wide Expression Profiles. *Proceedings of the National Academy of Sciences* **102,** 15545–15550 (2005).

323. McCarthy, M. M., Pickett, L. A., VanRyzin, J. W. & Kight, K. E. Surprising Origins of Sex Differences in the Brain. *Hormones and Behavior* **76,** 3–10 (2015).

324. Morgan, C. P. & Bale, T. L. Sex Differences in microRNA Regulation of Gene Expression: No Smoke, Just miRs. *Biology of Sex Differences* **3,** 22 (2012).

325. Lin, Y.-C., Balakrishnan, C. N. & Clayton, D. F. Functional Genomic Analysis and Neuroanatomical Localization of miR-2954, a Song-Responsive Sex-Linked microRNA in the Zebra Finch. *Frontiers in Neuroscience* **0** (2014).

326. Radhakrishnan, B. & Alwin Prem Anand, A. Role of miRNA-9 in Brain Development. *Journal of Experimental Neuroscience* **10,** 101–120 (2016).

327. Ruminot, I., Schmälzle, J., Leyton, B., Barros, L. F. & Deitmer, J. W. Tight Coupling of Astrocyte Energy Metabolism to Synaptic Activity Revealed by Genetically Encoded FRET Nanosensors in Hippocampal Tissue. *Journal of Cerebral Blood Flow and Metabolism: Official Journal of the International Society of Cerebral Blood Flow and Metabolism* **39,** 513–523 (2019).

328. Tang, C. *et al.* Neural Stem Cells Behave as a Functional Niche for the Maturation of Newborn Neurons through the Secretion of PTN. *Neuron* **101,** 32–44.e6 (2019).

329. González-Castillo, C., Ortuño-Sahagún, D., Guzmán-Brambila, C., Pallàs, M. & Rojas-Mayorquín, A. E. Pleiotrophin as a Central Nervous System Neuromodulator, Evidences from the Hippocampus. *Frontiers in Cellular Neuroscience* **8,** 443 (2015).

330. Curmi, P. A. *et al.* Stathmin and Its Phosphoprotein Family: General Properties, Biochemical and Functional Interaction with Tubulin. *Cell Structure and Function* **24,** 345–357 (1999).

331. Ohkawa, N., Fujitani, K., Tokunaga, E., Furuya, S. & Inokuchi, K. The Microtubule Destabilizer Stathmin Mediates the Development of Dendritic Arbors in Neuronal Cells. *Journal of Cell Science* **120,** 1447–1456 (2007).

332. Watabe-Uchida, M., John, K. A., Janas, J. A., Newey, S. E. & Van Aelst, L. The Rac Activator DOCK7 Regulates Neuronal Polarity through Local Phosphorylation of Stathmin/Op18. *Neuron* **51,** 727–739 (2006).

333. Dickson, B. J. Molecular Mechanisms of Axon Guidance. *Science* **298,** 1959–1964 (2002).

334. Song, H.-j. & Poo, M.-m. The Cell Biology of Neuronal Navigation. *Nature Cell Biology* **3,** E81–E88 (2001).

335. Wang, S. *et al.* Sexual Dimorphism of Inhibitory Synaptic Transmission in RA Projection Neurons of Songbirds. *Neuroscience Letters* **709,** 134377 (2019).

336. Nordeen, E. J., Voelkel, L. & Nordeen, K. W. Fibroblast Growth Factor-2 Stimulates Cell Proliferation and Decreases Sexually Dimorphic Cell Death in an Avian Song Control Nucleus. *Journal of Neurobiology* **37,** 573–581 (1998).

337. Nordeen, E. J. & Nordeen, K. W. Sex Difference among Nonneuronal Cells Precedes Sexually Dimorphic Neuron Growth and Survival in an Avian Song Control Nucleus. *Journal of Neurobiology* **30,** 531–542 (1996).

338. Johnson, F., Hohmann, S. E., DiStefano, P. S. & Bottjer, S. W. Neurotrophins Suppress Apoptosis Induced by Deafferentation of an Avian Motor-Cortical Region. *Journal of Neuroscience* **17,** 2101–2111 (1997).

339. Akutagawa, E. & Konishi, M. Transient Expression and Transport of Brain-Derived Neurotrophic Factor in the Male Zebra Finch's Song System during Vocal Development. *Proceedings of the National Academy of Sciences* **95,** 11429–11434 (1998).

340. Chen, X., Agate, R. J., Itoh, Y. & Arnold, A. P. Sexually Dimorphic Expression of trkB, a Z-Linked Gene, in Early Posthatch Zebra Finch Brain. *Proceedings of the National Academy of Sciences* **102,** 7730–7735 (2005).

341. Knight, J. C., Scharf, E. L. & Mao-Draayer, Y. Fas Activation Increases Neural Progenitor Cell Survival. *Journal of Neuroscience Research* **88,** 746–757 (2010).

342. Strauss, J. *Yen & Jaffe's Reproductive Endocrinology: Physiology, Pathophysiology, and Clinical Management* ISBN: 978-0-323-47912-7 (Elsevier, Philadelphia, PA, 2019).

343. Grisham, W., Tam, A., Greco, C. M., Schlinger, B. A. & Arnold, A. P. A Putative 5α-Reductase Inhibitor Demasculinizes Portions of the Zebra Finch Song System. *Brain Research* **750,** 122–128 (1997).

344. Friedrich, S. R., Lovell, P. V., Kaser, T. M. & Mello, C. V. Exploring the Molecular Basis of Neuronal Excitability in a Vocal Learner. *BMC Genomics* **20,** 629 (2019).

345. Clayton, D. F. Role of Gene Regulation in Song Circuit Development and Song Learning. *Journal of Neurobiology* **33,** 549–571 (1997).

346. Velho, T. A. F., Lovell, P. & Mello, C. V. Enriched Expression and Developmental Regulation of the Middle-Weight Neurofilament (NF-m) Gene in Song Control Nuclei of the Zebra Finch. *The Journal of Comparative Neurology* **500,** 477–497 (2007).

347. Shi, Z. *et al.* Dynamic Transcriptome Landscape in the Song Nucleus HVC between Juvenile and Adult Zebra Finches. *Advanced Genetics* **2,** e10035 (2021).

348. Nordeen, K. W. & Nordeen, E. J. Projection Neurons within a Vocal Motor Pathway Are Born during Song Learning in Zebra Finches. *Nature* **334,** 149–151 (1988).

349. Wang, J., Sakaguchi, H. & Sokabe, M. Sex Differences in the Vocal Motor Pathway of the Zebra Finch Revealed by Real-Time Optical Imaging Technique. *Neuroreport* **10,** 2487–91 (1999).

350. Akutagawa, E. & Konishi, M. Two Separate Areas of the Brain Differentially Guide the Development of a Song Control Nucleus in the Zebra Finch. *Proceedings of the National Academy of Sciences* **91,** 12413–12417 (1994).

351. Herrmann, K. & Arnold, A. P. Lesions of HVC Block the Developmental Masculinizing Effects of Estradiol in the Female Zebra Finch Song System. *Journal of Neurobiology* **22,** 29–39 (1991).

352. Johnson, F. & Bottjer, S. W. Afferent Influences on Cell Death and Birth during Development of a Cortical Nucleus Necessary for Learned Vocal Behavior in Zebra Finches. *Development* **120,** 13–24 (1994).

353. Burek, M. J., Nordeen, K. W. & Nordeen, E. J. Initial Sex Differences in Neuron Growth and Survival within an Avian Song Nucleus Develop in the Absence of Afferent Input. *Journal of Neurobiology* **27,** 85–96 (1995).

354. Tomaszycki, M. L. *et al.* Sexual Differentiation of the Zebra Finch Song System: Potential Roles for Sex Chromosome Genes. *BMC Neuroscience* **10,** 24 (2009).

355. Diddens, J. *et al.* DNA Methylation Regulates Transcription Factor-Specific Neurodevelopmental but Not Sexually Dimorphic Gene Expression Dynamics in Zebra Finch Telencephalon. *Frontiers in Cell and Developmental Biology* **9** (2021).

356. De Vries, G. J. Minireview: Sex Differences in Adult and Developing Brains: Compensation, Compensation, Compensation. *Endocrinology* **145,** 1063–1068 (2004).

357. Lucas, P. C. & Granner, D. K. Hormone Response Domains in Gene Transcription. *Annual Review of Biochemistry* **61,** 1131–1173 (1992).

358. Fuentes, N. & Silveyra, P. in *Advances in Protein Chemistry and Structural Biology* (ed Donev, R.) 135–170 (Academic Press, 2019).

359. O'Lone, R., Frith, M. C., Karlsson, E. K. & Hansen, U. Genomic Targets of Nuclear Estrogen Receptors. *Molecular Endocrinology* **18,** 1859–1875 (2004).

360. Frankl-Vilches, C. & Gahr, M. Androgen and Estrogen Sensitivity of Bird Song: A Comparative View on Gene Regulatory Levels. *Journal of Comparative Physiology A* **204,** 113–126 (2018).

361. Catchpole, C. K. & Slater, P. J. B. *Bird Song: Biological Themes and Variations, 2nd Ed* xi, 335. xi, 335. ISBN: 978-0-521-87242-3 (Cambridge University Press, New York, NY, US, 2008).

362. Slater, P. J. B. & Mann, N. I. Why Do the Females of Many Bird Species Sing in the Tropics? *Journal of Avian Biology* **35,** 289–294 (2004).

363. Webb, W. H. *et al.* Female Song Occurs in Songbirds with More Elaborate Female Coloration and Reduced Sexual Dichromatism. *Frontiers in Ecology and Evolution* **4** (2016).

364. Wilkins, M. R., Odom, K. J., Benedict, L. & Safran, R. J. Analysis of Female Song Provides Insight into the Evolution of Sex Differences in a Widely Studied Songbird. *Animal Behaviour* **168,** 69–82 (2020).

365. Krieg, C. A. & Getty, T. Not Just for Males: Females Use Song against Male and Female Rivals in a Temperate Zone Songbird. *Animal Behaviour* **113,** 39–47 (2016).

366. Odom, K. J., Hall, M. L., Riebel, K., Omland, K. E. & Langmore, N. E. Female Song Is Widespread and Ancestral in Songbirds. *Nature Communications* **5,** 3379 (2014).

367. Odom, K. J., Omland, K. E. & Price, J. J. Differentiating the Evolution of Female Song and Male–Female Duets in the New World Blackbirds: Can Tropical Natural History Traits Explain Duet Evolution? *Evolution* **69,** 839–847 (2015).

368. Price, J. J., Lanyon, S. M. & Omland, K. E. Losses of Female Song with Changes from Tropical to Temperate Breeding in the New World Blackbirds. *Proceedings of the Royal Society B: Biological Sciences* **276,** 1971–1980 (2009).

369. Price, J. J. Evolution and Life-History Correlates of Female Song in the New World Blackbirds. *Behavioral Ecology* **20,** 967–977 (2009).

370. Riebel, K., Hall, M. & Langmore, N. Female Songbirds Still Struggling to Be Heard. *Trends in Ecology & Evolution* **20,** 419–20 (2005).

371. Goodwin, D. & Woodcock, M. *Estrildid Finches of the World* 328 pp. ISBN: 978-0-8014-1433-6 (British Museum (Natural History), 1982).

372. Geberzahn, N. & Gahr, M. Undirected (Solitary) Birdsong in Female and Male Blue-Capped Cordon-Bleus (Uraeginthus Cyanocephalus) and Its Endocrine Correlates. *PLoS ONE* **6,** e26485 (2011).

373. Gahr, M. & Güttingery, H.-R. Functional Aspects of Singing in Male and Female Uraeginthus Bengalus (Estrildidae). *Ethology* **72,** 123–131 (1986).

374. Ota, N., Gahr, M. & Soma, M. Tap Dancing Birds: The Multimodal Mutual Courtship Display of Males and Females in a Socially Monogamous Songbird. *Scientific Reports* **5,** 16614 (2015).

375. Boman, J. *et al.* The Genome of Blue-Capped Cordon-Bleu Uncovers Hidden Diversity of LTR Retrotransposons in Zebra Finch. *Genes* **10** (2019).

376. Soma, M. & Garamszegi, L. Z. Evolution of Courtship Display in Estrildid Finches: Dance in Relation to Female Song and Plumage Ornamentation. *Frontiers in Ecology and Evolution* **3** (2015).

377. Odom, K. J. *et al.* Typical Males and Unconventional Females: Songs and Singing Behaviors of a Tropical, Duetting Oriole in the Breeding and Non-Breeding Season. *Frontiers in Ecology and Evolution* **4,** 14 (2016).

378. Illes, A. E. Context of Female Bias in Song Repertoire Size, Singing Effort, and Singing Independence in a Cooperatively Breeding Songbird. *Behavioral Ecology and Sociobiology* **69,** 139–150 (2015).

379. Price, J. J., Yunes-Jiménez, L., Osorio-Beristain, M., Omland, K. E. & Murphy, T. G. Sex-Role Reversal in Song? Females Sing More Frequently Than Males in the Streak-Backed Oriole. *The Condor* **110,** 387–392 (2008).

380. Rose, E. M., Mathew, T., Coss, D. A., Lohr, B. & Omland, K. E. A New Statistical Method to Test Equivalence: An Application in Male and Female Eastern Bluebird Song. *Animal Behaviour* **145,** 77–85 (2018).

381. Arcese, P., Stoddard, P. K. & Hiebert, S. M. The Form and Function of Song in Female Song Sparrows. *The Condor* **90,** 44–50 (1988).

382. Beletsky, L. D. Vocalizations of Female Northern Orioles. *The Condor* **84,** 445–447 (1982).

383. Langmore, N. E. Functions of Duet and Solo Songs of Female Birds. *Trends in Ecology & Evolution* **13,** 136–140 (1998).

384. Morton, E. S. in *Ecology and Evolution of Acoustic Communication in Birds* 258–268 (Cornell University Press, 1996).

385. Sikora, J. G., Moyer, M. J., Omland, K. E. & Rose, E. M. Large Female Song Repertoires and Within-Pair Song Type Sharing in a Temperate Breeding Songbird. *Ethology* **127,** 166–175 (2021).

386. Illes, A. E. & Yunes-Jimenez, L. A Female Songbird Out-Sings Male Conspecifics during Simulated Territorial Intrusions. *Proceedings of the Royal Society B: Biological Sciences* **276,** 981–6 (2009).

387. Farabaugh, S. M. in *Acoustic Communication in Birds* 85–124 (Academic Press, New York, 1982).

388. Hall, M. L. A Review of Hypotheses for the Functions of Avian Duetting. *Behavioral Ecology and Sociobiology* **55,** 415–430 (2004).

389. Rose, E. M. *et al.* Why Do Females Sing?—Pair Communication and Other Song Functions in Eastern Bluebirds. *Behavioral Ecology* **30,** 1653–1661 (2019).

390. Langmore, N. E. in *Animal Signals: Signalling and Signal Design in Animal Communication* 317–324 (Tapir Academic Press, 2000). ISBN: 978-82-519-1545-8.

391. Cooney, R. & Cockburn, A. Territorial Defence Is the Major Function of Female Song in the Superb Fairy-Wren, Malurus Cyaneus. *Animal Behaviour* **49,** 1635–1647 (1995).

392. Cresswell, W. Song as a Pursuit-Deterrent Signal, and Its Occurrence Relative to Other Anti-Predation Behaviours of Skylark (Alauda Arvensis) on Attack by Merlins (Falco Columbarius). *Behavioral Ecology and Sociobiology* **34,** 217–223 (1994).

393. MacDougall-Shackleton, S. A. & Ball, G. F. Comparative Studies of Sex Differences in the Song-Control System of Songbirds. *Trends in Neurosciences* **22,** 432–436 (1999).

394. Brenowitz, E. A. & Arnold, A. P. Interspecific Comparisons of the Size of Neural Song Control Regions and Song Complexity in Duetting Birds: Evolutionary Implications. *Journal of Neuroscience* **6,** 2875–9 (1986).

395. Gahr, M., Sonnenschein, E. & Wickler, W. Sex Difference in the Size of the Neural Song Control Regions in a Dueting Songbird with Similar Song Repertoire Size of Males and Females. *Journal of Neuroscience* **18,** 1124–31 (1998).

396. Lobato, M. *et al.* Mismatch in Sexual Dimorphism of Developing Song and Song Control System in Blue-Capped Cordon-Bleus, a Songbird Species with Singing Females and Males. *Frontiers in Ecology and Evolution* **3** (2015).

397. Hall, Z. J., MacDougall-Shackleton, S. A., Osorio-Beristain, M. & Murphy, T. G. Male Bias in the Song Control System despite Female Bias in Song Rate in Streak-Backed Orioles (Icterus Pustulatus). *Brain, Behavior and Evolution* **76,** 168–75 (2010).

398. Ball, G. F. & MacDougall-Shackleton, S. A. Sex Differences in Songbirds 25 Years Later: What Have We Learned and Where Do We Go? *Microscopy Research and Technique* **54,** 327–34 (2001).

399. Benichov, J. I. *et al.* The Forebrain Song System Mediates Predictive Call Timing in Female and Male Zebra Finches. *Current Biology* **26,** 309–318 (2016).

400. Clayton, N. S. Song Discrimination Learning in Zebra Finches. *Animal Behaviour* **36,** 1016–1024 (1988).

401. Nelson, D. A., Marler, P., Soha, J. A. & Fullerton, A. L. The Timing of Song Memorization Differs in Males and Females: A New Assay for Avian Vocal Learning. *Animal Behaviour* **54,** 587–597 (1997).

402. Lauay, C., Gerlach, N. M., Adkins-Regan, E. & DeVoogd, T. J. Female Zebra Finches Require Early Song Exposure to Prefer High-Quality Song as Adults. *Animal Behaviour* **68,** 1249–1255 (2004).

403. Mello, C. V., Kaser, T., Buckner, A. A., Wirthlin, M. & Lovell, P. V. Molecular Architecture of the Zebra Finch Arcopallium. *The Journal of Comparative Neurology* **527,** 2512–2556 (2019).

404. Nevue, A. A., Lovell, P. V., Wirthlin, M. & Mello, C. V. Molecular Specializations of Deep Cortical Layer Analogs in Songbirds. *Scientific Reports* **10,** 18767 (2020).